



Australian Government
Department of Defence
Defence Science and
Technology Organisation

A Review of Australian and New Zealand Investigations on Aeronautical Fatigue During the Period April 2011 to March 2013

Editor: Phil Jackson

Air Vehicles Division
Defence Science and Technology Organisation

DSTO-TN-1166

ABSTRACT

This document has been prepared for presentation to the 33rd Conference of the International Committee on Aeronautical Fatigue and Structural Integrity (ICAF) scheduled to be held in Jerusalem, Israel June 3rd to 4th 2013. The report contains summaries of the research and associated activities in the field of aircraft fatigue and structural integrity at research laboratories, universities and aerospace companies in Australia and New Zealand during the period April 2011 to March 2013. The review covers fatigue-related research programs as well as fatigue investigations on specific military and civil aircraft.

RELEASE LIMITATION

Approved for public release

Contents

1. INTRODUCTION.....	1
2. AUSTRALIA	2
2.1 RESEARCH ACTIVITIES.....	2
2.1.1 Prediction models for stable tearing during fatigue crack growth - Mohd Fairuz Ab Rahman ^{a,b} , Chun Wang ^a , Graham Clark ^a (RMIT University).....	2
2.1.2 Damage tolerance based life assessment for helicopter components - Sunny Chan, Graham Clark, Chun Wang (RMIT University)	2
2.1.3 Quantitative fractography for the determination of fatigue crack growth rates in Aluminium and Titanium structures - Marcus McDonald, Rob Boykett (DSTO) and Malcolm Jones(Fortburn)	3
2.1.4 Fatigue Testing of AA7050-T7451 with Various Corrosion Prevention Surface Treatments - Macus McDonald, Rob Boykett, (DSTO), Malcolm Jones, (Fortburn)	5
2.1.5 New Threshold and Short Crack (TASC) Data for Improved Predictions of Combat Aircraft Fatigue Life [1] - Madeleine Burchill, Simon Barter, (DSTO), E. Amsterdam, (NLR).....	8
2.1.6 Development and validation of improved experimental techniques and modelling for fatigue crack growth under constant amplitude and spectrum loading - Kevin Walker, DSTO and RMIT University Australia, and James Newman, Jr., Mississippi State University USA.....	12
2.1.7 A new approach to determine near-threshold fatigue crack growth rate properties in high-strength coarse grain titanium alloy with rough and torturous fatigue surfaces - Kevin Walker, (DSTO and RMIT University Australia), and James Newman, Jr., (Mississippi State University USA)	15
2.1.8 The Harman-Schjive Variant for the Calculation of Crack Growth - Rhys Jones (Monash University), Loris Molent and Simon Barter (DSTO).....	18
2.1.9 The Lead Crack Fatigue Lifting Framework - Loris Molent and Simon Barter (DSTO) and Russell Wanhill (NLR).....	21
2.1.10 A New Closed-Form Stress Intensity Factor Solution For Equal Cracks Emanating From A Central Circular Hole In A Rectangular Plate - Witold Waldman (DSTO).....	22
2.1.11 Beta Factors For Collinear Asymmetrical Cracks Emanating From An Offset Circular Hole In A Rectangular Plate - Witold Waldman (DSTO).....	25
2.1.12 Elasto-Plastic Contact Analysis Using Abaqus Of The K_t Of A Hole Fitted With Neat-Fit Fastener For LIF Hawk Filled-Hole Coupon - Witold Waldman (DSTO)	27

2.1.13	Managing the Effects of Environmental Degradation on the Airworthiness of RAAF Aircraft - Bruce Crawford, Khan Sharp, Chris Loader, Qanchu Liu, Alex Shekhter, (DSTO) and T.J. Harrison (RMIT University)	30
2.1.13.1	Corrosion Structural Integrity Roadmap	30
2.1.13.2	Pitting Corrosion of 7050-T7651	31
2.1.13.3	Pitting Data Consolidation.....	32
2.1.13.4	Criticality of Pitting Corrosion	32
2.1.13.5	Certification of Retrogression and Re-ageing.....	33
2.1.13.6	Modelling of Intergranular Corrosion in AA7075-T651	34
2.1.14	Managing Fatigue from Corrosion Pits - Loris Molent, (DSTO)	36
2.1.15	On the Fatigue Crack Growth Analysis of Spliced Plates under Sequential Tensile and Shear Loads - Xiaobo Yu, (DSTO)	37
2.1.16	Forced Dynamic Response Analysis for an Industrial Mistuned Integrally Bladed Disk - Guan Xia Chen and Jianfu Hou (DSTO)	38
2.1.17	In Situ Structural Health Monitoring using Acousto-Ultrasonics, Optical Fibre Sensors and Thermoelastic Stress Analysis - Nik Rajic, Claire Davis and Steve Galea, (DSTO)	42
2.1.17.1	Enhanced Experimental Facility for Durability and Performance Characterisation of Piezoelectric Transducers [3].....	43
2.1.17.2	Thermoelastic Stress Analysis (TSA) for Structural Health Monitoring (SHM) [8, 9]	45
2.1.18	Improving Structural Risk Analysis by Updating the Probabilistic Distribution of the Equivalent Initial Flaw Sizes based on the Bayes' Theorem - Ribí Torregosa and Weiping Hu, (DSTO)	49
2.1.19	Probabilistic Risk Analysis Of A Fatigue-Critical Location On A Transport Aircraft Considering Multi Site Damage Using FracRisk - Ribí Torregosa and Weiping Hu, (DSTO)	51
2.1.20	Recent Development in Fatigue Damage and Crack Growth Analysis: Verification and Validation, and Application in Lifting Airframe Structures - Chris Wallbrink and Weiping Hu, (DSTO)	54
2.1.21	Seeing the Invisible: Taking a look at Stresses in Aircraft Fatigue Analysis - Albert Wong (DSTO)	55
2.2	FULL SCALE TEST ACTIVITIES	58
2.2.1	F/A-18A/B Hornet Outer Wing StAtic Testing (HOWSAT) - Wayne Foster, (DSTO)	58
2.2.2	F/A-18A-D Flaw IdeNtification through the Application of Loads (FINAL) Program - Geoff Swanton, (DSTO)	60
2.3	IN-SERVICE STRUCTURAL INTEGRITY MANAEMENT	63
2.3.1	Beta solutions for C-130J-30 wing damage tolerance locations based on handbook methods - Rebecca Evans, Manfred Heller (DSTO), Rebecca Gravina, A Clarke, and C Rock (QinetiQ Australia)	63
2.3.2	User Manual for the C-130J DSTO Global Finite Element Model Version C130J-DSTO-v1.0 - Michael Opie, (DSTO)	65

2.3.3	C-130J Wing Fatigue Test Article Finite Element Model Validation and Determination of Test Representativeness - Michael Opie, (DSTO) and Jack Lubacz, (Qinetiq Australia)	66
2.3.4	P-3C Structural Management Update - Andrew Walliker (DSTO), Kevin Watters (QinetiQ Australia) and FLTLT Greg Brick (ASI-DGTA).....	68
2.3.5	P-3 Skin Panel Assessment - S. Bandara, T. Cooper, Kevin Watters (QinetiQ Australia)	73
2.3.6	C-130J Counter Measure Dispenser System Structural Substantiation - S. Bandara, Kevin Watters, R. Stewart (QinetiQ Australia)	75
2.3.7	Assessment of Training Aircraft Full Scale Fatigue Test Data for Reliable Validation of Global Finite Element Models - Xiaobo Yu, Robert Kaye and Michael Opie, (DSTO)	77
2.3.8	Integration of Load Path Analysis and Harmonic Regression for Usage Monitoring of Helicopter Dynamic Components - Xiaobo Yu and John Vine, (DSTO)	79
2.3.9	Helicopter Airframe Fatigue Spectrum Generation and Truncation - Luther Krake (DSTO)	80
2.3.10	E-7A Wedgetail Usage Monitoring System Certification, Testing and Implementation - Tom Matley, (DSTO) and Ian Coker, (Directorate General Technical Airworthiness)	83
2.3.11	Regulation of UAS for use by the ADF - Callum Wright, (DSTO)	85
2.3.12	DEF STAN 00 970 Equivalent Safety Finding Methodology for RAAF PC-9/A FAR23 Certified Repairs - Z. Louli, S. Trezise, Kevin Watters (QinetiQ Australia)	87
2.3.13	Development of Flight Manoeuvre Recognition Software for Rotary Wing Platforms - A. Castelow, A. McArlein, C. McGregor (QinetiQ Australia).....	88
2.3.14	Black Hawk CRT Calculations/Individual Asset Calculations - A. Jackson, T. Frisch, C. Cowx, B. Hindmarsh, D. Moorhead, J. Turner, J. Lamshed, K. Watters, R. Lockett, K. Jackson, J. Moews (QinetiQ Australia)	89
2.4	FATIGUE INVESTIGATIONS OF MILITARY AIRCRAFT.....	90
2.4.1	Failure Analysis Examples in Military Aircraft - Nick Athinotis, (DSTO)	90
2.4.2	Life Extension of F/A-18 LAU-7 Missile Launchers Using Rework Shape Optimisation and Cold Rolling - Manfred Heller, Jaime Calero, Simon Barter, Ron Wescott, Jireh Choi, (DSTO)	92
2.5	FATIGUE INVESTIGATIONS OF CIVIL AIRCRAFT.....	96
2.5.1	Fatigue and Structural Integrity of Light Aircraft - AEA Aerospace Group Pty Ltd and Dave Morris, (Civil Aviation Safety Authority)	96
2.5.1.1	Cessna 210 Carry through rework	96
2.5.1.2	Cessna 441 life extension STC.....	97

2.5.1.3	CASA 212 fatigue assessment of landing gear following Antarctic operations.....	98
3.	NEW ZEALAND.....	99
3.1.1	CT4-E Fatigue Life - Stephen Campbell, (Defence Technology Agency).....	99
3.1.2	C-130 Gust Spectrum- Stephen Campbell, (Defence Technology Agency)	100

1. INTRODUCTION

This document presents a review of Australian and New Zealand work in fields relating to aeronautical fatigue and structural integrity in the period April 2009 to March 2011, and is made up from inputs from the organisations listed below. The editor acknowledges these contributions with appreciation. Enquiries should be addressed to the person identified against the item of interest.

DSTO	Defence Science and Technology Organisation, 506 Lorimer Street, Fishermans Bend VIC 3207, Australia
DTA	Defence Technology Agency, Auckland Naval Base, New Zealand
QinetiQ Australia	Level 3, 210 Kings Way, South Melbourne, VIC 3205, Australia.
Monash University	Dept of Mechanical Engineering, PO Box 72, Monash University, VIC 3800, Australia.
RMIT University	Dept of Aerospace, Mechanical and Manufacturing Engineering, PO Box 71 Bundoora, VIC 3083
Civil Aviation Safety Authority	Aviation House, PO Box 2005 Canberra, ACT 2601
Royal Australian Air Force	Deputy Director ASI, Directorate General Technical Airworthiness, RAAF Williams, Laverton, VIC, 3027

2. AUSTRALIA

2.1 RESEARCH ACTIVITIES

2.1.1 Prediction models for stable tearing during fatigue crack growth - Mohd Fairuz Ab Rahman^{a,b}, Chun Wang^a, Graham Clark^a (RMIT University)

Stable tearing features a rapid “jump” of crack length, usually at a macro-scale, in one loading cycle, after which normal fatigue crack growth resumes with crack growth increments on a micro-scale. Fatigue crack growth with bands of stable tearing result in a pattern of fatigue crack growth that consists of periods of slow fatigue crack growth interspersed with periods of fast, but *stable*, fracture by tearing. Prediction of the tearing jump has been limited to the magnitude of the stress intensity factor for the first onset of stable tearing, and it is still not possible to predict the size for each tearing jump length. A prediction model for stable tearing could be integrated into overall fatigue life prediction to further improve its accuracy, although the major benefit is likely to be related to identifying the probable current size of cracking for NDE purposes. Such a model would also be useful during fractographic analysis of variable amplitude fatigue fracture surfaces, which exhibit multiple tearing jumps, and would assist with post-fracture analysis of failures.

The curved crack front at the arrest of tearing complicates determination of the stress intensity factor. A three-dimensional finite element analysis was undertaken to develop a model based on a parametric solution that correlates the stress intensity factor values at the mid-thickness with tearing crack jump length of three variable amplitude stable tearing jumps. This model was validated against multiple tearing jump lengths produced in various aluminium alloys used in aircraft structures. Salient features of this new model are that the tongue-shaped region of stable tearing is idealised as a trapezoidal shape and the average of area ratio of tearing is approximately constant. Comparisons between the model predictions and experimental results indicate that this new model produces satisfactory prediction of stable tearing crack jump length in aluminium alloys of different cross-sectional thickness. The features of this model have also been used to extend the Forsyth and Schijve concepts of post-fracture analysis of tearing, to provide alternative methods for predicting stable tearing jump length. These models are very useful as post-failure analysis tools during fractographic analysis of fatigue fracture surfaces, especially in estimating the loading conditions that caused the stable tearing.

^aSchool of Aerospace, Mechanical and Manufacturing Engineering, RMIT University, Bundoora, Victoria 3083, Australia

^bDepartment of Occupational Safety and Health, Level 2, 3 & 4, Block D3, Complex D, 62530 Putrajaya, Malaysia

2.1.2 Damage tolerance based life assessment for helicopter components - Sunny Chan, Graham Clark, Chun Wang (RMIT University)

For many years the helicopter community has used the safe life approach to design against fatigue. Variability in safe life prediction varies substantially with loading and hence with

test life, and at low-load, long cyclic lives, therefore requires relatively large safety factors to minimise the risk. This leads to a less efficient use of components as many components are replaced while still having a substantial remaining life. Because of this problem and the success of damage tolerance based fatigue life management for fixed wing aircraft, the Federal Aviation Administration (FAA) added a requirement to tolerate damage and flaws in rotary wing aircraft (FAR 29.571). However, it is difficult to translate the damage tolerance methodology for fixed wing applications due to the differences in loading between fixed wing and rotary wing aircraft. For example, at the helicopter blade root, loading is typically applied at a rate of 2 to 20 Hz and there are many of these low amplitude loadings. In contrast, at a transport aircraft wing root, the loading rate is typically less than 1Hz, and cyclic life is shorter. Adopting a damage tolerance approach for helicopters can lead to very short inspection intervals, and, crucially, inspections for very small cracks, which can make the damage tolerance approach not very practical. Helicopter loadings, in conjunction with the smaller initial crack size, also lead to life prediction relying on the more poorly understood near-threshold regime. This project examines the key factors involved in potential application of damage tolerance methods to an Australian fleet of helicopters for which loading data is available, with the aim of improving prediction methods.

One area that has been explored in this research is the effect of fracture surface roughness on roughness induced crack closure, which is believed to play a key role in the threshold region. By collecting the fracture surface roughness perpendicular to the crack growth direction, and plotting them with the stress intensity factor, with the material used, it was found that there is a relationship between roughness and stress intensity factor independent of the stress ratio. The trend of the relationship matches the trend observed for crack growth in the threshold region. This relationship leads to potential for further development of a roughness model that could be used to enhance prediction, which will in turn improve the application of damage tolerance methods to helicopters.

2.1.3 Quantitative fractography for the determination of fatigue crack growth rates in Aluminium and Titanium structures - Marcus McDonald^{1c}, Rob Boykett¹ (DSTO) and Malcolm Jones²(Fortburn)

The determination of crack growth rates in metallic materials is essential for damage tolerance assessments of fatigue cracking in airframe components. Reading the microscopic deformations 'recorded' on the fracture surface of a metal fatigue failure, or Quantitative Fractography (QF), can reveal information about the rate at which the fatigue crack grew under the applied in-flight loading. This is done by destructively opening up the cracked component and, under the microscope, associating the fracture surface deformations back to the individual in-flight loading events, thus enabling a plot of the crack size against flight-hours to be generated. This can provide previously unavailable data for the purpose of fatigue design validation and fatigue modelling improvement.

¹ Defence Science and Technology Organisation, Melbourne, Australia.

² QinetiQ Australia, Melbourne, Australia.

^c corresponding author: marcus.mcdonald@dsto.defence.gov.au

QF data is not always easy to obtain as different metals have different propensities for creating visible fracture surface deformations. A recent joint-study by DSTO & NLR on Aluminium Alloy 7050 revealed that the deformations can be made more visible by forcing the crack path to change direction for small periods of time by inserting special load patterns into the applied flight load spectrum. These load patterns were exploited to force the fatigue crack to 'grow' a microscopic light-reflector on the fracture surface at a particular point in the flight spectrum. These reflectors are significantly easier to identify under an optical microscope compared to the deformations caused by the normal flight loading.

This work presents load patterns that were found to create optical reflectors for Titanium Ti-6Al-4V, which has traditionally been very difficult to read and so there is very little available data on the growth rate of small cracks in this material. Fatigue tests for Titanium were performed to fine-tune these load patterns such that they produced optical bands small enough that they did not significantly affect the overall component life and yet were still visible (see Figure 1). It was also found that load 'pulses' could be applied to effectively create a 'barcode' if needed (see Figure 2). Titanium is used extensively in the skeleton of modern combat airframes, and hence this technology is currently being used to provide new, more comprehensive, crack growth rate information that will improve the accuracy and efficiency of durability and damage tolerance assessments for these modern combat aircraft.

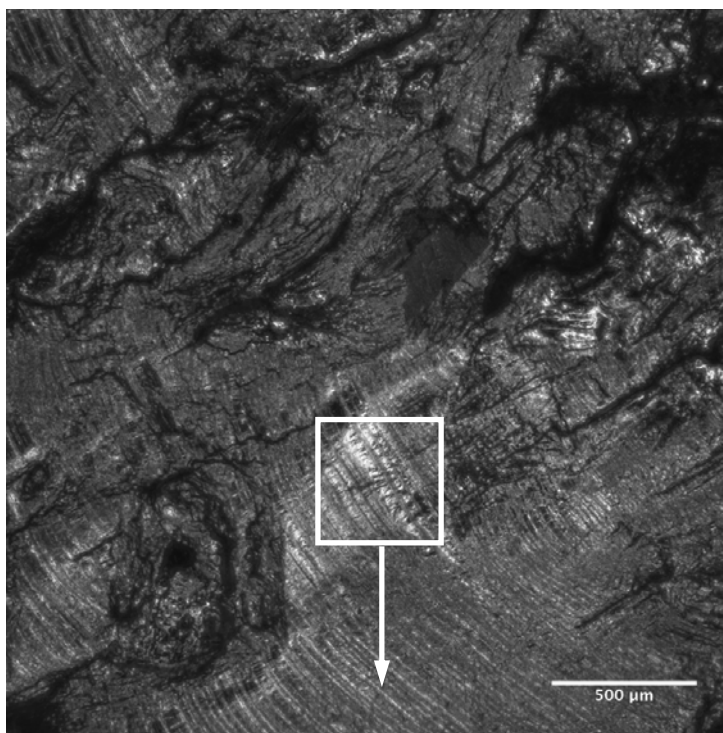


Figure 1: A view of a Titanium fracture surface showing the relatively reflective 'marker band' amongst usual flight load markings.

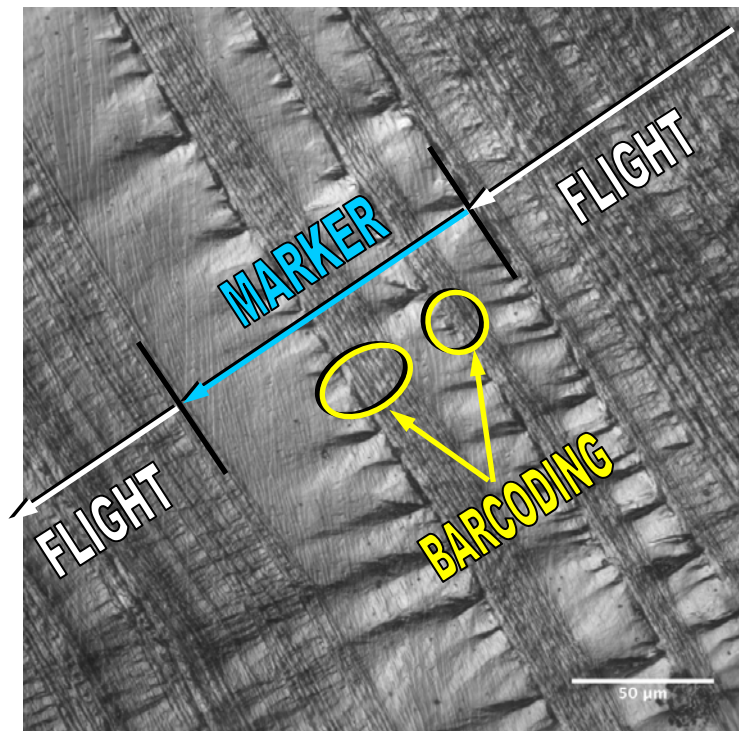


Figure 2: A zoomed view of a Titanium fracture surface showing an example of 'barcoding' within a 'marker band'.

2.1.4 Fatigue Testing of AA7050-T7451 with Various Corrosion Prevention Surface Treatments - Macus McDonald, Rob Boykett, (DSTO), Malcolm Jones, (Fortburn)

Corrosion preventative surface treatments are commonly used on metallic components of modern combat aircraft to help prevent environmental effects - corrosion, from degrading the integrity of the structure. However, some metals are known to be more susceptible to damage from the surface treatment, such as pitting that can occur during the application of the surface treatment. Such pits can, in turn potentially reduce the fatigue life of the component, through the presence of more numerous and larger fatigue crack initiation sites compared to un-treated materials with their inherent discontinuities - second phase particles, machining marks, etc.

A fatigue coupon test program has been completed [1], which investigated the potential effects on fatigue lives of four different surface treatments on AA7050-T7451, a material commonly used in modern combat aircraft and known to be susceptible to chemical pitting attack [2]. The surface treatments tested in this fatigue program were: machined (bare as-machined; with and without post machining polishing), anodised and etched as per the etching process used prior to Ion Vapour Deposited aluminium (IVD) being applied to the surface as a corrosion preventative (Boeing specification used on F/A-18 aircraft).

The tested coupons consisted of two different geometries as shown in Fig.1, representing both high and low stress concentration geometries. The coupons were subjected to a combat wing root bending moment spectrum that had the addition of marker loads [3] to allow for the crack-growth progression to be measured, Fig 1c.

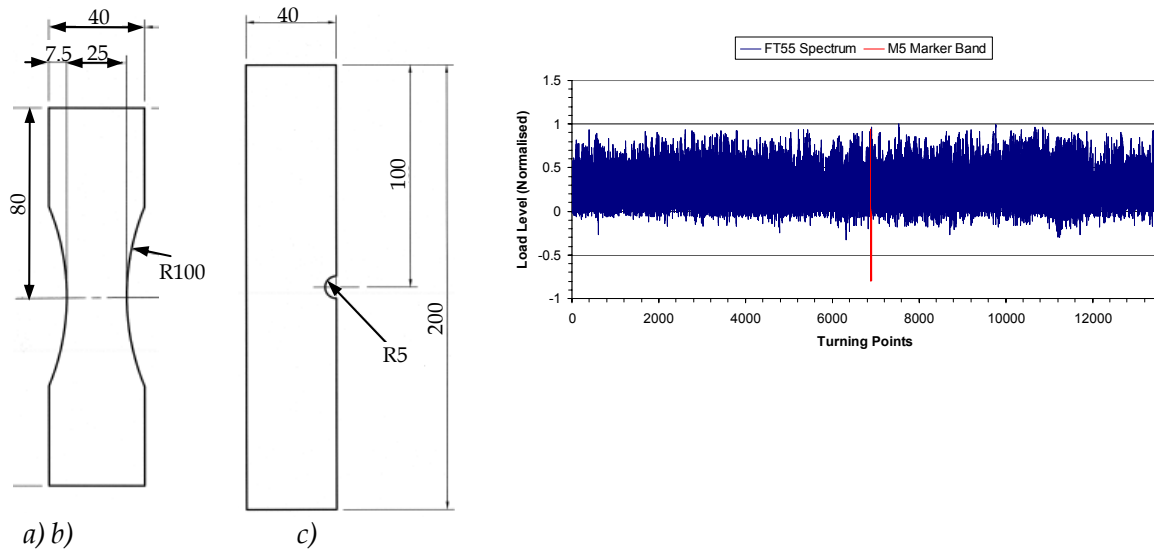


Figure. 1: Coupon geometries a) low K_t dog-bone and b) high K_t side-notched and RAAF F/A-18 wing root bending moment spectrum with marker band loads.

The results of the coupon test program showed the fatigue life of the anodised and etched coupons were shorter than those of the machined coupons, especially in the lower stress concentration geometries. A summary of the coupon fatigue test lives is shown in Fig.2.

The discontinuities that lead to the onset of each of the main fatigue cracks were examined, (Fig 3) and it was found that initiation typically occurred at either inclusions (either cracked and intact or pulled out as a result of the machining) or pits. These discontinuities were significantly larger and more frequent in the anodised coupons, where they were exclusively pits, when compared to the machined coupons, where they were mostly pulled out or damaged inclusion clusters. An investigation into the anodising process indicated the cause of the initiation features was likely the chemical cleaning process prior to anodising. The crack initiators in the pre-etched IVD coupons were also pits, although these tended to be smaller than the anodising pits.

This project was carried out to aid the RAAF to better understand the effects that surface treatments have on the fatigue performance of the aluminium alloy 7050-T7451. This effect can vary significantly between the processes used by individual aircraft manufacturers, and therefore this work may assist in the conduct of structural integrity compliance finding and technical risk assessments. This may help the RAAF to better assess and manage the safety, availability and cost of ownership of its air vehicles.

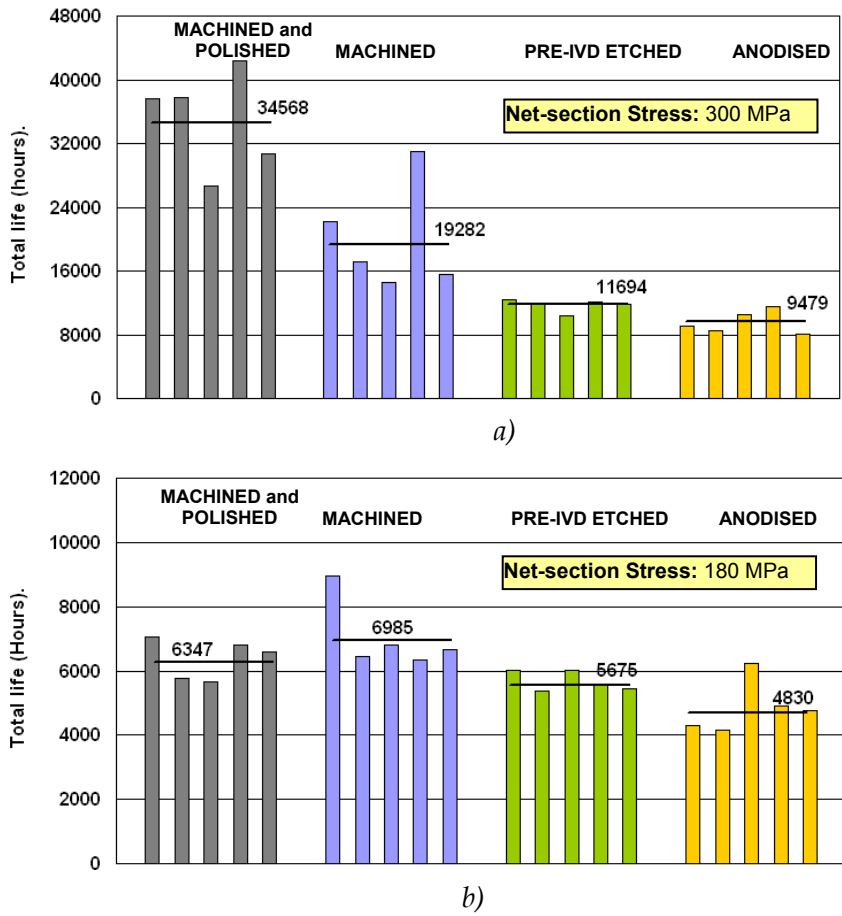


Figure 2: Fatigue test results summary for a) low Kt dogbone and b) high Kt side notched coupons

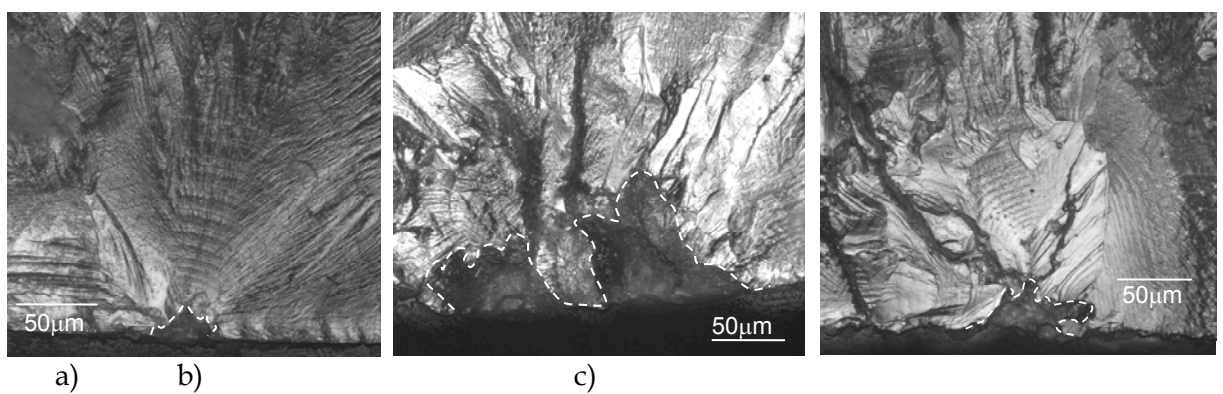


Figure. 3: Typical initial flaws (shown by the white dotted line) from : a) bare machined (unpolished) surface finish, b) anodised and c) pre-IVD etched

References:

- [1] McDonald, M., Boykett, R. and Jones, M. (draft) *Fatigue Testing of AA7050-T7451 with Various Corrosion Prevention Surface Treatments*. Defence Science and Technology Organisation Technical Report DSTO-TR-XXXX, Australia
- [2] Wanhill, R. J. H. (1995) *Damage tolerance engineering property evaluations of aerospace aluminium alloys with emphasis on fatigue crack growth*. National Aerospace Laboratory Report NLR TP 94177U, NLR Amsterdam, The Netherlands.
- [3] McDonald, M., Boykett, R. and Jones, M. (2012) *Quantitative fractography markers for determining fatigue crack growth rates in aluminium and titanium aircraft structures*. ICAS 2012, 23-28 September 2012, Brisbane, Australia.

2.1.5 New Threshold and Short Crack (TASC) Data for Improved Predictions of Combat Aircraft Fatigue Life [1] - Madeleine Burchill, Simon Barter, (DSTO), E. Amsterdam, (NLR)

Fatigue cracks in the metallic materials used in combat aircraft typically start from small surface discontinuities that are about 0.01mm deep and the growth is often well represented as being exponential in nature [2]. Thus, a significant portion of the component's fatigue life is usually spent while such cracks are very short. Crack growth predictions for combat airframe components have historically been based on fatigue data acquired using well established test methodologies, such as those in American Society for Testing and Materials (ASTM) standards, ASTM E647 [3]. However, results from such testing have been found by researchers to be deficient for calculating the lives of short cracks, using linear elastic fracture mechanics (LEFM) methodologies. Figure 1 shows a typical example for aluminium alloy 7050-T7541 (AA7050) coupons tested under a variable amplitude loading spectrum based on RAAF F/A 18 Hornet wing root bending moment measurements [4]. Commonly available "hand-book" AA7050 long crack growth data, such as that found in [5] and [6], under estimates the crack growth rate when cracks are short, and typically, as in this case, initial crack sizes need to be increased in the prediction to produce a sensible result. This is a result of the "hand-book" data has stress intensity threshold (ΔK_{th}) values that will not allow growth at the observed initial crack/discontinuity size, a_i .

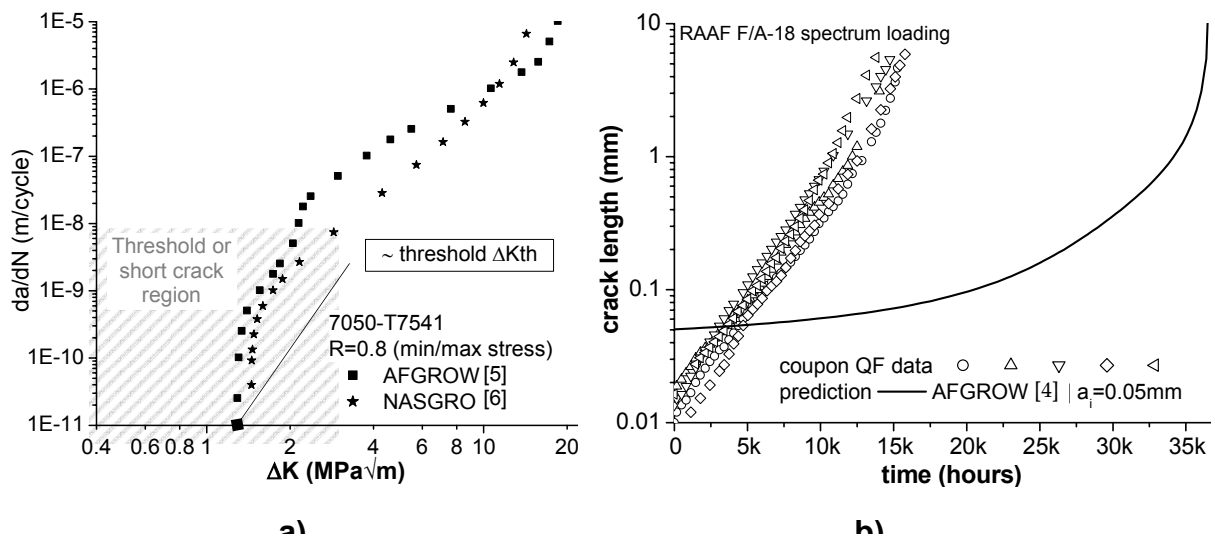


Figure. 1: AA7050 crack growth a) da/dN v ΔK data and b) analytical LEFM prediction of coupon(QF - quantitative fractography) test results with RAAF F/A-18 Hornet wing root bending moment spectrum.

The Defence Science and Technology Organisation (DSTO) & the National Aerospace Laboratory (NLR) of the Netherlands, drawing upon a wide range of experience in identifying, measuring and assessing fatigue cracks, [7 - 9] is developing tools to improve the accuracy and efficiency in generating, collecting and validating new short crack growth data. Using a combination of novel testing and advanced microscopy techniques, load sequences for fatigue testing have been selected to create visible marks that can be seen on the fatigue crack fracture surfaces of short cracks in coupons. An example of the coupon geometry and a typical test load sequence is given in Figure 2.

Optical and field emission gun scanning electron microscopy (FEGSEM) images, such as those shown in Fig. 3 show that the repeated constant amplitude block load sequence was able to generate clearly visible alternating patterns on the fracture surface for a significant range of crack sizes. Crack growth bands down to $1\mu\text{m}$ in width were measured optically, whereas, FEGSEM examination at very short ($\sim 0.2\text{mm}$) crack lengths, allowed measurements of growth bands that were as short as 20nm wide.

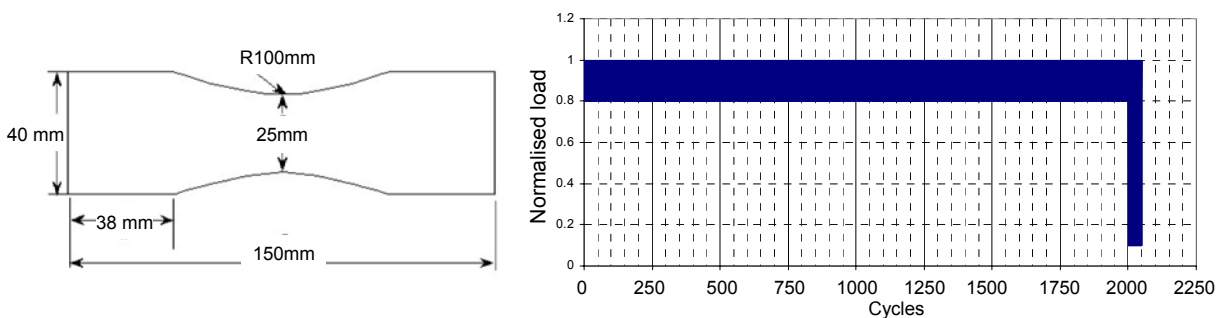


Figure. 2: Coupon geometry and test load sequence

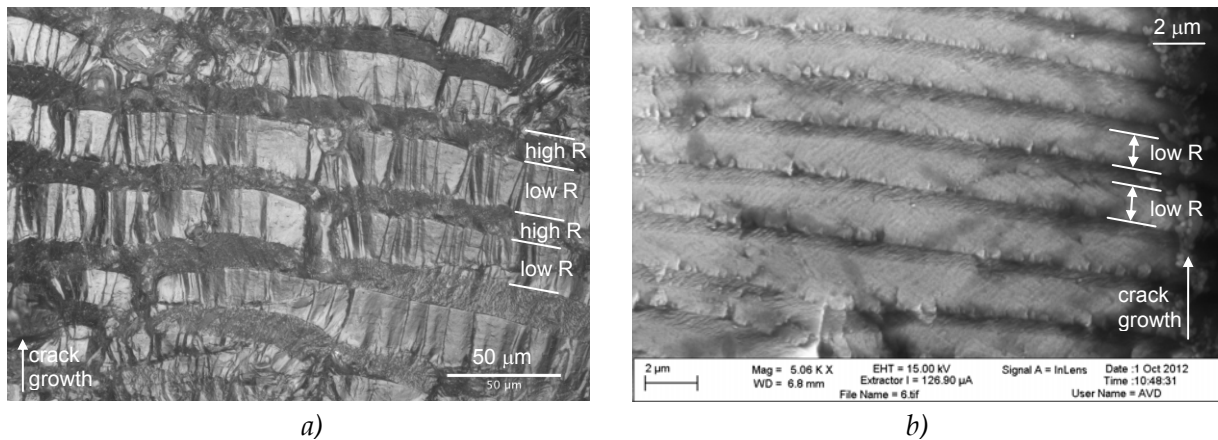


Figure.3: Growth bands (low R and high R) on AA7050 coupon taken at various magnifications (note scale) : a) via an optical microscope at crack depth $\sim 3.00\text{mm}$ and b) via the FEGSEM at crack depth $\sim 0.25\text{mm}$.

Evidence, from the crack growth band measurements, clearly shows that cracks grow at values of $\Delta K \sim 0.6 \text{ MPa}\sqrt{\text{m}}$, well below current material threshold limits; and possibly considerably lower. Two new crack growth rate material curves for AA7050 have been developed Fig. 4a. Version 1 results from a prior study, using a similar method to measure crack growth rates and “boot strapping” against several different loading spectra as reported in [10] and Version 2, based solely on the results generated during this study.

The crack growth predictions presented previously in Figure 1b were re-analysed, and are presented in Figure 4b. These results indicate that both the Version 1 and Version 2 da/dN v ΔK data curves produce more accurate predictions of the short crack growth behaviour of coupons tested under a typical combat aircraft wing root bending moment spectrum. Previously, growth in the short crack region was significantly under-estimated and hence un-conservative. These results highlight the benefits from this work via an improvement in predicting fatigue crack growth progression for a wider range of crack sizes. Future work is planned to consider additional aluminium and titanium alloys, validating against a variety of spectra and further investigating the short fatigue crack growth mechanism.

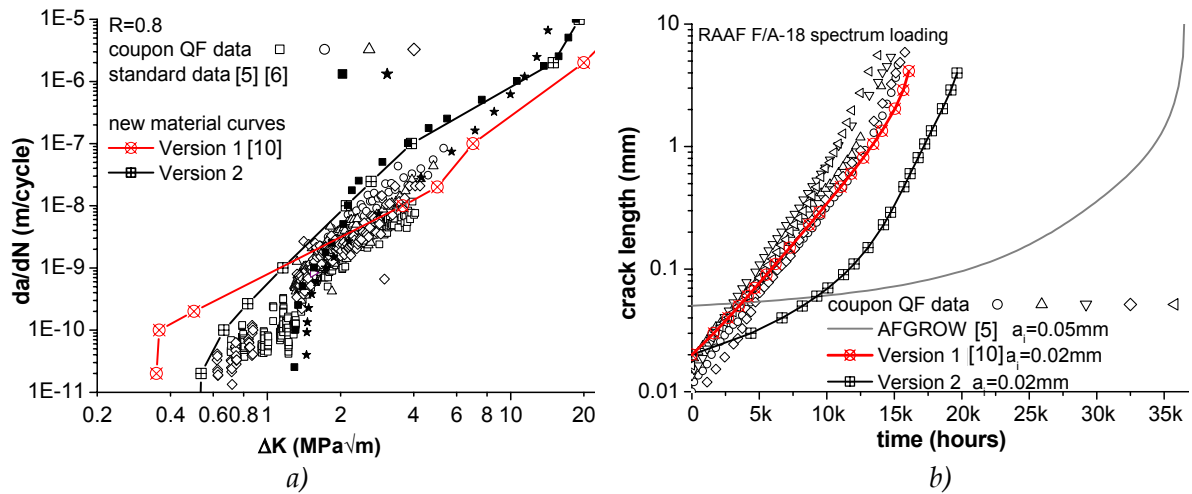


Figure. 4: New AA7050 short crack constant amplitude data used to: a) create updated da/dN v ΔK material input curves ($R=0.8$) and, b) predict fatigue crack growth in coupons tested with a RAAF combat spectrum (from Fig.1)

References:

- [1] Burchill, M., Barter, S. and Amsterdam, E. *Improved Fatigue Life Predictions for Combat Aircraft Fatigue Life from a Novel Testing Program*. AIAC Australian International Aerospace Congress 26-28 February 2013, Melbourne Australia.
- [2] Barter, S., Molent, L., Goldsmith, N. and Jones, R (2005) An experimental evaluation of fatigue crack growth. *Engineering Failure Analysis* 12 (1) 99-128.
- [3] ASTM E647-05 - Standard Test Methods for Measurement of Fatigue Crack Growth Rates. (2005). American Society for Testing and Materials.
- [4] McDonald, M., Molent, L. and Green, A. J. (2006) Assessment of fatigue crack growth prediction models for F/ A-18 representative spectra and material. DSTO-RR-0312, DSTO.
- [5] Harter, J. A. (2006) AFGROW Users Guide and Technical Manual. AFRL-VA-WP-TR-206-XXXX, WPAFB OH USA, Air Vehicles Directorate, Air Force Research Laboratory.
- [6] NASA-JSC and SwRI (2002) NASGRO® Fracture Mechanics and Fatigue Crack Growth Analysis Software, Version 4.02.
- [7] Barter, S., Wanhill, R. (2008) Marker Loads for Quantitative Fractography (QF) of Fatigue in Aerospace Alloys. NLR-TR-2008-644, The Netherlands, National Aerospace Laboratory.

[8] White, P., Barter, S. A. and Wright, C. (2009) Small crack growth rates from simple sequences containing underloads in AA7050-T7451. *International Journal of Fatigue* 31 2009 1865-1874.

[9] White, P., Barter, S. and Molent, L. (2007) Observations of crack path changes caused by periodic underloads in AA7050-T7451. *International Journal of Fatigue* 30 (7) 1267-1278.

[10] Walker, K. F., Barter, S. A. (2011) The Critical Importance of Correctly Characterising Fatigue Crack Growth Rates in the Threshold Regime. 26th ICAF Symposium 1-3 June pp 249-263

2.1.6 Development and validation of improved experimental techniques and modelling for fatigue crack growth under constant amplitude and spectrum loading - Kevin Walker, DSTO and RMIT University Australia, and James Newman, Jr., Mississippi State University USA

The ability to accurately model and understand the formation and growth of fatigue cracking in high strength metallic aircraft structures is critical in terms of both safety and cost. Structural integrity management must be based on high fidelity analysis and interpretation of test data. In order to account for uncertainty it is necessary to be conservative, which means that inspections are typically carried out more frequently, life enhancing modifications are incorporated more urgently, and retirement times are earlier than otherwise might be the case. Recent experience with the Royal Australian Air Force P-3C Maritime Patrol aircraft fleet [1] has clearly demonstrated the benefits which can be realized through improvements in the analytical models, and the fundamental material characterization data behind them.

In the case of fatigue crack growth analysis, the baseline constant amplitude rate characterization data are crucially important. The threshold and near threshold region are particularly important because a large portion of the total life is spent in that regime. Traditionally the baseline rate data are determined from testing on either Compact Tension (C(T)) or Middle Tension (M(T)) in accordance with methods described in ASTM Standard Test Method E647 [2]. Data in the threshold region are often derived using a tension pre-cracking followed by load reduction method. Ohata et al. [3] and Minakawa and McEvily [4] showed a rise in the crack-closure levels as the threshold is approached using load reduction methods similar to the ASTM E647 technique. The behaviour was attributed to roughness- and fretting-debris-induced crack-closure effects. Newman [5, 6] and McClung [7] also showed a rise in crack closure associated with the load-reduction method using strip-yield and finite-element models respectively. The models showed that the test method exhibits anomalies due to load-history effects from residual-plastic deformations.

Compression pre-cracking methods have been demonstrated [8] to avoid many of the problems associated with the ASTM E647 tension pre-cracking load reduction technique. Some materials are more sensitive than others. 7050-T7451 for example was found to be very sensitive, but 7075-T651 was found to not be significantly affected [8]. Data for 7050-

T7451 generated by the compression pre-cracking method were compared by Walker and Barter [9] with naturally occurring (no notch or pre-crack) short crack data measured using a novel marker load and Quantitative Fractography (QF) method. The two separately derived data sets were in very good agreement. The data were then used with the analytical fatigue crack closure based code FASTRAN to conduct an analysis for crack growth under variable amplitude spectrum loading. The analytical results correlated very well with the test data [10].

The material of concern in the wing structure of the P-3C aircraft is 7075-T651 extrusion. Many of the coupons tested in support of the P-3C program were however manufactured from 7075-T6 sheet. Comparisons of test results suggested that the -T6 and -T651 behaviour is very similar, but it was considered that a detailed and comprehensive set of fundamental baseline testing of the -T6 material should be carried out to verify that assertion. This also provided an opportunity to further develop the overall modelling, and in particular to evaluate an updated and improved version of the FASTRAN code [11].

Another very important issue is to determine whether the pre-cracking method (tension or compression) has any influence on the subsequent fatigue crack propagation under variable amplitude spectrum loading. Materials which have been found to exhibit sensitivity in the constant amplitude case such as 7050-T7451 have been found to have no such sensitivity when the subsequent fatigue cycling is under a spectrum loading [12]. Testing on that matter has been conducted using both C(T) and M(T) specimens and the results suggest that as for the 7050 there is very little, if any, effect for the 7075-T6/T651 alloys.

The testing of 7075-T6 C(T) coupons confirmed that the properties are very similar to the 7075-T651 material. Baseline Compression Pre-crack Constant Amplitude (CPCA) and Load Reduction (CPLR) tests were conducted for a range of stress ratios from threshold through to fracture. Spike overload tests and variable amplitude spectrum load tests with both compression and tension pre-cracking were also conducted. An improved material characterization model was developed and evaluated using the updated version of FASTRAN, Version 5.36 [11]. The model was then evaluated against a variety of spectrum loading examples from Australian and US tests on 7075-T6/T651 M(T) coupons. The analytical results compared very well with the test data. An example of the spike overload correlation is shown in Figure 1, and an example for the spectrum loading is shown in Figure 2.

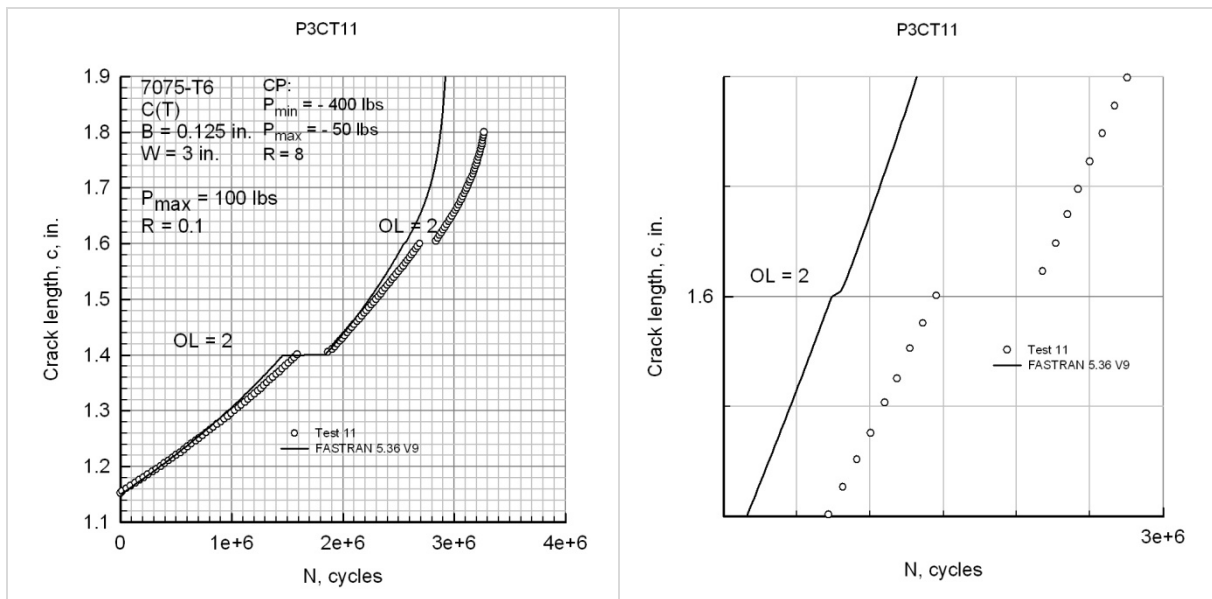


Figure 1 : Results comparison for Factor 2 spike overload test. Plot on right shows detail for the second factor 2 overload.

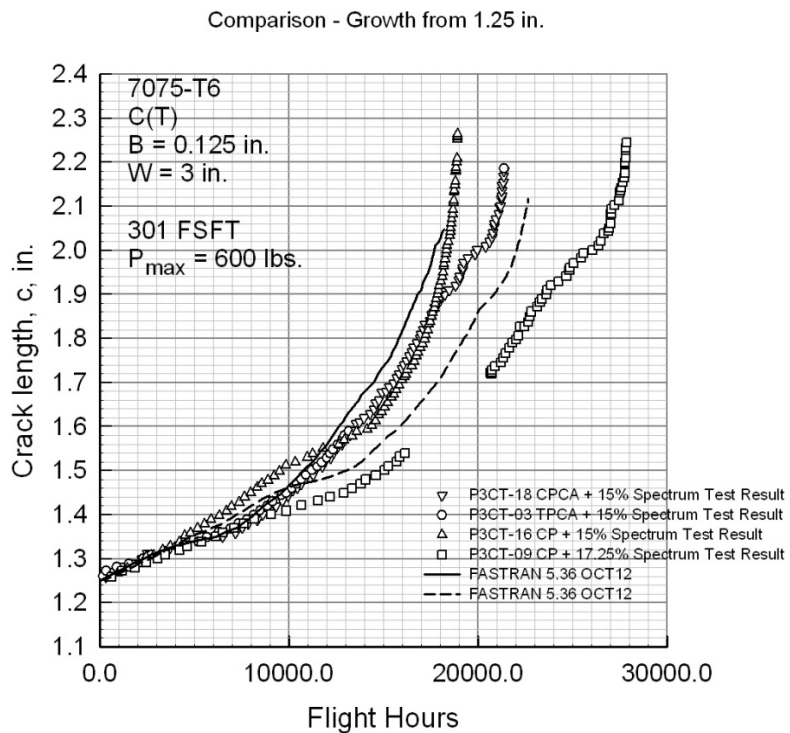


Figure 2 : 600 lbs scaling level spectrum crack growth comparisons

References:

1. Walker, K., Walliker, A., Meadows, L., and Matricciani, E., *A comprehensive testing and analytical model development program to assure ongoing structural integrity of the aging Australian P-3C fleet*, in *Aircraft Airworthiness and Sustainment Conference*. 2012: Baltimore, MD, USA.
2. Anon, *Standard Test Method for Measurement of Fatigue Crack Growth Rates*, ASTM, Editor. 2011, ASTM International.
3. Ohta, A., and Sasaki E., *A method for determining the stress intensity threshold level for fatigue crack propagation*. *Eng Fract Mech*, 1977. **9**(3): p. 655-62.
4. Minakawa, K., and McEvily, A.J. *On near-threshold fatigue crack growth in steels and aluminum alloys*. in *International Conference on Fatigue Thresholds*. 1981. Stockholm, Sweden.
5. Newman, J.C., Jr., *A nonlinear fracture mechanics approach to the growth of small cracks. Behaviour of short cracks in airframe components*, 1983(AGARD CP-328): p. P. 6.1-6.27.
6. Newman, J.C., Jr., *Analysis of fatigue crack growth and closure near threshold conditions*. ASTM STP-1372, 2000: p. 227-51.
7. McClung, R.C., *Analysis of fatigue crack closure during simulated threshold testing*. ASTM STP-1372, 2000: p. 209-26.
8. Newman Jr, J.C. and Y. Yamada, *Compression precracking methods to generate near-threshold fatigue-crack-growth-rate data*. *International Journal of Fatigue*, 2010. **32**(6): p. 879-885.
9. Walker, K.F., and Barter, S.A., *The critical importance of correctly characterising fatigue crack growth rates in the threshold regime*, in *International Committee on Aeronautical Fatigue*. 2011: Montreal, Canada.
10. Newman, J.C., Jr., *FASTRAN II - A fatigue crack growth structural analysis program*. 1992, NASA.
11. Newman, J.C., Jr., *FASTRAN. A fatigue crack growth life prediction code based on the crack-closure concept. Version 5.3. User Guide*. 2010, Fatigue and Fracture Associates LLC.
12. Newman, J.C., Jr., Shaw, J.W., Annigeri, B.A., and Zeigler, B.M. *Fatigue and crack growth in 7050-T7451 aluminium alloy under constant- and variable-amplitude loading*. in *Turbine Technical Conference and Exposition ASME Turbo Expo*. 2012. Copenhagen, Denmark.

2.1.7 A new approach to determine near-threshold fatigue crack growth rate properties in high-strength coarse grain titanium alloy with rough and torturous fatigue surfaces - Kevin Walker, (DSTO and RMIT University Australia), and James Newman, Jr., (Mississippi State University USA)

Fatigue crack growth rate properties are typically determined by experimental methods in accordance with ASTM Standard E647 [1]. These traditional methods use standard notched specimens which are pre-cracked under cyclic tensile loads before the main test. The data which are produced using this approach have been demonstrated elsewhere to be flawed [2], particularly in the threshold region where load-reduction methods are also required. Coarse grained materials which exhibit rough and torturous fatigue surfaces have been

observed to be strongly affected [3]; in part because the anomalies caused by crack closure and roughness induced closure become more important. The focus of the work reported in this paper was to develop and validate a method to determine the fatigue crack growth rate properties from threshold through to fracture for coarse-grained, β -annealed, titanium alloy Ti-6Al-4V ELI thick plate material. New approaches which differ from the ASTM Standard included compression pre-cracking, load reduction starting from a lower load level, and continuing the test beyond rates where crack growth would otherwise be considered below threshold. Two load reduction methods were also investigated; the ASTM method [1], and a method proposed by Wu *et al.* [4], where the load is reduced with crack growth such that the crack mouth opening displacement is held constant, in an attempt to avoid remote closure. Constant amplitude fatigue crack growth rate data were produced from threshold to fracture for the titanium alloy at a variety of stress ratios. Spike overload tests were also conducted. These data were then used to develop an improved analytical model to predict crack growth under spectrum loading and the predictions were found to correlate well with further test results.

Figure 1 shows an example of the rough nature of the fatigue surface, including one significant asperity of about 1.5 mm. That asperity coincided with a significant rise in closure (ratio of opening load to max load) from about 0.4 to 0.6 at a crack length to width aspect ratio of about 0.35 as shown in Figure 2. Despite the limitation of not modelling roughness induced closure explicitly, a modelling approach using FASTRAN was shown to correlate well with crack growth testing under spectrum loading under a mini-Falstaff sequence as shown in Figure 3. This work makes a strong contribution toward a better understanding of fatigue crack growth mechanisms in a complex material.



Figure 1: Crack surface on specimen 4A showing significant 1.5 mm asperity at a crack length of about 13-15 mm.

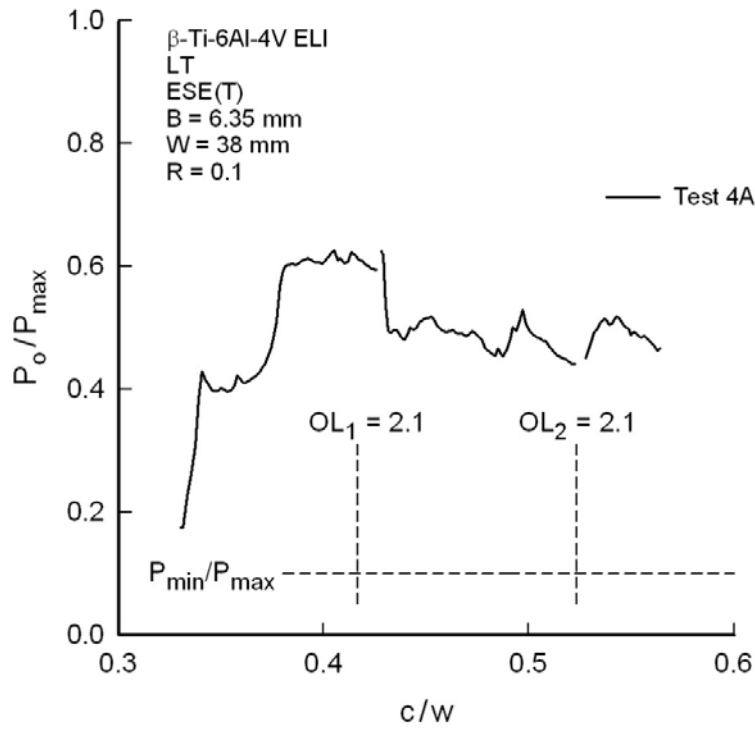


Figure 2: Measured crack opening loads at R=0.1 CPCA with overloads

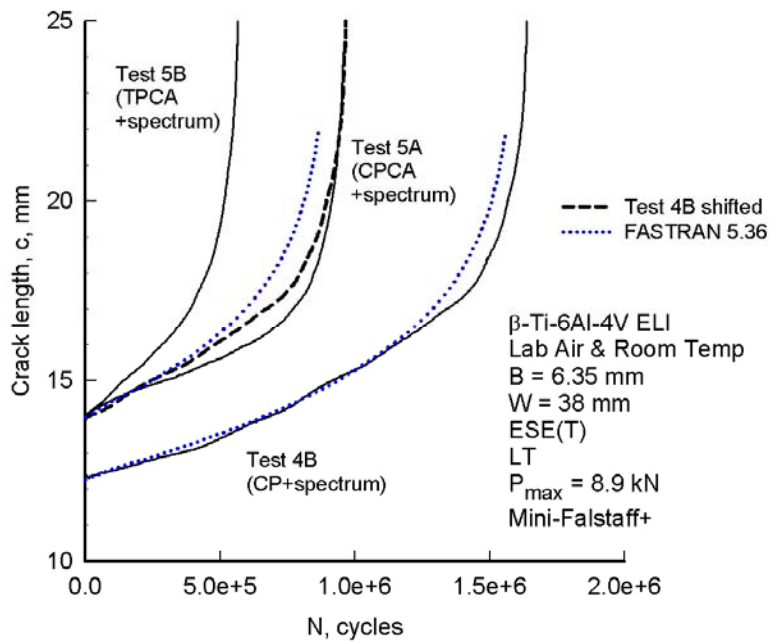


Figure 3: Comparison of test results and FASTRAN analysis for Variable Amplitude Spectrum loading case under mini-Falstaff+

References:

1. Anon, *Standard Test Method for Measurement of Fatigue Crack Growth Rates*, ASTM, Editor. 2011, ASTM International.
2. Newman, J.C., Jr., and Yamada, Y., *Compression precracking methods to generate near-threshold fatigue-crack-growth-rate data*. *International Journal of Fatigue*, 2010. **32**: p. 879-885.
3. Newman, J.C., Jr., Yamada, Y., and Newman, J. A., *Crack-closure behaviour of 7050 aluminum alloy near threshold conditions for wide range in load ratios and constant K_{max} tests*. *Journal of ASTM International*, 2010. **7**(4).
4. Wu, X.J., Wallace, W., and Koul, A.K., *A new approach to fatigue threshold*. *Fatigue and Fracture of Engineering materials and Structures*, 1995. **18**(7/8): p. 833-844.

2.1.8 The Harman-Schjive Variant for the Calculation of Crack Growth - Rhys Jones (Monash University), Loris Molent and Simon Barter (DSTO)

The majority of the life of metallic aircraft structures is spent in growing a physically short crack (deep ≤ 1 mm deep) which nucleates from small discontinuities (approximately 0.01mm deep) inherent in the material or induced during production [1, 2].

It has been shown that the crack growth rate in a large range of metallic materials fitted a variant of the Hartman-Schjive equation [3] where da/dN is a function of $(\Delta K - \Delta K_{thr})^\alpha$, where ΔK_{thr} is a parameter that reflects the apparent fatigue stress intensity threshold of the material, and α is approximately 2 [4]. For the case of AA7050-T7451 aluminium alloy the same equation was shown to fit both long and short crack growth data once the appropriate ΔK_{thr} was chosen for each specific data set (see [4] and Figures 1 to 2). This equation has been used to produce accurate predictions of the fatigue crack growth in AA7050-T7451 aluminium alloy specimens with both a low and high stress concentration subjected to two combat aircraft loading spectra. The analyse of the growth of small cracks, with initial depths that varied from approximately 2 to 9 μm , at a 6.35mm diameter fastener hole in 10mm thick AA7050-T7451 specimens tested under a typical RAAF F/A-18 Hornet operational load spectrum (of approximately 325 simulated flight hours) with a peak (net section) stress of 155 MPa [5] is shown in Figure 3.

Thus, it is postulated that if long crack data are fitted to the variant of the Hartman-Schjive equation then accurate predictions can be made in the short crack regime for a wide range of materials.

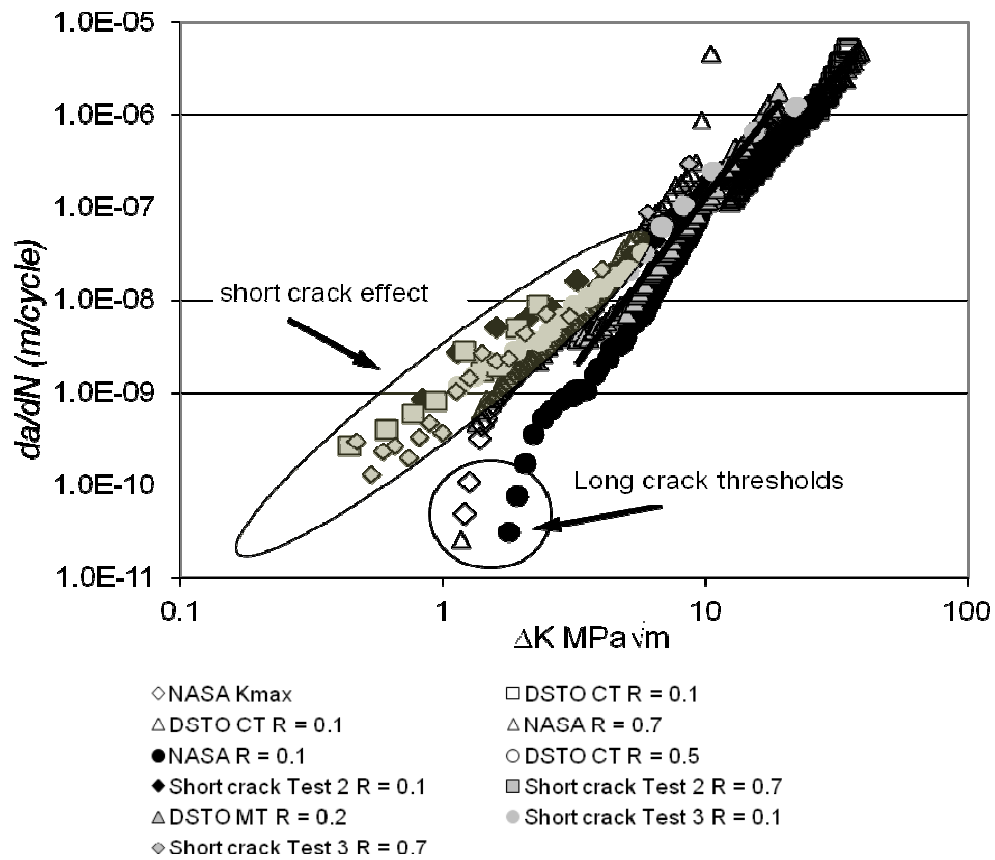


Figure 1: Comparison of the various da/dN versus ΔK test data for AA7050-T7451 [4]

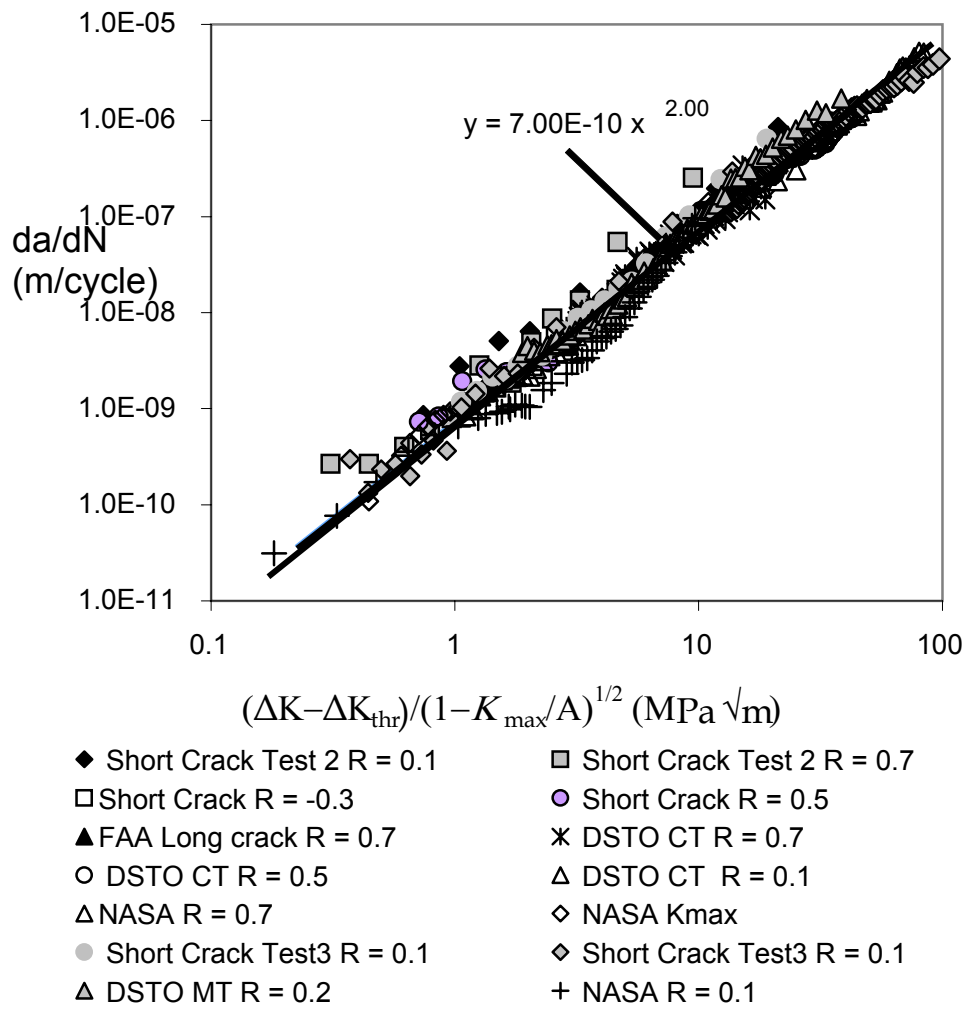


Figure 2: Long and short crack data for AA7050-T7451.

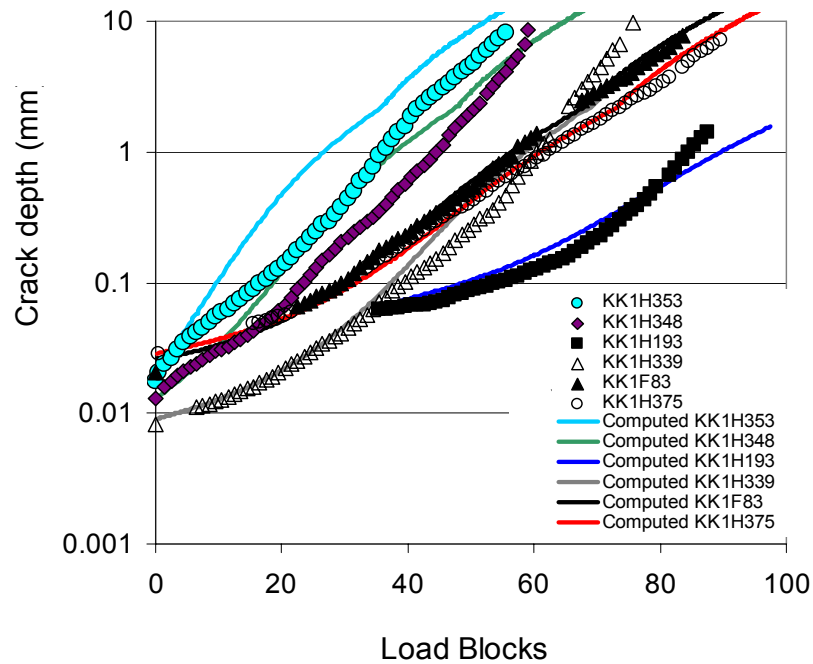


Figure 3. Measured and computed crack depth histories under a RAAF operational load spectrum where one block represents approximately 325 flight hours. Each of the data points was measured using quantitative fractography. They represent a crack increment caused by one block of loading.

References:

1. Molent, L. Fatigue Crack growth from flaws in combat aircraft. International Journal of Fatigue 32 (2010) 639-649.
2. Barter SA, Molent L, Wanhill RJH. Typical fatigue-initiating discontinuities in metallic aircraft structures, J Fatigue 2012 ; 41:11-22.
3. Hartman, A. and Schijve J., The effects of environment and load frequency on the crack propagation law for macro fatigue crack growth in aluminium alloys. Engineering Fracture Mechanics 1970; 1/ 4: 615-631.
4. Jones R, Molent L., Walker K., Fatigue crack growth in a diverse range of materials, International Journal of Fatigue 2012; 40: 43-50.
5. Huynh J., Molent L., and Barter S., Experimentally derived crack growth models for different stress concentration factors. International J Fatigue 2008; 30(10-11):1766-1786.

2.1.9 The Lead Crack Fatigue Lifting Framework - Loris Molent and Simon Barter (DSTO) and Russell Wanhill (NLR)

A fatigue lifting framework using a lead crack concept has been developed by the DSTO for metallic primary airframe components [1]. The framework is based on years of detailed inspection and analysis of fatigue cracks in many specimens and airframe components, and is an important additional tool for determining aircraft component fatigue lives in the Royal Australian Air Force (RAAF) fleet. Like the original Damage Tolerance (DT) concept developed by the United States Air Force (USAF), this framework assumes that fatigue

cracking begins as soon as an aircraft enters service. However, there are major and fundamental differences. Instead of assuming initial crack sizes and deriving early crack growth behaviour from back-extrapolation of growth data for long cracks, the DSTO framework uses data for real cracks growing from small discontinuities inherent to the material and the production of the component [2]. Furthermore, these data, particularly for lead cracks, are characterized by exponential crack growth behaviour. Because of this common characteristic, the DSTO framework can use lead crack growth data to provide reasonable (i.e. not overly conservative) lower-bound estimates of typical crack growth lives of components, starting from small natural discontinuities and continuing up to crack sizes (thus encompassing short-to-long crack growth) that just meet the residual strength requirements. Scatter factors based on engineering judgement are then applied to these estimates to determine the maximum allowable service life (safe life limit).

References:

1. Molent L, Barter SA and Wanhill RJH. The Lead Crack Fatigue Lifting Framework, *Int J Fatigue*; 33 (2011) 323–331.
2. Barter SA, Molent L, Wanhill RJH. Typical fatigue-initiating discontinuities in metallic aircraft structures, *Int J Fatigue* 2012 ; 41:11-22.

2.1.10 A New Closed-Form Stress Intensity Factor Solution For Equal Cracks Emanating From A Central Circular Hole In A Rectangular Plate - Witold Waldman (DSTO)

The Structural and Damage Mechanics Group of DSTO has been undertaking computational work into calculating stress intensity factors for situations involving multi-site fatigue damage [1]. This is an issue of critical interest in relation to the fatigue life management of ageing aircraft structures, and the topic of probabilistic failure analysis of structures is receiving continued attention. Some new results have been developed concerning a closed-form solution for the stress intensity factor associated with equal (symmetrical) collinear through-thickness cracks emanating from a central circular hole in a uniaxially-loaded finite two-dimensional plate (see Figure 1).

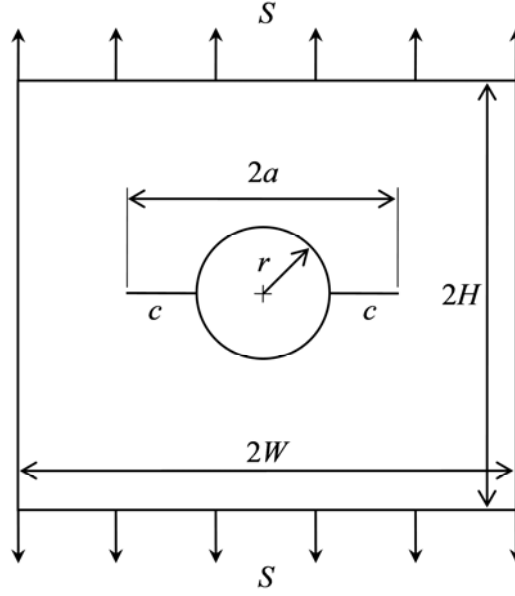


Figure 1: Geometry for two equal collinear through thickness cracks emanating from a central circular hole in a finite-width plate subjected to a uniform uniaxial remote tension stress.

As only limited handbook solutions exist for this particular configuration (eg [2]), a modified two-dimensional boundary element technique based on distributed dislocations [3] was used to study the behaviour of these two interacting cracks. The particular implementation that was used consisted of the FADD2D code [4], and during benchmarking it produced stress intensity factor results that were in excellent agreement with the highly-accurate solutions obtained by Newman [2].

The new closed-form solution for computing the Beta factor F_c associated with a pair of equal through cracks of length c emanating from a central hole of radius r in a long strip of finite width $2W$ is presented in Equation 2.

$$K = S\sqrt{\pi c} F_c \quad (1)$$

$$F_c = F_\infty F_h F_w F_l$$

$$F_\infty = 1 + \frac{1}{2\left(\frac{c}{r}\right)^2 + 1.93\left(\frac{c}{r}\right) + 0.539} + \frac{1}{2\left(\frac{c}{r} + 1\right)} \quad (2)$$

$$F_h = \sqrt{\sec\left(\frac{\pi r}{2W}\right)} \quad F_w = \sqrt{\sec\left(\frac{\pi r}{2W}\left(1 + \frac{c}{r}\right)\right)} \quad F_l = \sqrt{\cos\left(\frac{\pi r}{2W}\left(\frac{c}{W-r}\right)\right)}$$

The equation for F_c involves a new boundary correction factor, F_l , that accounts for the effect of the uncracked ligament length, $l = W - r$, in combination with the size of the hole relative to the plate width, r/W . For any given combination of plate width and hole size, it is noted that the effect of F_l decreases with increasing crack length. The three remaining

geometry corrections factors, F_∞ (from [5]), F_h (from [6, 7]) and F_w (from [6]), have previously been reported in the literature.

The accuracy of Equation 2 has been compared to numerical results obtained using the FADD2D program for a plate of aspect ratio $H/W = 8$. It has been found to be within 1% for $0 \leq r/W \leq 0.25$ and $c/(W-r) \leq 0.8$, while providing reasonably accurate results in the range $0.25 < r/W \leq 0.5$ and $0.8 < c/(W-r) \leq 0.9$ (see Figure 2).

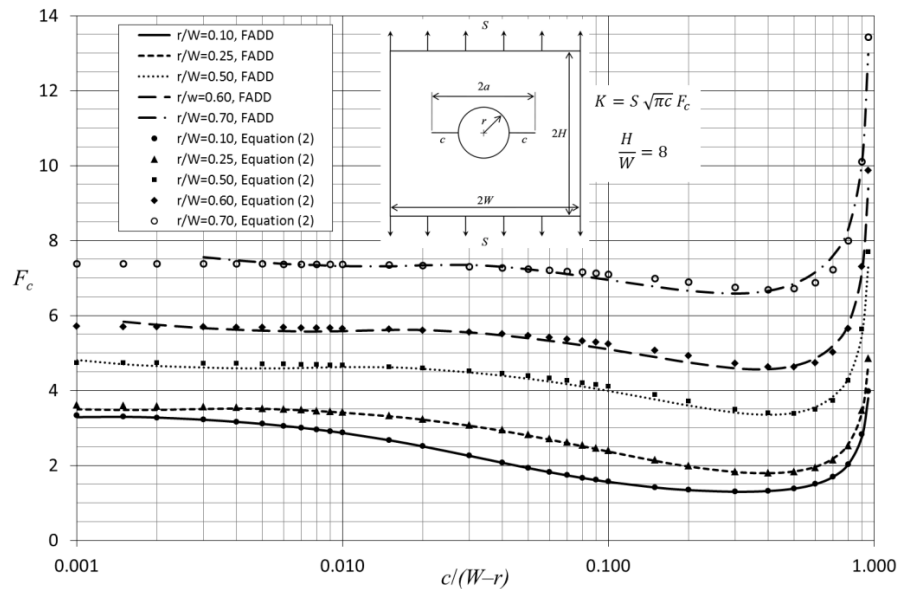


Figure 2: Beta factors F_c for two equal collinear through cracks emanating from a central circular hole in a finite-width plate subjected to a uniform uniaxial remote tension stress for various r/W ratios.

References:

- 1 W Waldman. Beta factors for collinear asymmetrical cracks emanating from an offset circular hole in a rectangular plate. DSTO Minute, File B2/129/PT4, 23 January 2013.
- 2 JC Newman Jr. An improved method of collocation for the stress analysis of cracked plates with various shaped boundaries. NASA TN D-6376, August 1971.
- 3 C Chang, ME Mear. A boundary element method for two dimensional linear elastic fracture analysis. International Journal of Fracture, Vol 74, 1995, pages 219–251.
- 4 JC Newman Jr, C Chang, L Xiao, ME Mear, VJ Kale. FADD2D: Fracture Analysis by Distributed Dislocations, Version 1.0, User Guide for Personal Computers with Demonstration Example. October 2006.
- 5 J Schijve. Stress intensity factors of hole edge cracks. Comparison between one crack and two symmetric cracks. International Journal of Fracture, Vol 23, 1983, pages R111–R115.
- 6 JC Newman Jr. Predicting failure of specimens with either surface cracks or corner cracks at holes. NASA Technical Note TN D-8244, June 1976.
- 7 CE Feddersen. Discussion: Plane Strain crack toughness testing of high strength metallic materials (by WF Brown Jr and JE Srawley). In: Plane Strain Crack Toughness Testing, ASTM STP 410, pages 77–79, 1966.

2.1.11 Beta Factors For Collinear Asymmetrical Cracks Emanating From An Offset Circular Hole In A Rectangular Plate - Witold Waldman (DSTO)

Multi-site fatigue damage is an issue of concern in the probabilistic risk assessment and fatigue life management of aircraft structures. This has led to a research activity being undertaken in the Structural and Damage Mechanics Group of the Air Vehicles Division in DSTO to investigate the interactions that occur between multiple growing fatigue cracks [1]. The specific idealised scenario of interest is a two-dimensional one, consisting of asymmetrical collinear through-thickness cracks emanating from an offset circular hole in a uniaxially-loaded finite plate (see Figure 1). Here the stress intensity Beta factors intrinsically include interaction effects between the left-hand and right-hand cracks, as well as proximity effects related to the distance of the hole and the cracks from the edges of the plate.

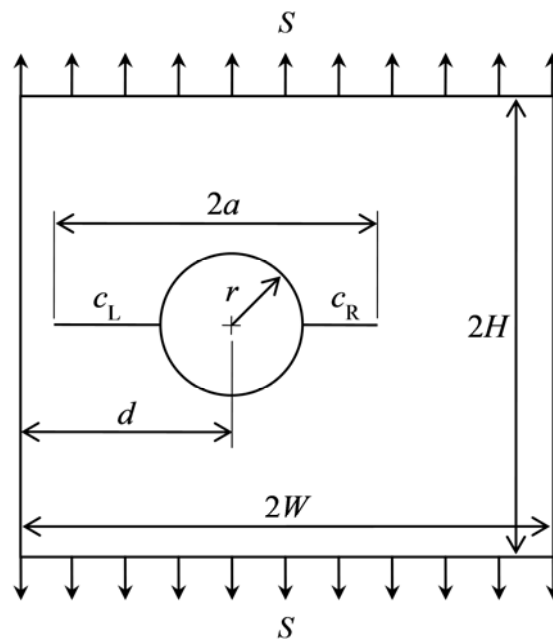


Figure 1: Geometry for two asymmetrical collinear cracks emanating from an offset circular hole in a finite-width plate subjected to a uniform uniaxial remote tension stress.

As no prior handbook solutions exist for the configuration of interest, a general purpose numerical approach was used consisting of a modified two-dimensional boundary element technique based on distributed dislocations [2]. The particular implementation was the FADD2D code [3]. It was benchmarked against a number of known published solutions for similar geometries, including: equal cracks emanating from a central hole in a finite plate [4], equal and unequal cracks emanating from a hole in an infinite plate [5], and unequal cracks emanating from an offset hole in a finite plate. The results obtained using FADD2D were found to be in excellent agreement with the known solutions. This provided confidence in the accuracy of the results that were subsequently to be obtained for the problem of interest.

Beta factors for the two unequal cracks were computed over the following ranges of parameters (subject to physical constraints): $0.1 \leq d/W \leq 1.0$, $0.05 \leq r/W \leq 0.2$, $0.01 \leq c_L/r \leq 2.0$ and $0.01 \leq c_R/r \leq 2.0$. A H/W ratio of 4 was used to define a rectangular plate, one that can be considered to be nominally large relative to the largest hole size of $r/W = 0.20$. Some typical Beta factors as obtained for the left-hand crack for $d/W = 0.5$ and $r/W = 0.2$ are shown in Figure 2(a), while those for the associated right-hand crack are shown in Figure 2(b).

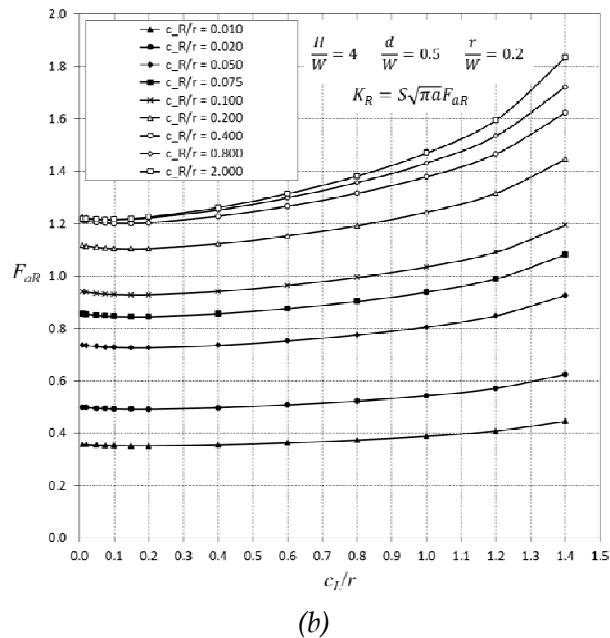
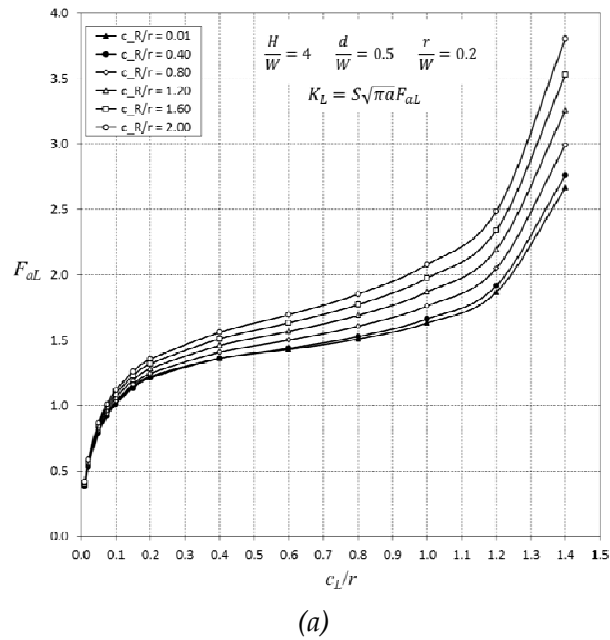


Figure 2: Beta factors F_{aL} for the left-hand crack and F_{aR} for the right-hand crack for two unequal collinear through cracks emanating from an offset circular hole in a finite-width plate subjected to a uniform uniaxial remote tension.

References:

- 1 W Waldman. Beta factors for collinear asymmetrical cracks emanating from an offset circular hole in a rectangular plate. DSTO Minute, File B2/129/PT4, 23 January 2013.
- 2 C Chang, ME Mear. A boundary element method for two dimensional linear elastic fracture analysis. *International Journal of Fracture*, Vol 74, 1995, pages 219–251.
- 3 JC Newman Jr, C Chang, L Xiao, ME Mear, VJ Kale. FADD2D: Fracture Analysis by Distributed Dislocations, Version 1.0, User Guide for Personal Computers with Demonstration Example. October 2006.
- 4 JC Newman Jr. An improved method of collocation for the stress analysis of cracked plates with various shaped boundaries. NASA TN D-6376, August 1971.
- 5 DP Rooke, J Tweed. Opening-mode stress intensity factors for two unequal cracks at a hole. Royal Aircraft Establishment, Technical Report 79105, August 1979.
- 6 JA Harter, D Taluk. Life analysis development and verification, Delivery Order 0012: Damage tolerance application of multiple through cracks in plates with and without holes (Final Report for 25 August 1997 – 31 July 2002). AFRL-VA-WP-TR-2004-3112, October 2004.

2.1.12 Elasto-Plastic Contact Analysis Using Abaqus Of The K_I Of A Hole Fitted With Neat-Fit Fastener For LIF Hawk Filled-Hole Coupon - Witold Waldman (DSTO)

A 3D elasto-plastic finite element analysis (FEA) has been undertaken to study the effects of contact interaction between a neat-fit unloaded titanium alloy pin and a fastener hole in an aluminium alloy plate loaded in uniaxial tension [1]. The idealised configuration is shown in Figure 1, and is representative of a Lead-In Fighter (LIF) Hawk Filled Hole Coupon, which is typical dog-bone specimen, with a plate thickness of 6.0 mm and a centrally-located hole with a nominal hole diameter of 6.35 mm. This coupon is being used for validation of test interpretation activities associated with the BAE Systems LIF Hawk full-scale fatigue test. The coupon has previously been the subject of a detailed linear-elastic contact analysis [2].

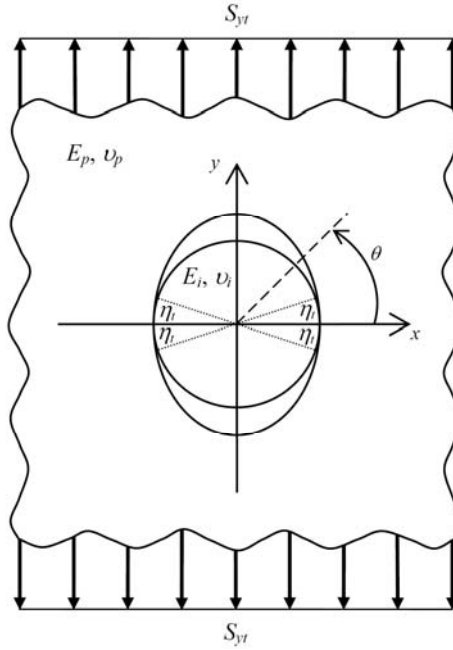


Figure 1: Geometrical configuration of a plate with a hole loaded by a uniaxial tensile stress S_{yt} at infinity showing the contact angle η_t between the plate and the circular disk insert.

The elasto-plastic 3D analysis was conducted using the Abaqus/Standard 6.11-1, and $\frac{1}{4}$ -symmetry was utilised in order to reduce computation time. The maximum applied load was $P = 35$ kN, and the stress distribution around the hole was found to remain linear-elastic up to a load of $P = 15.75$ kN, beyond which plastic deformation began to occur.

The typical variation of the normalised tangential stress, σ_{tt}/S_{yt} , around the boundary of the hole at the mid-plane of the plate and a range of tension load levels is shown in Figure 2. The response obtained here was found to be qualitatively similar to that reported in [3] and [4]. At any given load level, the peak value of σ_{tt}/S_{yt} corresponds to the K_t for the hole-pin combination. At load levels $P \leq 15.75$ kN, where the response is linear-elastic, the tensile K_t was determined to be $K_t = 3.005$ at a point lying on the mid-plane of the coupon at an angle of $\theta = \eta_t = 19.6^\circ$. This value of K_t is about 11% lower than the result obtained for the open-hole case. At $\theta = 0^\circ$ it was determined that $K_t = 2.715$, which is about 10% lower than that which occurs at $\theta = \eta_t$. When $P > 15.75$ kN, material plasticity begins to come into play, and the peak value of σ_{tt}/S_{yt} decreases with increasing levels of plasticity. Interestingly, the location of the peak value remains constant at $\theta = 19.6^\circ$. At the maximum load $P = 35$ kN, the tensile K_t at the mid-plane was $K_t = 2.377$ at $\theta = \eta_t = 19.6^\circ$, while at $\theta = 0^\circ$ it was found that $K_t = 1.943$, which is 18% lower than at $\theta = \eta_t$. As the peak tangential stress occurs at the $\theta = \pm 19.6^\circ$ and $\theta = \pm 160.4^\circ$ locations around the hole boundary, fatigue cracking in the coupon is expected to initiate in the vicinity of those locations, rather than at the $\theta = 0^\circ$ and $\theta = 180^\circ$ positions.

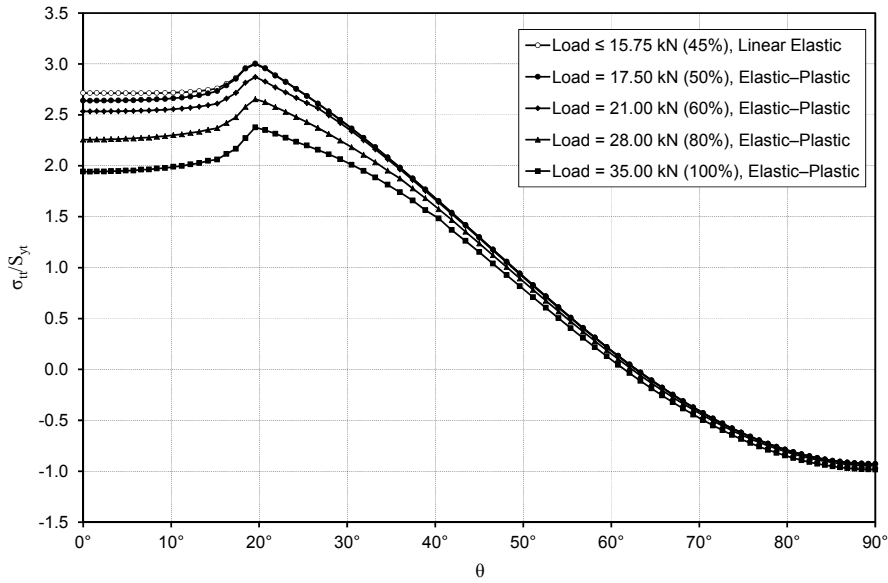


Figure 2: Normalised tangential stress around the hole boundary hole at the mid-plane of the plate for the filled-hole case and a range of tension load levels, corresponding to linear-elastic and elasto-plastic response regimes.

The von Mises stress in the plastic zone around the hole boundary under hole-pin contact conditions for the maximum applied load of $P = 35$ kN is shown in Figure 3(a). The colour contours have been configured to display only those von Mises stresses that exceed the cyclic proportional limit of the aluminium alloy coupon material of $\sigma_{cpl} = 276.89$ MPa. At the maximum load, the depth of the plastic zone, d_p , is approximately 76% of the hole radius, with $d_p/r = 0.76$ ($d_p = 2.42$ mm) at the mid-plane surface and $d_p/r = 0.63$ ($d_p = 2.00$ mm) at the free surface. The total area of the plastic zones at the mid-plane surface is $A_p = 20.2$ mm², which is equivalent to 63.9% of the area of the hole. In comparison, it was found that the area of the plastic zones at the free surface is about 19% smaller than at the mid-plane surface.

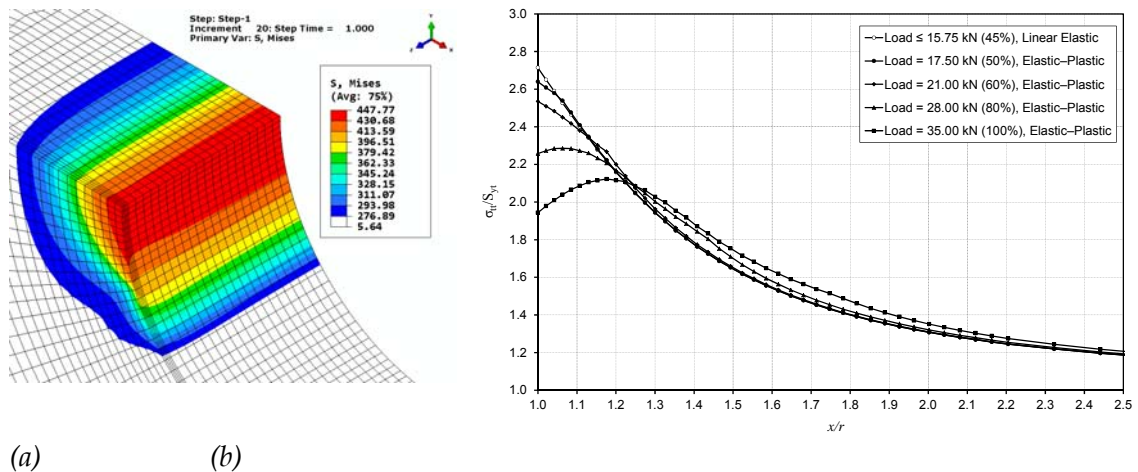


Figure 3: (a) Von Mises stress in the plastic zone around the hole boundary in the coupon at the maximum applied load, $P = 35$ kN. (b) Normalised tangential stress as a function of radial distance away from the edge of the hole at the $\theta = 0^\circ$ location at the plate mid-plane.

The variation of the normalised tangential stress σ_{tt}/S_{yt} versus the distance from the hole centre normalised to the hole radius, x/r , is shown in Figure 3(b) for $1.0 \leq x/r \leq 2.5$ and a range of load levels. σ_{tt}/S_{yt} decays away quickly with increasing distance from the hole edge. By $x/r = 2.0$ the tangential stress has been reduced to between 32% and 35% of the gross-section average stress. The peak value of σ_{tt}/S_{yt} reduces with increasing plastic deformation, and for higher load levels the peak occurs within the body of the plate material. This results in a redistribution of stress, such that each elasto-plastic σ_{tt}/S_{yt} curve crosses over the linear-elastic response curve and has some portion of its response lying above the linear-elastic response curve. At the maximum load level of $P = 35$ kN, the peak value $\sigma_{tt}/S_{yt} = 2.122$ occurs at $x/r = 1.18$, which is slightly in from the edge of the hole, while at the hole surface ($x/r = 1.00$) the stress is $\sigma_{tt}/S_{yt} = 1.943$, which is about 8% lower.

References:

- 1 W Waldman. Elasto-plastic contact analysis using Abaqus of the K_t of a hole fitted with neat-fit fastener for LIF Hawk filled-hole coupon. DSTO Minute, File B2/129/PT4, 1 August 2011.
- 2 M Opie, W Waldman. Finite element derivation of stress concentration at edge of hole with close-fit fastener representative of Hawk fatigue coupons. DSTO Minute, File B2/129/PT4, July 2010.
- 3 G Karami. Boundary element analysis of elasto-plastic contact problems. *Computers & Structures*. Vol. 41, No. 5, 1991, pp. 927-935.
- 4 D Martín, MH Aliabadi. Boundary element analysis of two-dimensional elastoplastic contact problems. *Engineering Analysis with Boundary Elements*, Vol. 21, Issue 4, 1998, pp. 349-360.

2.1.13 Managing the Effects of Environmental Degradation on the Airworthiness of RAAF Aircraft - Bruce Crawford, Khan Sharp, Chris Loader, Qanchu Liu, Alex Shekhter, (DSTO) and T.J. Harrison (RMIT University)

2.1.13.1 Corrosion Structural Integrity Roadmap

Contributors: B.R. Crawford, P.K. Sharp and C. Loader

Like many other aircraft operators, the Royal Australian Air Force (RAAF) faces a major challenge in managing corrosion damage in its fleet. Over the last 15 years, DSTO has developed several successful models of how corrosion affects aircraft structural integrity (Figure 1) [1-12].

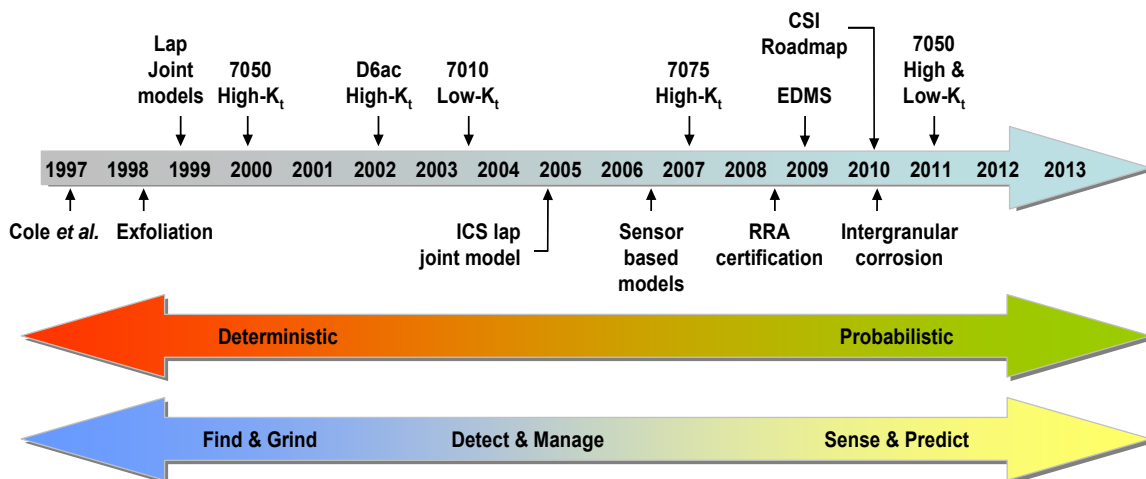


Figure 1: Timeline of DSTO research into the effects of corrosion on aircraft structural integrity

DSTO is now working to transfer these models into service on Royal Australian Air Force aircraft [13]. It is concentrating on developing predictive models of the effects of pitting, intergranular, and exfoliation corrosion on structural integrity and transferring these models into the RAAF's Environmental Degradation Management toolbox.

2.1.13.2 Pitting Corrosion of 7050-T7651

Contributors: B.R. Crawford and P.K. Sharp

DSTO has recently published the results of a joint program with the USAF on the effect of pitting corrosion on the fatigue life of 7050-T7651 [7]. DSTO's interest in 7050-T7451 came from the in-flight loss of a trailing edge flap from a RAAF F/A-18 in the 1990s [14]. This alloy is the primary structural alloy for the F/A-18 and the lug that held the trailing edge flap to the aircraft was made of this material.

This project found that pitting corrosion greatly reduced the fatigue endurance of pitted high- k_t specimens. A scanning electron microscope was used to measure the dimensions of the corrosion pits on the fracture surfaces of the specimens. The fatigue crack growth prediction software AFGROW was then used to model the fatigue life of the specimens using these dimensions. It was found that pit tip radius had the strongest effect on fatigue life. However, this metric cannot be measured in-service. Therefore, pit depth was used as the primary metric, which was referred to as an equivalent crack size (ECS). Conversely, the width of the pit in these high- k_t specimens was found to be insignificant. This conclusion was supported by comparing finite element models of narrow and wide pits with a model for a crack.

DSTO are further developing this work on 7050-T7451 by combining it with the Corrosion Criticality Model described below to allow the prediction of fatigue lives and failure locations in corroded material and components [2].

2.1.13.3 *Pitting Data Consolidation*

Contributors: B.R. Crawford, P.K. Sharp, T.J. Harrison and C. Loader

As a result of its research, DSTO has collected a large amount of experimental data on the effect of pitting corrosion on the fatigue life and structural integrity of four alloys. DSTO has investigated the effect of corrosion on the fatigue endurance of three aluminium alloys (7010-T7651, 7050-T7451 and 7075-T6) [5-7, 15] and one steel (D6ac) [8]. DSTO is now consolidating all of these data into a single database, which will allow the data to be analysed as a whole. This is important as the methods used to analyse the data evolved over time as knowledge was gained. Ideally, this would not be the case. The consolidation of the data will also allow DSTO to share its dataset, where possible, with collaborators.

2.1.13.4 *Criticality of Pitting Corrosion*

Contributors: B.R. Crawford, P.K. Sharp, C. Loader, Q. Liu and T.J. Harrison

In addition to reducing fatigue life, corrosion can also affect where fatigue failures occur. DSTO has studied this effect for pitting corrosion in 7010-T7651 [4]. This study used a Monte-Carlo simulation to predict how the location of fatigue failures in corroded low- k_t fatigue specimens differed from that in uncorroded specimens. Figure 2 compares the model's fatigue life predictions with fatigue life data from Crawford et al. [5, 6] for the same material. It also shows experimental results from fatigue life specimens which were corroded at offset locations. The match between the experimental data and model predictions is very good except at the lowest stress level where there are some near-runouts that were not predicted by the model.

Figure 3 shows the model's predictions of the proportion of fatigue failures due to dual symmetric corrosion strikes versus the distances of these strikes from the middle of the specimen. This figure also shows the proportion of pit induced failures from an experimental trial of 16 specimens with symmetric dual corrosion strikes at offset distances of 30 mm, 38 mm and 45 mm. There is good agreement between the results of the experimental trial and the modelling despite the small number of specimens tested.

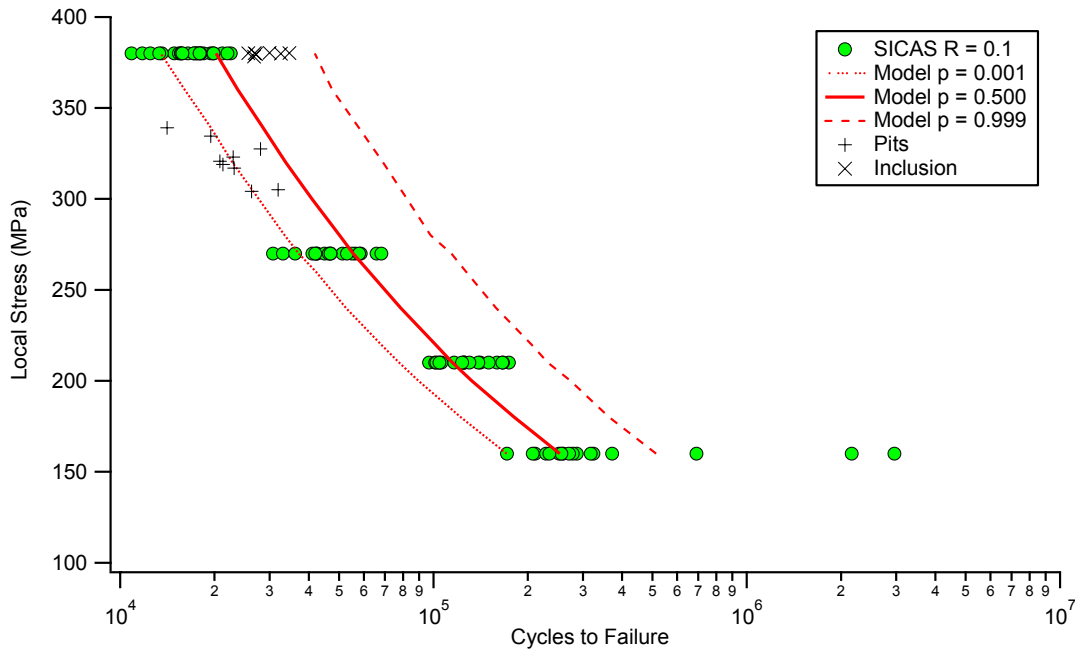


Figure 2: Comparison of fatigue life results for 7010-T7651 from Crawford et al. with those obtained from the offset-corrosion fatigue life tests and the predictions of the criticality model.

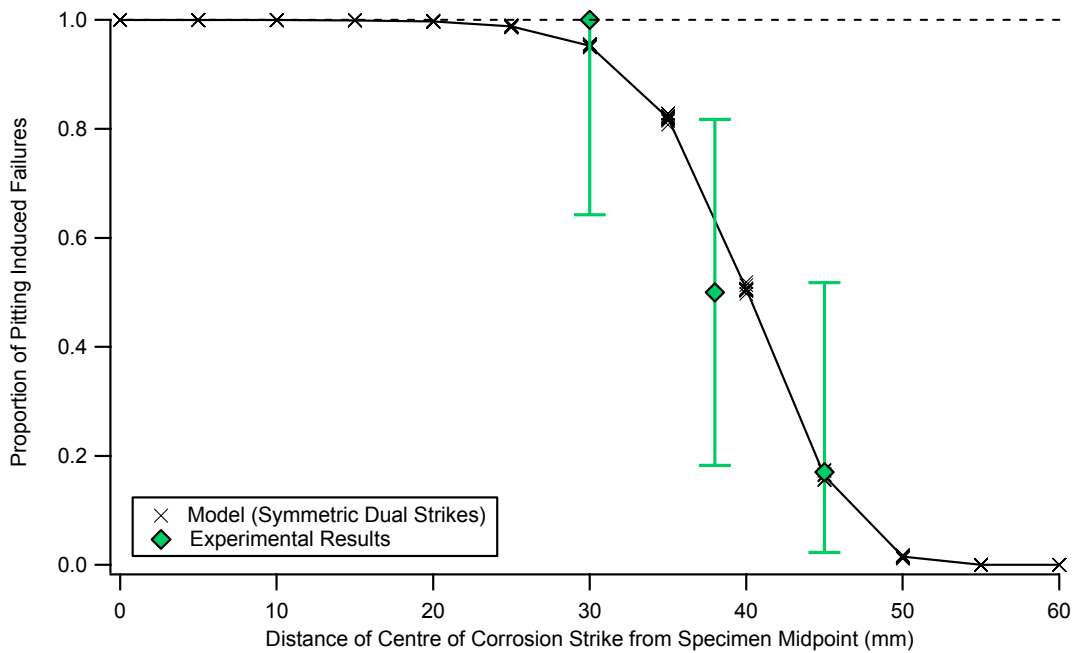


Figure 3: Proportion of experimental and predicted failures due to pitting for single and dual symmetric corrosion strikes vs. distance from the midpoint of the specimen. $\sigma_{\max} = 380$ MPa, $R = 0.1$ and each data point represents 5,000 replicates.

2.1.13.5 Certification of Retrogression and Re-ageing

Contributors: B.R. Crawford, P.K. Sharp, C. Loader and A. Shekhter

DSTO, in collaboration with the NRC of Canada, has been working on certifying the Retrogression and Re-ageing (RRA) heat treatment on RAAF aircraft, such as the C-130, since 2004. DSTO has now completed this certification effort [16, 17] and has in-principle design acceptance from the sponsor of this work. DSTO has shown that RRA can be performed reliably on components of extruded 7075-T6 of 6.35 to 25.4 mm thickness and up to 3.2 meter long. DSTO is now conducting a trial of the use of RRA on the AP-3C Orion. This trial is a precursor to the certification of the RRA treatment of extruded 7075-T6 of less than 6.35 mm thickness.

2.1.13.6 Modelling of Intergranular Corrosion in AA7075-T651

Contributors: T.J Harrison (RMIT).B. R. Crawford.

A “Brick Wall” model has been developed to describe and predict the path taken by intergranular corrosion in extruded 7075-T651 by treating the microstructure as a “brick wall” of grains, based on their size distributions. In the work described here, the corrosion has started on the ST-LT plane (representing the bore of a fastener hole) and proceeds in the L direction (along the rolling direction, parallel to the surface).

This model requires inputs of the grain length and width distribution, probability that the corrosion will “turn” when it reaches a grain boundary junction rather than just continuing straight (which is based on analysis of corrosion samples) and the average length of the corrosion. The model describes the corrosion path by stepping along a “grain length” where it then calculates if it will jump up or down a layer of grains or continue on the same grain layer. It then steps again along a “grain length”. This then continues until the corrosion path reaches the length given. The model will calculate a number of paths (in this case 1000) and highlight the path with the highest deviation, as well as a randomly selected path (Figure 4).

This model has been validated against lab-produced intergranular corrosion [18] using a modified version of the protocol found in Salagaras *et al.* [19] which can produce IGC up to 3 mm in depth (Figure 5).

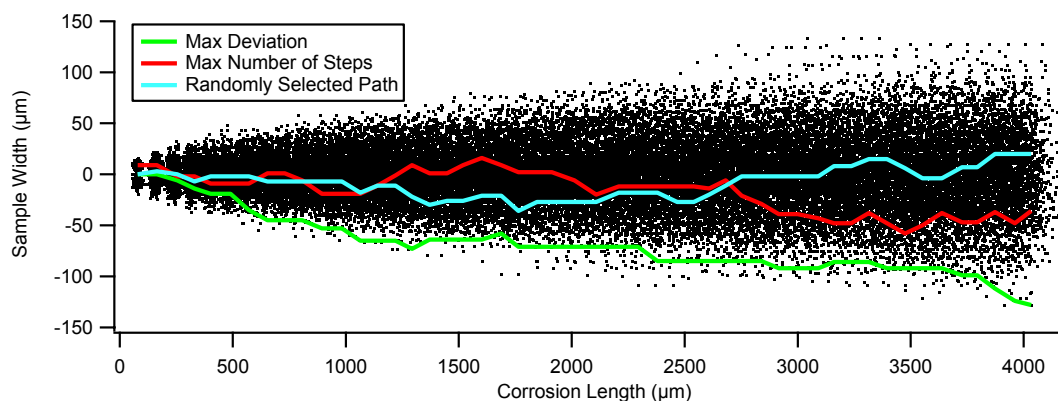


Figure 4: Microstructural paths of intergranular corrosion predicted by the Brick Wall model.



Figure 5: Optical micrograph of a path of intergranular corrosion in 7075-T6.

References:

1. Crawford, B. R. (2006) *An Assessment of the Initial Discontinuity State (IDS) Concept*. DSTO-TR-1957, [Technical Report] Melbourne, Defence Science and Technology Organisation.
2. Crawford, B. R., Harrison, T., Loader, C., Sharp, P. K. (2012) *Experimental Plan for the Development of Equivalent Crack Size Distributions and a Monte Carlo Model of Fatigue in Low and High-kt Specimens of Corroded AA7050-T7451*. DSTO-TN-1073, Melbourne, DSTO.
3. Crawford, B. R., Loader, C., Hay, D., Urbani, C., Spence, S. (2006) *Initiation and Growth of Fatigue Cracks from Pits in Pre-Corroded 7010-T7651*. In: *Structural Integrity Forum 2006*: 2006.
4. Crawford, B. R., Loader, C., Liu, Q., Harrison, T. (2013) *A Methodology for Predicting the Fatigue Behaviour of Corroded Aircraft Components*. Draft, Melbourne, DSTO.
5. Crawford, B. R., Loader, C., Sharp, P. K., Clark, G., Urbani, C., Hay, D., Ward, A., Bache, M., Evans, W. J., Stonham, A., Spence, S. (2005) *Structural Integrity Assessment of Corrosion in Aircraft Structures*. DSTO-RR-0294, Melbourne, DSTO.
6. Crawford, B. R., Loader, C., Ward, A. R., Urbani, C., Bache, M. R., Spence, S. H., Hay, D. G., Evans, W. J., Clark, G., Stonham, A. J. (2005) *The EIFS distribution for anodised and pre-corroded 7010-T7651 under constant amplitude loading*. *Fatigue and Fracture of Engineering Materials and Structures* **28** (9) 795-808.
7. Crawford, B. R. and Sharp, P. K. (2012) *Equivalent Crack Size Modelling of Corrosion Pitting in an AA7050-T7451 Aluminium Alloy and its Implications for Aircraft Structural Integrity*. In Review, [Technical Report] Melbourne, DSTO.
8. Mills, T., Sharp, P. K. and Loader, C. (2002) *The Incorporation of Pitting Corrosion Damage into F-111 Fatigue Life Modelling*. DSTO-RR-0237, [Research Report] Melbourne, DSTO.
9. Mills, T. B., Honeycutt, K. T., Brooks, C. L., Sharp, P. K., Loader, C., Crawford, B. R. (2004) *Development and Demonstration of an Holistic Structural Integrity Process using the Initial Discontinuity State Concept for 7050-T7451 Aluminum*. APES.
10. Sharp, P. K. and Crawford, B. R. (2006) *FATIGUE CRACK INITIATION FROM CORROSION DAMAGE ON AGEING AIRCRAFT STRUCTURES*. TTCP-MAT-TP1-7-2006, Melbourne, Australia, TTCP.
11. Sharp, P. K., Mills, T., Clark, G., Russo, S. (2000) *Recent Advances in Modelling Exfoliation Corrosion*. In: *Australian Fracture Group Conference*, Sydney: 2000, Australian Fracture Group.

12. Sharp, P. K., Mills, T., Russo, S., Clark, G., Liu, Q. (2000) Effects of Exfoliation Corrosion on the Fatigue Life of Two High-Strength Aluminium Alloys. In: *Fourth Joint FAA/DoD/NASA Ageing Aircraft Conference*, St Louis, Missouri USA, FAA/DoD/NASA.
13. Crawford, B. R., Loader, C. and Sharp, P. K. (2010) *A Proposed Roadmap for Transitioning DSTO's Corrosion Structural Integrity Research into Australian Defence Force Service*. DSTO-TR-2475, [Technical Report] Melbourne, Defence Science and Technology Organisation.
14. Barter, S. A., Sharp, P. K. and Clark, G. (1994) The failure of an F/A-18 trailing edge flap hinge. *Engineering Failure Analysis* 1 (4) December 1994 255-266.
15. Shekhter, A., Loader, C., Hu, W., Crawford, B. R. (2007) *Assessment of the effect of pitting corrosion on the safe life prediction of the P3-C*. DSTO-TR-2080, [Technical Report] Defence Science and Technology Organisation.
16. Loader, C., Crawford, B. R. and Shekhter, A. (2012) *Retgression and Re-Aging In-Service Demonstrator Trial: Stage II Component Test Report*. DST-TR-2686, Melbourne, DSTO.
17. Loader, C., Crawford, B. R. and Shekhter, A. (2012) *Retgression and Re-Aging In-Service Demonstrator Trial: Stage III Component Test Report*. DSTO-TR-2687, Melbourne, DSTO.
18. Harrison, T. (2012) Intergranular Corrosion Protocol Development for 7075-T651 Extrusion. In: *ICAS 2012: 28th Congress of the International Council of the Aeronautical Sciences*, Brisbane: 23-28 September, ICAS.
19. Salagaras, M., Wythe, A. and Trathen, P. (2012) Methodology for Producing Intergranular Corrosion on AA7075-T651. In: *Proceedings of the Australasian Corrosion Association Conference*, Melbourne: November.

2.1.14 Managing Fatigue from Corrosion Pits - Loris Molent, (DSTO)

Despite corrosion prevention or protection schemes/treatments and corrosion prevention and control plans, in-service corrosion does occur and has the potential to impact the structural integrity of aircraft. Whilst the fatigue management of the aircraft is generally well understood as reflected in typical Aircraft Structural Integrity Management Plans (ASIMP), which in some cases contain environmental degradation plans, limited provision beyond *find and fix* exists for corrosion repair. Thus the repair of corrosion can be a major through life cost driver as well as an aircraft availability degrader. This *find and fix* policy exists largely because tools are currently too immature to accurately assess the structural significance of corrosion when it is detected.

The work summarised in [0] provides a basis for the justification of allowing detected pitting corrosion to remain in service for a limited period of time (e.g. to the next planned or scheduled servicing). The method is intended to maintain a probability of failure consistent with ASIMP requirements for fatigue cracks initiating from corrosion pits for a specific period. Unanticipated maintenance costs significantly more than planned maintenance. Delaying the repair of pitting corrosion until the next scheduled maintenance, should save considerable resources and improve aircraft availability.

Traditionally one complicating aspect when assessing the importance of corrosion is the concern that a corrosive environment may accelerate the growth of fatigue cracks that may subsequently nucleate. However, recent findings have shown that for combat aircraft there appears to be little corrosion activity in flight when fatigue cracking may be active due to the cold, dry in-flight environments that largely suspended³corrosion activity, see Trathan [0], Barter and Molent [0], Burns et al. [0]. These independent findings suggest that (in general) for combat aircraft the effect of the environment on fatigue crack growth can be decoupled. This significantly simplifies the problem (i.e. the growth of fatigue cracks in these aircraft is not environmentally assisted). Thus, if an appropriate metric for the size of the initiating corrosion pit (referred to here as the Effective Pre-crack Size (EPS)) is determined then fatigue prediction can be made using laboratory generated non-environmentally assisted crack growth rate data and an appropriate crack growth algorithm [0].

The development of analytical tools capable of accurately assessing the effect of corrosion on the durability of a structure would be considered a major advance for the ASIMP.

References:

1. Molent, L. *Managing fatigue from corrosion pits – a proposal*. Proc. AIAC 15, Melb. 25-28 Feb 2013.
2. Trathan P. *Corrosion monitoring systems on military aircraft*, Proceedings 18th International Conference on Corrosion, Perth 20th -24th November, 2011.
3. Barter S.A. and Molent L. *Investigation of an in-service crack subjected to aerodynamic buffet and manoeuvre loads and exposed to a corrosive environment*, Proceedings 28th International Congress of the Aeronautical Sciences, Brisbane, 23-28th September, 2012.
4. Burns JT, Gangloff RP and Bush RW. *Effect of environment on corrosion induced fatigue crack formation and early propagation in aluminum alloy 7075-T651*. Proc. DoD Corrosion Conference, La Quinta CA, 31 Jul-5 Aug., 2011.

2.1.15 On the Fatigue Crack Growth Analysis of Spliced Plates under Sequential Tensile and Shear Loads - Xiaobo Yu, (DSTO)

On a propeller powered aircraft, the spliced joints between the wing panels are subject to sequentially applied tensile and shear load cycles, as illustrated in Figure 1. This study [see reference] aims to propose an approach to address the fatigue crack growth (FCG) issue in this scenario. The proposal is based on a general understanding of the FCG behaviour under non-proportional mixed-mode loads, and a detailed analysis of a generic spliced plate under tension and shear loads. As shown in Figure 2, the analysis revealed shear-induced-bearing at fastener holes, and predicted both shear-induced- K_I and shear-induced- K_{II} at a 0° crack emanating from the fastener hole. For a short crack, the K_I component dominates and therefore has the potential to cause shear-induced-mode I

³ This may not apply for aircraft that spend extended periods flying low in hot and salty environments or are carrying corrosive payloads (e.g. fire bombers, transport aircraft around toilets etc.).

overload. As the crack grows longer, the shear-induced- K_{II} increases, and may induce both short-range acceleration and long-range retardation.

As such, the engineering problem of FCG in a spliced plate with sequential tensile and shear loads was converted into a more generally understood problem of FCG with cyclic mode I and intermittent cyclic mixed-mode loading. This proposed approach is significantly different from a routine approach that treats the fastener hole as an open hole, or replaces the shear-induced-bearing with tension-induced-bearing.

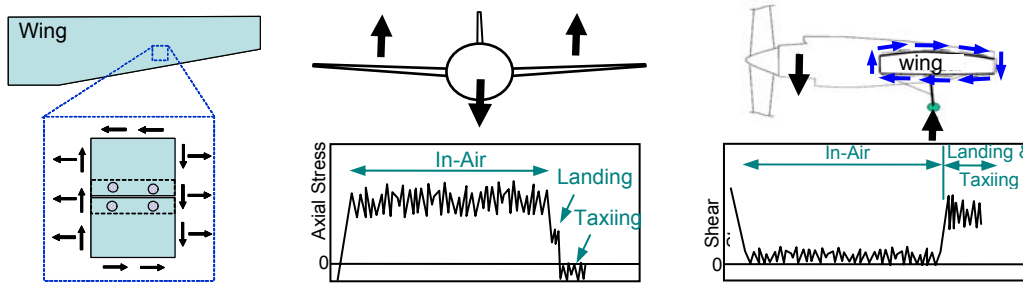


Figure 1. A spliced joint between wing panels subject to sequential tension and shear.

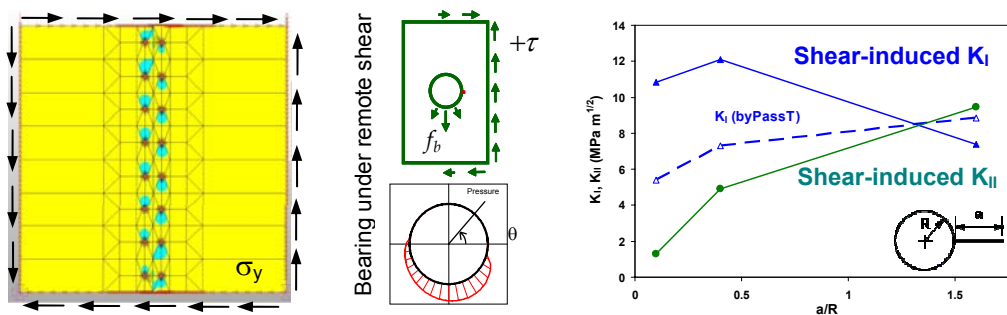


Figure 2. Selected results from the detailed analysis of a generic spliced plate.

Reference:

Xiaobo Yu, On the fatigue crack growth analysis of spliced plates under sequential tensile and shear loads, In: The Tenth International Conference on Multiaxial Fatigue & Fracture, ICMFF10, 3-6 June 2013, , Kyoto, Japan.

2.1.16 Forced Dynamic Response Analysis for an Industrial Mistuned Integrally Bladed Disk - Guan Xia Chen and Jianfu Hou (DSTO)

High cycle fatigue (HCF) failures have been increasingly considered as one of the major cost drivers for conventional aircraft engines, and having a significant negative impact on safety, cost of ownership and engine availability. As one of the top factors contributing to unscheduled shop visits and maintenance, HCF issues have been reported in RAAF

engines and some HCF related cracking instances have been investigated during the past decade.

Small variations among blade sectors, termed as mistuning, usually increase the blade forced response and may detrimentally affect engine HCF life. The engine blades for modern aircraft, like the JSF, are manufactured as a one-piece integrally bladed disk – termed as blisk. As a result of the utilisation of more blisks, HCF related issues are becoming more dominant regarding airworthiness and hence characterising mistuning through analysis has become particularly important. Therefore, it is essential to build up a capability of predicting the forced response of a blisk due to mistuning in an accurate and efficient manner.

As mistuning patterns in blisks have a large impact on the forced response even due to a small amount of mistuning, it is very important to study the sensitivities of mistuning strength for a typical pattern on the forced response. In this study, sensitivity analyses on the forced response of a blisk for different mistuning strengths were carried out using a Subset of Nominal Modes (SNM) method [1].

An FE model for a sector of a perfectly tuned blisk was created in ANSYS [2], shown in Figure 1. A cyclic dynamic analysis was performed using the FE model and the stiffness matrix and forced response results were produced for the tuned blisk. The results for the tuned case were depicted in Figure 2(a).

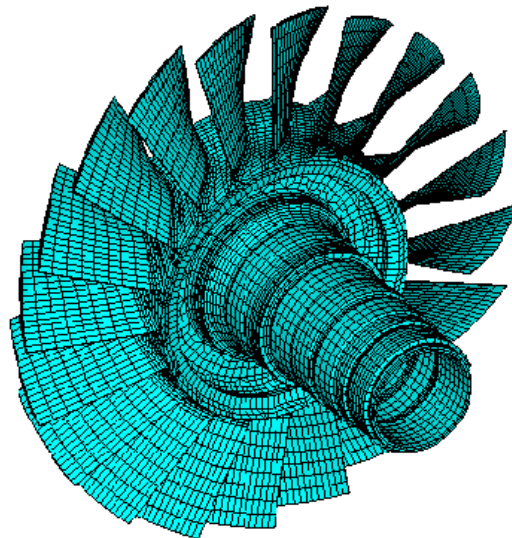


Fig.1. A full cyclic symmetric FE model for the blisk.

After the cyclic symmetric modal analysis for the tuned blisk was carried out, these modal results and model information data were transferred into a mistuning analysis system developed in MATLAB [2], where the mistuning analysis was conducted using the SNM method.

The mistuning analysis system casts the data into the modal domain and adds the information of the mistuning pattern. It then solved an algebraic eigenvalue problem with only a few hundred unknown parameters for the mistuned system. Finally, the mode shapes of the mistuned blisk are calculated using a weighted sum of the nominal tuned modes. Such a weighted sum is determined based on the cyclic symmetric FE model of the tuned blisk. Therefore, it uses relatively much shorter computational time and smaller model size than those for using a full blisk model. Furthermore, only the modes with natural frequencies close to the modes of interest are considered to make a significant contribution to the response. As a result, the forced response for a mistuned blisk is determined by a relatively small range of the nominal tuned blisk modes. This further saved computational time and storage space.

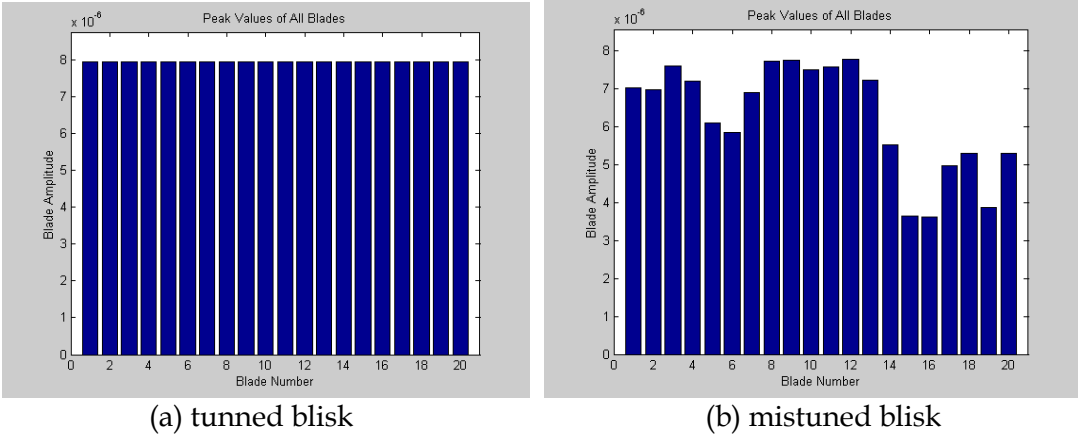


Fig. 2 Peak values of all blades

Four mistuning cases were studied under different engine order excitation. For these cases, only one sector is mistuned. The mistuned frequency ratios are 0.98, 0.95, 0.90 and 0.85 (denoting 2%, 5%, 10%, and 15% mistuning strength) respectively for the four cases with all other sectors' frequency ratios being 1. The final results from the investigation are plotted in Figure 3. In this figure, The maximum blade amplitude changes with different mistuning ratios, which are depicted as a function of maximum frequency changes. As can be seen in Figure 3, the 5% mistuning strength represents the worst case.

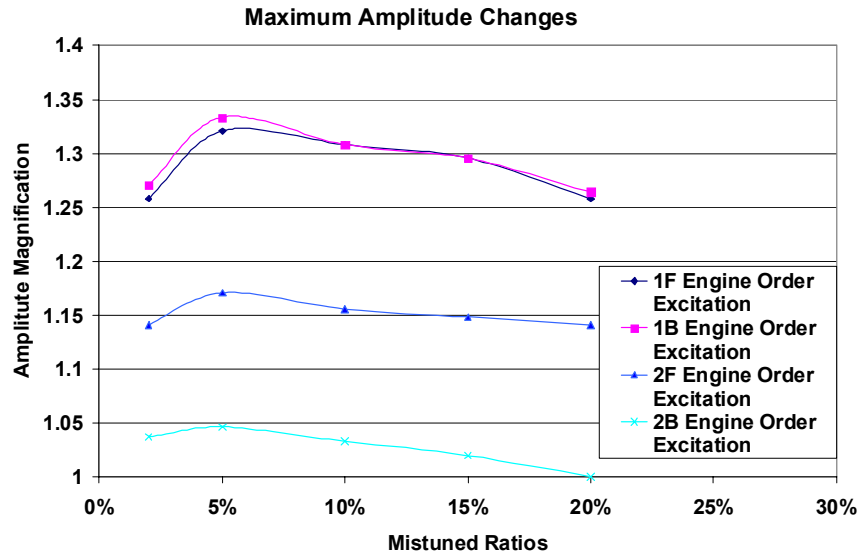


Fig. 3. The maximum blade amplitude change vs. maximum frequency changes for various excitations: 1st Forward (1F), 1st Backward (1B), 2nd Forward (2F) and 2nd Backward (2B) Engine Order Excitations.

Based on the analysis results shown in Figure 3, the following conclusions can be drawn:

- The introduction of a mistuned sector changes both the frequencies and the responses of each individual blade; and
- The 5% frequency change represents the worst case for the studied range of frequency changes.

Most importantly, as the amplitude magnification exhibits a peak with respect to small mistuning strength for the blisk, this research result provides two important insights. Firstly to design engineers, it presents an idea of starting with sufficient mistuning to keep the nominal design on the other side of peak. Secondly to maintenance engineers, it can be used as guidance for blending repairs to avoid the sensitive mistuning strength and to increase the safety margin during maintenance of engine components.

The future work will include further evaluations of the sensitivity of mistuning strength under the presence of random mistuning patterns, and the correlations between the predictions and laboratory tests as results are available.

References:

1. Yang, M.-T., and Griffin, J. H., 1999, "A Reduced Order Model of Mistuning Using a Subset of Nominal System Modes," Proc. 44th ASME Gas Turbine and Aeroengine Technical Congress, Exposition and Users Symposium, ASME, New York.
2. ANSYS Inc. 2010, ANSYS V.13 Mechanical User Guide. Pittsburgh, U.S.A.
3. The Mathworks Inc. 2000, MATLAB 6 Getting Started Guide. Massachusetts, U.S.A.

2.1.17 In Situ Structural Health Monitoring using Acousto-Ultrasonics, Optical Fibre Sensors and Thermoelastic Stress Analysis - Nik Rajic, Claire Davis and Steve Galea, (DSTO)

A significant through life support cost driver for military aircraft is time-based non-destructive inspections for corrosion or defects, often in inaccessible regions, which are costly and time-consuming. The introduction of Structural Health Monitoring (SHM) systems, which utilised structurally integrated transducers, has the potential to reduce costs and increase aircraft availability. SHM facilitates improved component inspectability by lowering detection thresholds and removing the need for disassembly of the structure for access to difficult to inspect regions. Subsequently SHM enables cost effective earlier detection (and possibly characterisation) of 'hot spots' and defects compared to current conventional techniques and provides a critical underpinning technology for efforts to improve the efficiency of contemporary structural integrity management practice.

The Defence Science and Technology Organisation (DSTO) has a program of work aimed at developing autonomous, robust, reliable SHM systems, based on two techniques, viz., stress-wave or acousto-ultrasonic (AU) and thermoelastic stress analysis (TSA), with the specific aim of retro-fitment to existing aircraft. Both techniques offer SHM systems with the potential for effective broad area, low sensor density, low-cost and reliable means of non-destructive inspection. The former technique is based on elastic waves produced by a fixed source, typically using piezoceramic elements. These waves are sensed using either piezoceramic transducers or optical fibre sensors at separate receiving locations where variations from the baseline response are used to identify damage within the wave path. The 2011 ICAF input [1] described the demonstration of the feasibility of AU based SHM systems on realistic aircraft components, the development of an AU modelling capability, the mechanical performance of piezoceramic transducers and strategies for ensuring system robustness. The use of distributed strain sensing using optical fibre sensors (OFS) to achieve a novel damage metric was also described. Activities over the past two years have made further advancements in all these areas; AU modelling [2], piezoceramic durability [3], OFS as AU sensors [4, 5] and, packaging and attachment studies for OFS [6]. TSA is a powerful non-contact full-field stress measurement technique, which has potential in in-situ structural health monitoring (SHM). In providing both diagnostic and prognostic capabilities it may surpass the capabilities of many currently proposed SHM systems. The technique utilises the thermoelastic effect, viz., elastic deformation causes an object to undergo a small reversible change in the temperature. The temperature changes produced by thermoelasticity are small where a stress change of 1 MPa in aluminium alloy Al2024 produces a thermoelastic temperature change of under 3 mK which is significantly below the noise floor of a modern infrared detectors. Using the load signal as a reference, cross-correlation can be applied to achieve vastly improved stress measurement sensitivities, to levels approaching 1MPa. This approach forms the basis of operation of most TSA systems. DSTO has applied this approach to low cost, compact and rugged microbolometer infrared cameras to develop a unique (microbolometer detector based) thermoelastic stress analysis (TSA) capability [7] called MiTE (Microbolometer ThermoElasticity). An F/A-18 centre-fuselage full-scale structural fatigue test is employed as a case study to illustrate the practical feasibility of the approach [8, 9]. Although the case study focuses on an aircraft structure, the concept has potential application to a wide

variety of different engineering assets across the aerospace, civil and maritime sectors. Only the piezoceramic durability studies and the TSA work will be elaborated on here.

2.1.17.1 Enhanced Experimental Facility for Durability and Performance Characterisation of Piezoelectric Transducers [3]

An experimental facility, called Autonomous Mechanical Durability Experimentation and Analysis System (AMeDEAS), has been developed at the DSTO capable of performing an autonomous long-term mechanical durability test on piezoceramic transducers. AMeDEAS controls the load cycling of an instrumented specimen by suspending the mechanical loading after a designated number of cycles and instructs the interrogation electronics to switch through a series of transducers and take time domain acousto-ultrasonic and electro-mechanical impedance measurements autonomously. Once the transducer interrogation is completed the system continues mechanical loading, and automatically adjusts (normally increases) loading amplitudes as required. So in essence the testing requires minimal operator input throughout the testing program. The basic approach is illustrated in the schematics in Figure 1.

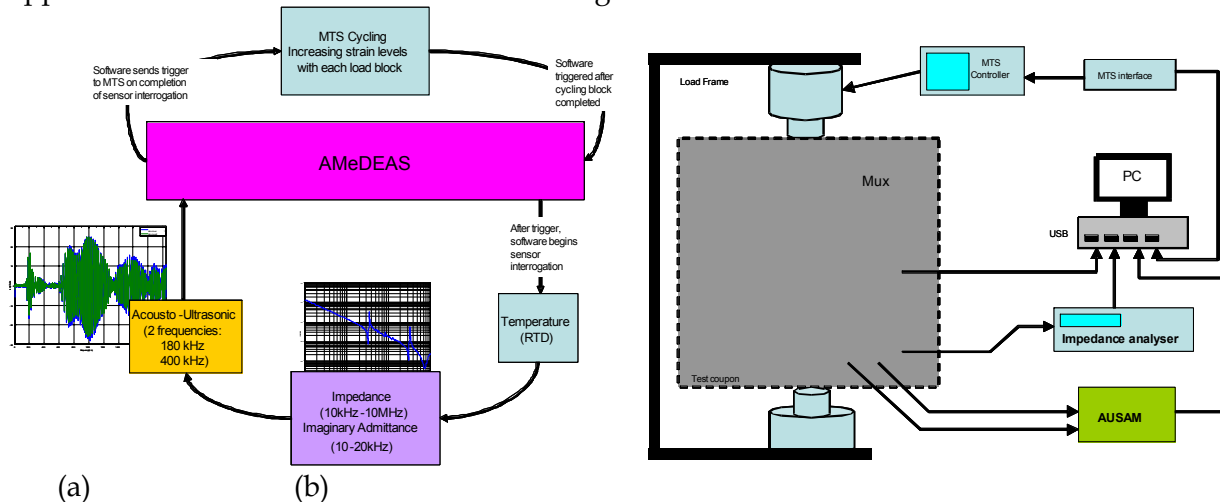
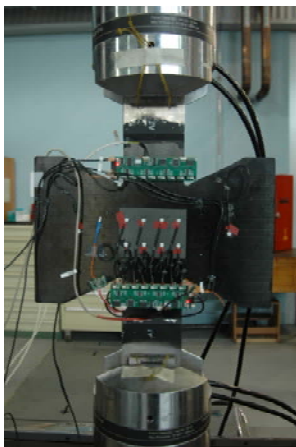


Figure.1: Schematic of the AMeDEAS (a) concept and (b) hardware test configuration.

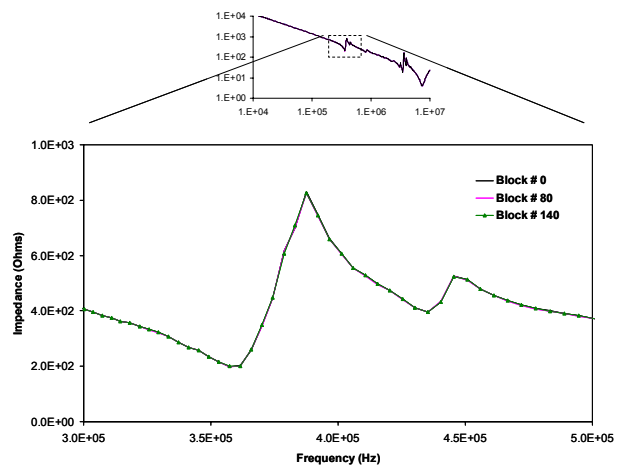
AMeDEAS was used to investigate the fatigue characteristics of a low-profile layered piezoceramic transducer package developed by DSTO. The specially designed test coupon, shown in Figure. a, was a 2.3 mm thick 16 ply quasi-isotropic carbon-BMI composite with a layup of $[90/-45/45/0]_{2s}$. It was designed to allow the durability testing of 16 transducers (8 on either side) as well as accommodating two additional transducers that would serve as reference AU sources and receivers. The 16 transducers under mechanical loading were tested under tension-dominated cyclic loading with peak-to-peak strain amplitude increased incrementally from $\sim 200 \mu\epsilon$ to $\sim 3000 \mu\epsilon$ with approximately 10^6 loading cycles completed at each strain level, except at the lowest strains which had only 500,000 cycles applied. The elements had a total of 7×10^6 cycles applied.

The reference elements are used to assess the transduction efficiency of the elements exposed to loading and consequently need to have stable performance. This is accomplished by the design of a distinctive 'winged' specimen, whereby large protrusions or 'wing' sections provide a nominally stress-free location for the reference elements (see Figure 2a). In addition, the wings were designed to increase the time-separation between incident and reflected wave packets within the working section of the sample.

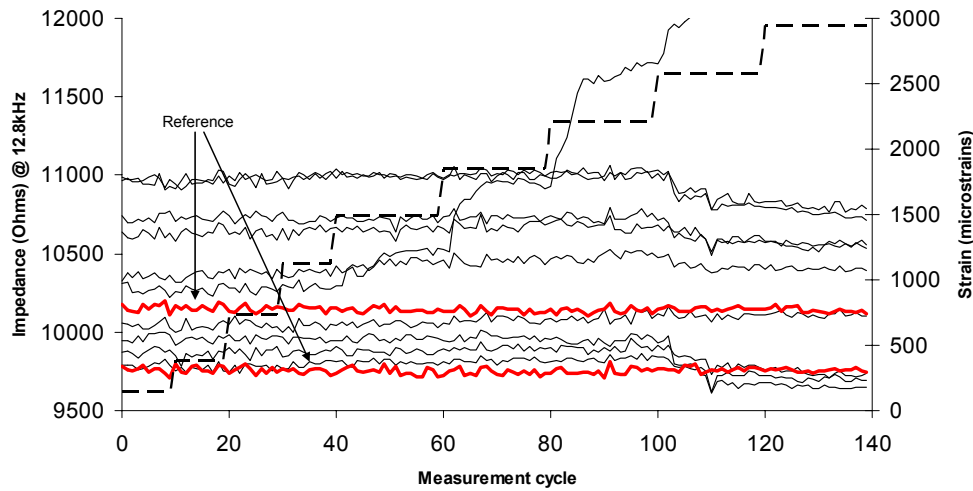
At a pre-determined number of loading cycles the test machine was paused and a transducer interrogation phase was commenced, which nominally took 40 min to complete. This consisted of measuring (1) electro-mechanical impedance of each element between 10 kHz and 10 MHz was measured (see Figure 2b for typical element output) and (2) the acoustic transduction efficiency of the fatigued elements by recording the AU time domain response between the reference and the working elements. No change in the impedance of the reference elements (see Figure 2b) indicates that the performance of the reference elements is constant with increasing number of loading cycles. For the fourteen active transducers (the wiring on two elements failed during the test), a plot of peak amplitude at the first lateral resonance of the electro-mechanical impedance response (see Figure 2c) showed that without exception, all transducers in the stress path showed significant variations in their impedance spectra at the first lateral resonant frequency. Some transducer showed variations in performance starting at strains as low as $1100 \mu\epsilon$ (peak-peak strain amplitude). Further detailed analysis of the impedance and AU response is continuing and the cause of variations in element performance is also being investigated. To this end a full 2D displacement scanning laser vibrometer field mapping before and after mechanically loading the system allows thorough electrical and mechanical characterisation of PZT transducers.



(a)



(b)



(c)

Figure. 2(a) Photograph of specimen showing transducers and AMeDEAS multiplexer boards required to take impedance and stress-wave time history response measurements. (b) Impedance spectrum (top) of reference transducer and enlarged inset (bottom). Transducer responses at the start, middle and end of the test program are shown but cannot be distinguished. (c) Plot of peak electro-mechanical impedance at the first lateral resonance. Reference (strain free) transducer data plotted in red (bold). Peak-peak strain amplitude is represented by dashed line.

Overall AMeDEAS has demonstrated its usefulness as an automated transducer endurance measurement system, capable of reliable uninterrupted operation over extended periods. Using a carefully designed specimen allowed placement of reference transducers in a stress free area ensuring stable performance and the generation of an interrogating wave-field without contributions from boundary reflections. Purpose-built multiplexers allow both electro-mechanical impedance and time history measurements to be carried out efficiently in a combined measurement cycle, and customised software allowed the measurements and mechanical cycling to be performed autonomously, with operator intervention only required during unavoidable test interruptions. The actual testing time was about four weeks for the 7×10^6 cycles due to system fine-tuning and unavoidable test machine shutdowns, but potentially the test could have been completed in about eleven days (or 1.6 weeks). Compare this to a previous test program using a semi-automated approach, where the operator needed to manually start the interrogations, which took of the order of 2 months to complete. The significant benefits of the automated approach has been demonstrated and can easily be adapted to test other variables such as spectrum loading and temperature variations on transducer performance.

2.1.17.2 Thermoelastic Stress Analysis (TSA) for Structural Health Monitoring (SHM) [8, 9]

It is proposed that in-situ TSA based SHM could be an integral part of any future SHM technology suite or toolbox. The technique offers a set of diagnostic and prognostic capabilities that are both significant and unique. TSA is a true imaging technique, which means an area of interest (the 'hot spot' region) can be observed passively from a remote

vantage point and be interrogated in detail and with full coverage. The technique provides a broad-field measurement of stress, where a single integrated TSA detector equipped with a modestly sized staring array is capable of providing a level of coverage equivalent to 75,000 separate strain gauges. That is stress mapping of a region is relatively straight forward provided the region is accessible and an unobstructed line of view is available. It has also been proposed that structural 'hot spots' can be identified pro-actively by means of a comprehensive TSA survey applied during full-scale structural fatigue testing of an airframe [10]. Continuous TSA monitoring of 'hot spot' locations offers a rich vein of information including:

- Measuring the actual stresses, and how they vary under different aircraft configurations and operational usage,
- Once a crack initiates the detection and tracking of a crack is generally not difficult and can in principle be done autonomously.
- The TSA response in the near-field zone surrounding the crack tip contains information that can be applied to determine the stress intensity factor. Moreover, since the measurements relate to the actual crack tip zone the effects of closure and residual stress are captured in the measurement meaning the approach yields the effective rather than the nominal stress intensity factor.

Demonstration of an Integrated TSA Monitoring Capability: An integrated TSA capability is demonstrated most effectively by providing a practical example taken from work done recently at DSTO. This work centres on a FSFT of the centre-barrel structure of the F/A-18. Over several years, MiTE has been applied in various aspects of this major engineering program, mostly in relation to the validation of FE model predictions [11, 12], and the assessment of structural repairs to critical regions. While this work has cast light on some important structural integrity problems, it is more broadly significant in its practical demonstration of the feasibility of integrated inspection, an approach specifically developed for these FSFT inspections. If not strictly an SHM application, the case is prescient in some important respects. The approach used here was to mechanically fix the detector to the structure which deviates from the customary practice of using a fixed vantage-point removed from the structure. Figure 3 illustrates the camera attached to the aft 488 bulkhead, using a small lightweight articulated arm. This approach offered several advantages that were instrumental in obtaining a useful result. By locking the detector to an appropriate part of the structure the motion of the observer and the observed are correlated, producing a result free of motion blur and other motion related artefacts. In the present example, the area of interest was resolved at 1:8mm per pixel, which was more than adequate for the exercise. The entire inspection took little more than half an hour to set-up and complete.

What made this approach feasible here, were in essence three factors; the relatively small size and low mass of the detector, its ruggedness and its low cost. The integrated inspection approach demonstrated has strong parallels with in situ SHM and, of course, the link could have been strengthened by leaving the systems in place and interrogating

the structure periodically, which is a straightforward extension of the present approach. Issues such as detector size, mass and ruggedness assume much greater importance, largely for the same reasons cited previously, but other considerations also enter into calculation, such as energy consumption, reliability, and how data is transferred to and from the system. In its present incarnation, the MiTE system is clearly unsuitable. For a start, the A20M used here is far too large, which conveniently brings us back to the original idea of the MiTE in 2002 which was conceived around the Indigo Omega, a much smaller device not much larger than a matchbox.

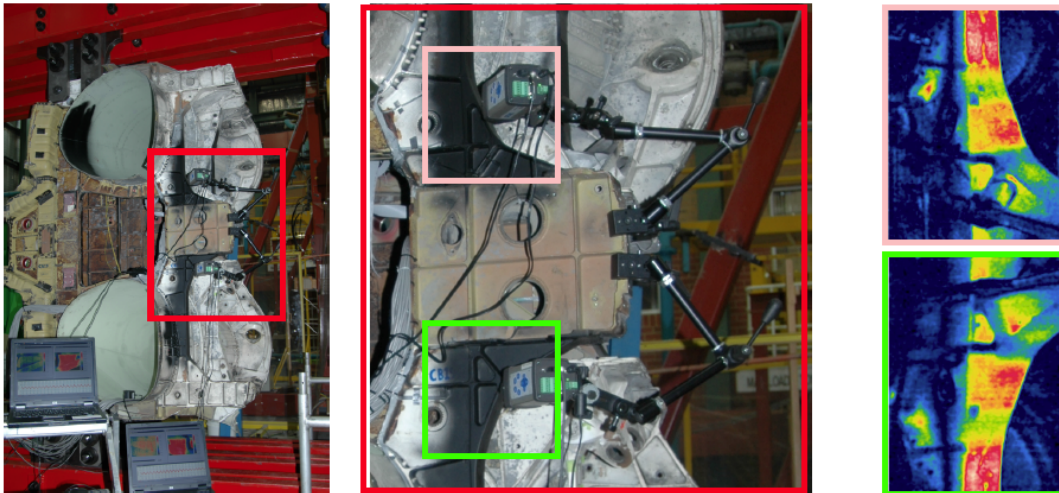


Figure. 3 TSA of the kickpoint region of the aft bulkhead in the Centre-Barrel of a Royal Australian Air Force F/A-18. Middle is a close-up showing two MiTE systems attached to the bulkhead. Right are representative results (bulk stress distributions) for the starboard (top) and port (bottom) sides, where red areas correspond to higher tensile stresses.

Microbolometer detectors considerably smaller and lighter than even the Omega are now available from several manufacturers. Compared to the A20M, these detectors are roughly two orders of magnitude smaller in volume, an order of magnitude lighter in mass, substantially lower in cost and draw much less power. These developments are all neatly aligned with the requirements for structurally integrated applications of TSA, including SHM. To this end, DSTO is presently developing the next generation of the MiTE system around several detectors in this miniature class. Figure 4 illustrates the broad concept that DSTO is working towards. It depicts a monitoring system comprising a network of miniature microbolometer detectors furnishing either real time IR imagery to a central processing hub, or fully-processed stress maps. The nodes are shown to operate wirelessly, which anticipates a capability not yet available in current microbolometers. Other than that, the type of scenario shown in Figure. could be realised within a relatively short period of time.

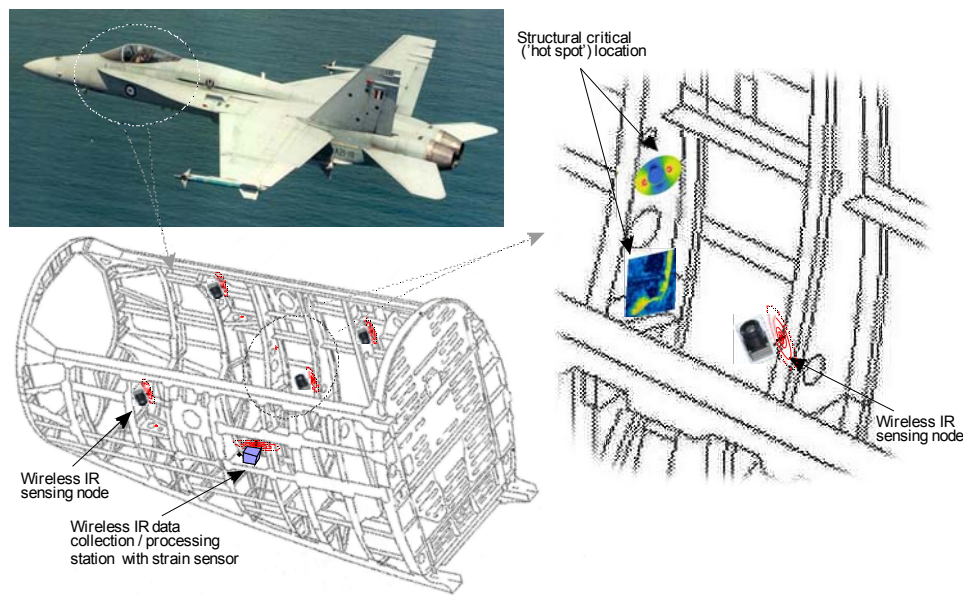


Figure. 4 Conceptual illustration of an in situ SHM system comprising a network of miniature microbolometer detectors with wireless comms and data transfer.

References:

- 1 "A Review of Australian and New Zealand Investigations on Aeronautical Fatigue During the Period April 2009 to March 2011", Editors: Phil Jackson and Christine Trasteli, DSTO-TN-0993, May 2011.
- 2 Rajic, N., Rosalie, C., Ong W. and Chiu, W.K., (2012), "Predictive Numerical Simulation of Lamb Wave Scattering from a Wing Skin Defect for Structural Health Monitoring System Design", Proceedings of the European Workshop on Structural Health Monitoring, Dresden, Germany, July 3-6.
- 3 George Jung, Steve Van der Velden, Kelly Tsoi and Nik Rajic, (2012) "An Enhanced Experimental Facility for Durability and Performance Characterisation of Piezoelectric Transducers for Structural Health Monitoring", Proceedings of the 4th APWSHM, Melbourne, Australia, 5-7 Dec, 2012
- 4 Cedric Rosalie, Patrick Norman, Joel Smithard, Claire Davis, Nik Rajic, "Optical Fibre Sensing of High Order Lamb Waves for Structural Health Monitoring", Proceedings of the ASME 2012 Conference on Smart Materials, Adaptive Structures & Intelligent Systems SMASIS 2012, September 19-21, 2012, Stone Mountain, Georgia, USA
- 5 Patrick Norman, Claire Davis, Cédric Rosalie, and Nik Rajic, "Interaction of high frequency Lamb waves with surface-mount sensor", Proceedings of the 4th APWSHM, Melbourne, Australia, 5-7 Dec, 2012
- 6 Tyler Schembri, Silvia Tejedor and Claire Davis, (2012) "Strain measurements using fibre Bragg gratings during full-scale structural testing of an F/A-18 centre barrel", Proceedings of the 4th APWSHM, Melbourne, Australia, 5-7 Dec, 2012
- 7 N. Rajic, S. Weinberg, and D. Rowlands, "Low-cost Thermoelastic Stress Analysis," Materials Australia, vol. 40, 2007.

- 8 Rajic, N., Rowlands, D. and Galea, S. "Probing the Limits - New Opportunities in Thermoelastic Stress Analysis", in Proc. 28th Congress of the International Council of the Aeronautical Sciences (P. I. Grant, ed.), 2012
- 9 N. Rajic, S. Galea and D. Rowlands, "Thermoelastic Stress Analysis - Emerging Opportunities in Structural Health Monitoring", in Proc. 4th Asia-Pacific Workshop on Structural Health Monitoring, Melbourne, Australia, 5-7 December, 2012.
- 10 A. Wong, "Making the Invisible Visible: Joining the Dots from Lord Kelvin to Fighter Jet Fatigue," in Proc. 28th Congress of the International Council of the Aeronautical Sciences (P. I. Grant, ed.), 2012.
- 11 N. Rajic, D. Rowlands, and K. A. Tsoi, "An Australian Perspective on the Application of Infrared Thermography to the Inspection of Military Aircraft," Proceedings of the 2nd International Symposium on NDT in Aerospace, Hamburg, Germany, 2010.
- 12 G. Swanton and L. Robertson, "Developments with the F/A-18 FINAL Centre Barrel Test Program," in Proceedings of AIAC14 - The Fourteenth Australian International Aerospace Congress, Melbourne, Australia, 2011.

2.1.18 Improving Structural Risk Analysis by Updating the Probabilistic Distribution of the Equivalent Initial Flaw Sizes based on the Bayes' Theorem - Ribi Torregosa and Weiping Hu, (DSTO)

Structural integrity assessment is a major activity for aircraft owners, regulators and operators, during acquisition and the subsequent operation. Due mainly to economic reasons, more and more military aircraft are operating close to their design lives or have their lives extended beyond the design goals through structural modifications and intensified inspections. For the continued operation of these aircraft, it is crucial to objectively quantify the risks involved. One of the risks is the probability of failure of key structural components by sudden fracture following accumulated fatigue damage. This type of risk is caused by many factors of uncertainty, relating to the material properties, service loads and manufacturing geometries and qualities. Increasingly, the theory of probability is used to quantify the structural risks rationally and systematically. Analyses show that a key input to risk analyses is the distribution of the equivalent initial flaw sizes (EIFS), which are obtained by regressing a set of observed cracks to the beginning of service life using a deterministic crack growth curve of the material for a specific load spectrum. To obtain a reliable distribution, a large number of crack data is required, but teardown crack data for a specific aircraft type at a given location are typically very few, and they are expensive to acquire. This problem of small sample size poses a big challenge to risk analysis for aircraft structures.

To address this problem, we used an updating technique based on the Bayes' theorem to enhance the quality of risk assessment by progressively improving the accuracy of the distribution of EIFS. Although the crack growth curve and the EIFS distribution both play a key role in determining the probability of failure by fracture for a given load profile, the crack growth curve is conventionally treated as deterministic while the EIFS is inherently probabilistic. Hence, the latter is a suitable candidate for Bayesian updating. Here, the successful flight hours of an aircraft are used as indirect information to update the prior

estimate of the EIFS distribution. For the analysis of a given aircraft, two types of Bayesian updating schemes may be devised, depending on whether the successful flight hours of the aircraft being analysed or those of similar aircraft in a fleet are used for the Bayesian updating. These two schemes are referred to as the Bayesian aircraft updating method and the Bayesian fleet updating method.

Bayesian updating technique was demonstrated by conducting a risk analysis on C-130H centre wing lower surface panel number 3 referred to as DTA location CW-1. The Bayesian aircraft updating method uses the successful flight hours of a particular aircraft in updating its own risk curve. Figure 3 shows the updated risk curve of a particular aircraft as compared to its calculated risk curve using the conventional (no-updating) method. On the other hand, the Bayesian fleet updating method uses the flight histories of all the aircraft in a fleet in updating the risk analysis of a fleet member. To demonstrate the effectiveness of the Bayesian fleet updating method, a specific case of a wing location on a transport aircraft was analysed using the Bayesian fleet updating method for both cases when a failure and no failure is observed at a specified flight hours. It was observed that the Bayesian fleet updating method produce lower risk values compared to the conventional method, when no failure is observed, as shown in Figure 4. In the same figure, it is also observed that the risk of failure will increase significantly when one failure among fleet members is observed.

It is demonstrated that the proposed Bayesian approach has advantages over the conventional method since it can refine the risk prediction when new information (e.g., failure or success at a specific flight hours) becomes available. Since the conventional (no-updating) risk analysis method does not accommodate indirect information, it is difficult to achieve such refinement systematically. The results from the test case also show that progressive updating ensures that the Bayesian risk results are always closer to the observed or experimental data than the results obtained from conventional non-updating method.

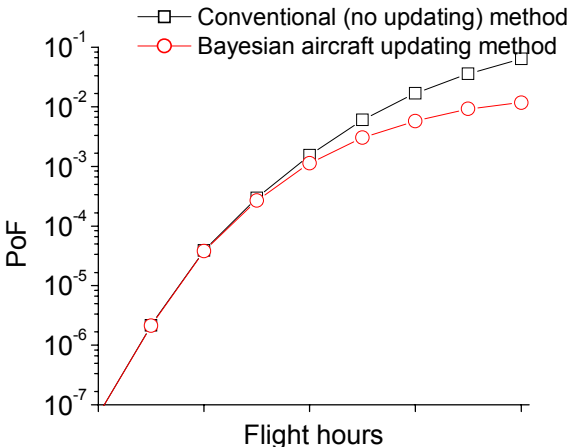


Figure 3 Bayesian aircraft updating method risk results compared with conventional method risk results

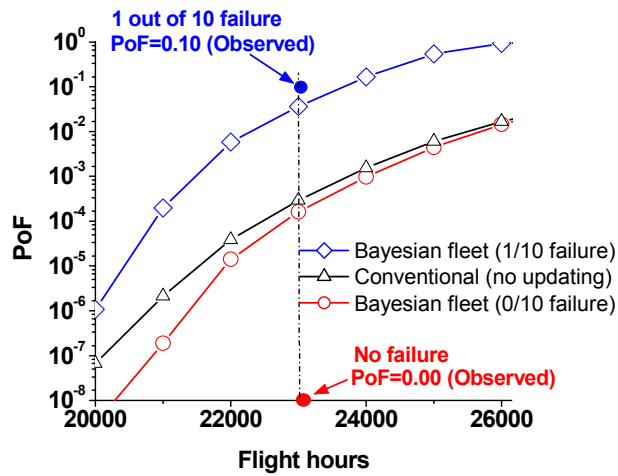


Figure 4 Bayesian fleet updating method risk results compared with conventional method risk results

2.1.19 Probabilistic Risk Analysis Of A Fatigue-Critical Location On A Transport Aircraft Considering Multi Site Damage Using FracRisk - Ribi Torregosa and Weiping Hu, (DSTO)

Aircraft structural integrity assessment is a major activity for all the aircraft owners and operators, during acquisition and the subsequent operation. For military aircraft that are operating near and beyond their design lives, it is crucial to quantify the risks involved in the continued safe operation. One of the risks is the probability of failure of a critical structural component by sudden fracture, after accumulated fatigue damage. This type of risks is caused by many factors of uncertainty and variability, relating to material properties, service load and geometries. Increasingly, the probabilistic approach is used to quantify this risk. In a complex structure, multiple holes and notches may exist and each of them may act as a site of crack initiation. One way of dealing with this is to assume that a lead crack starts from the most stressed location and grows in phases defined based on experience. This method works if the stress levels, hence the crack growth rates, at different locations are significantly different. If the crack growth rates at different locations are comparable, they need to be dealt with as multiple site damage (MSD), in order to capture the effect of the acceleration in crack growth rates caused by the interaction and coalescence multiple cracks.

Probabilistic risk analysis of a fatigue-critical location on a transport aircraft was conducted considering multiple site damage (MSD) from structural holes. The analysis was conducted using a Monte Carlo simulation technique. Five scenarios of Monte Carlo simulated MSD analysis were considered. These are illustrated in Figure 3. The MSD scenarios (a) to (e) show the different combinations of diametrical crack locations. Cases (a), (b), and (c) assume diametrical cracks that emanate from the outermost hole, the second hole and the third hole, respectively. Case (d) assumes diametrical cracks emanate from the outermost hole and a radial crack emanates from the remaining holes. Since the

outermost hole has a diametrical crack, its crack grows faster than the others and becomes the lead crack after the outer ligament fails. Case (e) is for diametrical cracks with random EIFS present in each hole. Case (f) is not an MSD case but a phase-by-phase approach included in the analysis to be compared with MSD scenario cases. A deterministic crack growth curve was assumed for both case scenarios during the simulation. For the analysis tool, a DSTO developed in-house risk analysis tool, FracRisk, was used. FracRisk, is an in-house DSTO risk analysis tool capable of analysing the probability of failure using the conventional method, the Bayesian risk updating method and the MSD cases.

The results indicated that an increase in the number of cracks in the MSD scenario will result to a corresponding increase in the risk of failure. This is illustrated in Figure 6. This shows why MSD should not be discounted when analysing risk of failure of airframe structural elements. It is also observed that the risk is highest when the diametrical crack is at the outermost hole of the structure as shown in Figure 7. This gives leverage to the assumption used in the phase-by-phase approach in which the crack was assumed to start at the outermost hole. However, MSD scenarios still gave more conservative results compared with the phase-by-phase approach. The following was concluded.

- 1.) The presence of multi-site damage significantly increases the risk of failure for a structural component
- 2.) The simplistic approach using only two sets of parameters to conduct risk analysis is shown to give lower risk values compared to the analysis using four parameters;
- 3.) An increase in the number of cracks resulted to a corresponding increase in the risk of fracture;
- 4.) Cracks closer to the edge of a component will result in a higher risk of failure due to its higher likelihood of becoming an edge crack.

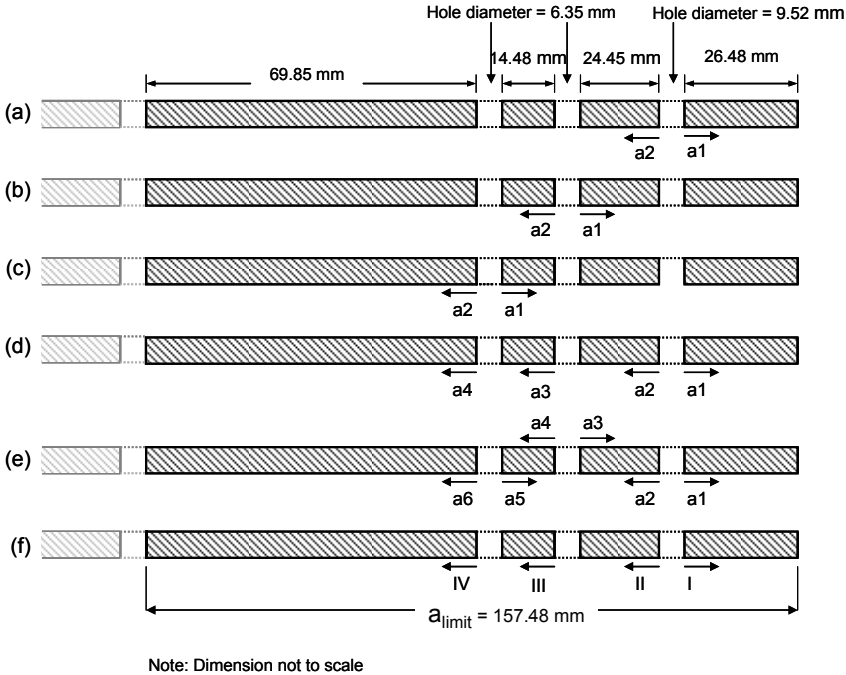


Figure 5 Crack scenarios analysed for MSD (cases a, b, c, d, e) and the phase-by-phase approach (case f)

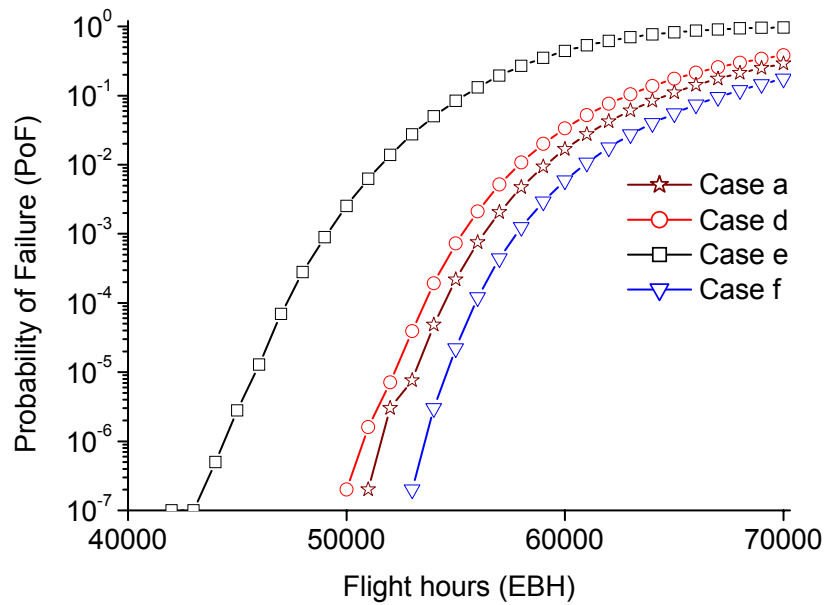


Figure 6 Risk curves showing the increase of PoF's corresponding to the increase of the number of cracks.

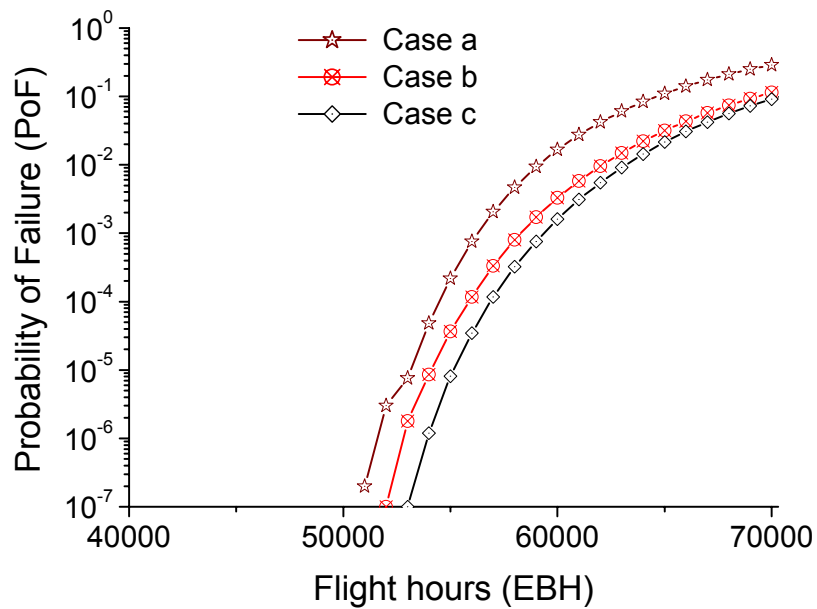


Figure 7 Comparison of risk values with varying locations of diametrical holes.

2.1.20 Recent Development in Fatigue Damage and Crack Growth Analysis: Verification and Validation, and Application in Lifting Airframe Structures - Chris Wallbrink and Weiping Hu, (DSTO)

The Australian Defence Force (ADF) requires quality advice relating to fatigue damage and crack growth analysis for the purpose of aircraft structural integrity management. This advice is critical to support the safe and economical operation of aircraft in the ADF. As such the Defence Science and Technology Organisation (DSTO) have been developing methods and codes to conduct fatigue life assessment in a robust and consistent manner. The result of this work is an in-house computer program known as CGAP. CGAP is a Microsoft Windows-based program with a graphical user interface, integrated database support, and modularised solvers for fatigue life and crack growth problems in metallic aircraft structures. Among CGAP's fatigue analysis capabilities are tools for predicting fatigue crack initiation life and crack growth. The fatigue crack initiation module in CGAP is based on the strain-life approach, and the crack growth modules are based on the concept of plasticity-induced crack closure. The CGAP solver also provides advanced capabilities for probabilistic crack growth and analysis of crack growth in notch-affected plastic zones. Extensive verification and validation have been conducted to ensure that CGAP functions as intended and to highlight its strengths and limitations. Over a thousand test cases have been run to check the functionality of the user interface elements. Each of the numerical modules has been verified using data available in the open literature or generated specifically for the purpose. The diagram in Figure 1 presents one verification activity used to assess the crack growth codes included in CGAP. The recent developments, verification and validation activities applied to CGAP have been reported widely [1-4].

References:

- 1 Wallbrink, C., Hu, W. and Torregosa, R. (2012). In: *The 2012 Aircraft Airworthiness & Sustainment Conference*, Baltimore, Maryland, USA: April 2-5
- 2 Wallbrink, C., Hu, W. and Torregosa, R. (2012). In: *Aircraft Airworthiness and Sustainment Conference*, Brisbane, Australia: 23-26th July
- 3 Hu, W. and Wallbrink, C. (2013). In: *15th Australian International Aerospace Congress*, Melbourne, Australia: 25-28 February
- 4 Hu, W. and Wallbrink, C. (2013). In: *ICAF*, Jerusalem, Israel: 3-7 June

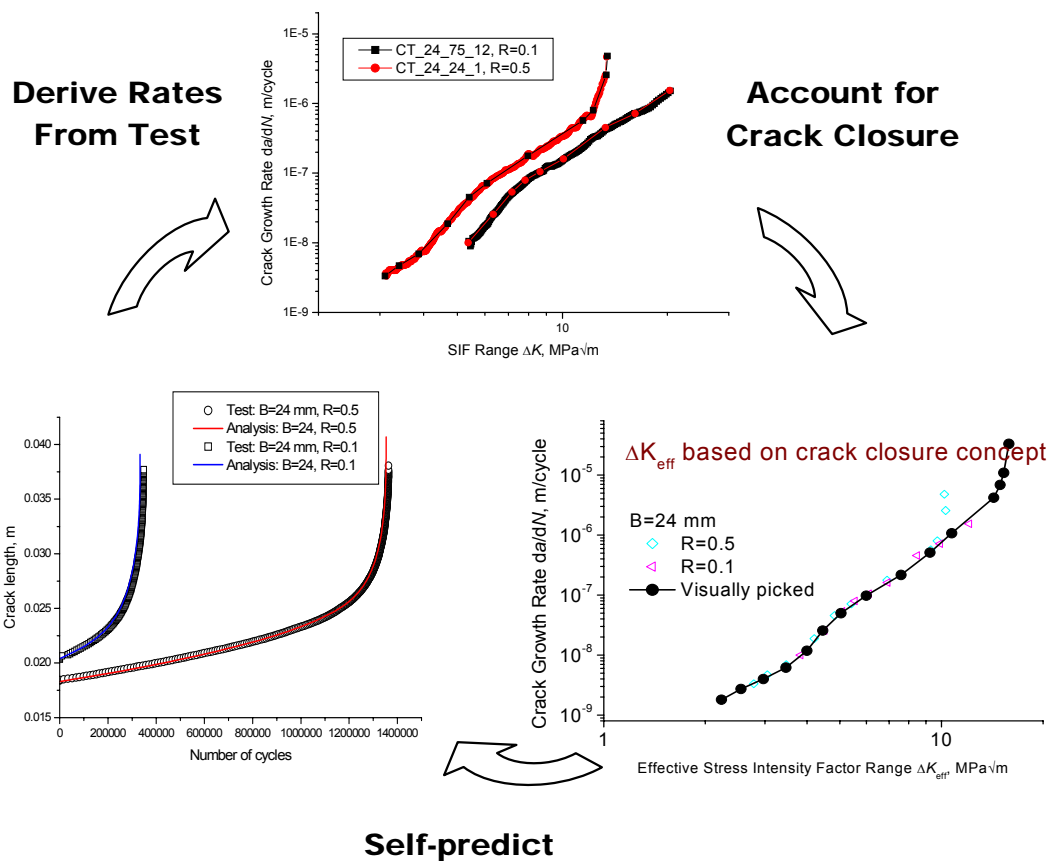


Figure. 1 CGAP verification: raw crack growth data are converted to crack growth rates for different stress ratios, which are then collapsed to a single curve using the FCGR converter; the resulting rates are then used to self-predict the original crack growth curves.

2.1.21 Seeing the Invisible: Taking a look at Stresses in Aircraft Fatigue Analysis - Albert Wong (DSTO)

Thermoelastic Stress Analysis (TSA) has been around for the past three decades, but to date, it has not been widely used or indeed widely known. Although there are devoted groups of practitioners in the automotive industry in Japan, this technology is practically unknown in the aerospace sector. On the other hand, the Defence Science and Technology Organisation (DSTO) has been in the forefront of this technology for some time, achieving many pioneering feats, including the development of the world's first high-speed focal plane TSA system, and more recently, the world's first microbolometer-based system. DSTO has also applied this technology with great effect on a number of practical problems involving Australian military aircraft components and structures.

To date, TSA has served as an effective validation tool for finite element models (FEM), and an example is shown in Figure 1 and 2 where the system was used as part of an investigation of an aircraft component failure. The system initially revealed discrepancies

in the original 2-D FEM developed to understand the failure. However, when the model was refined to include additional features such as skin dimpling in the region of interest, the correlation improved significantly and the component failure could be understood.

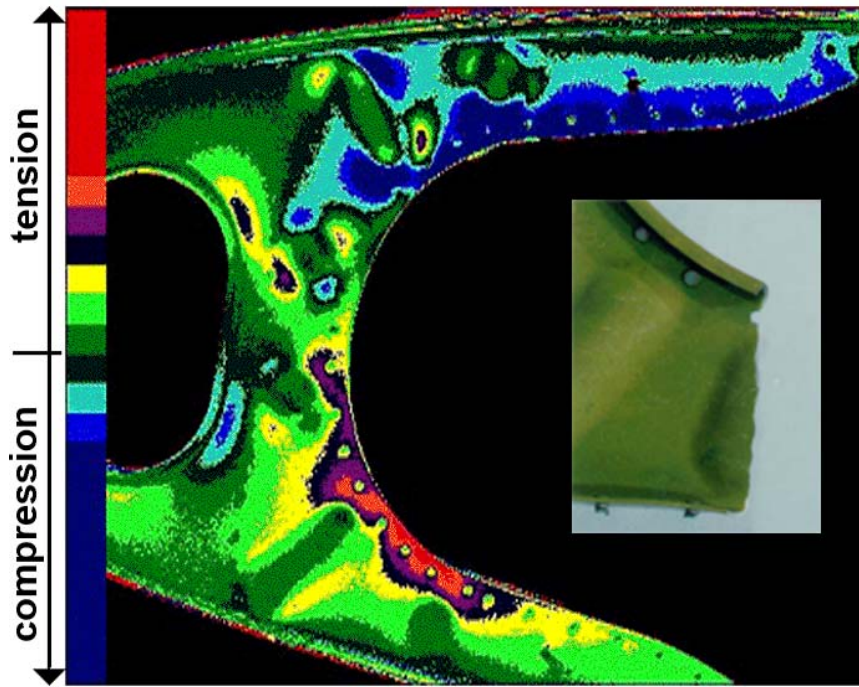


Figure 1. DSTO TSA scan of Orion WLE; inset: failed region of the test articles; dark-green in TSA scan indicates areas of low stresses in this image

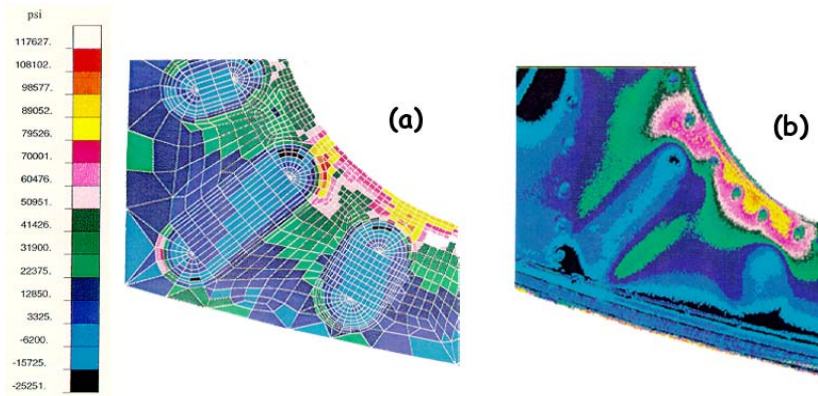


Figure 2. Analysis of critical region: a) 3-D FEA performed by NAVAIR, b) DSTO TSA scan; blue shading shows areas of low stresses

As the TSA technique allows non-contact measurement of stresses over broad areas of structures or components under cyclic load, it is an ideal technique for applications in fatigue tests. As an example, TSA was used as part of an experiment in an axial testing machine on the growth of cracks in a riveted splice joint. The system was firstly able to

show deficiencies in the design of the load transfer in the experiment and then errors in the loading alignment. Both problems would have led to difficulties in understanding the results of the experiment but could be corrected within a very short time with the aid of the TSA images. Figure 3 shows the TSA images before and after the re-alignment.

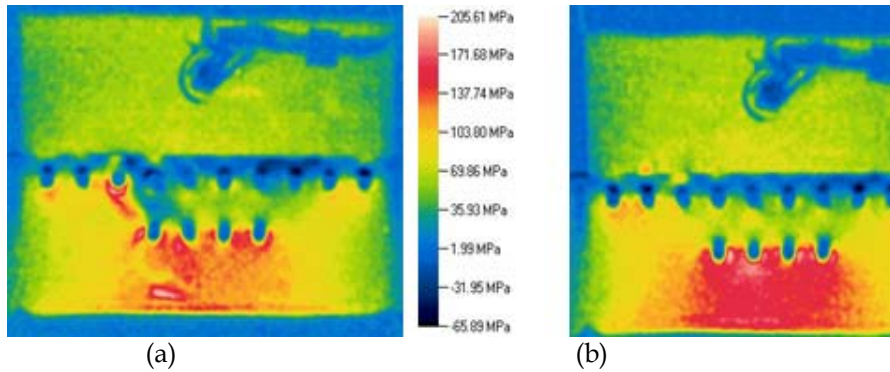


Figure 3. TSA scan of redesigned lap joint specimen: a) showing a degree of load misalignment, b) after re-alignment of specimen in the testing machine.

It is suggested that TSA has yet to make its greatest impact in the aerospace world, where it could take on a ubiquitous and persistent surveillance role in airframe full scale fatigue tests. Work is currently being undertaken in DSTO to demonstrate this capability.

Reference:

Wong, A.K. (2012), *Making the Invisible Visible: Joining the dots from Lord Kelvin to fighter jet fatigue*, Proc. 28th ICAS, Brisbane, Aust.

Wong, A.K. (2013), In: ICAF, Jerusalem, Israel: 3-7 June

2.2 FULL SCALE TEST ACTIVITIES

2.2.1 F/A-18A/B Hornet Outer Wing StAtic Testing (HOWSAT) - Wayne Foster, (DSTO)

Attempts to develop a through life management strategy for the outer wing of the F/A-18A/B Hornet aircraft, based on direct test interpretation of previous full-scale fatigue tests including FT93L (an Original Equipment Manufacturer test) and FT245 (International Follow-On Structural Test Project) have proven inconclusive mainly due to variations in the configuration of the wing tip stores in service and significant aerodynamic buffet. Loading at the outer wing representative of RAAF usage and store configuration was not achieved on either of these fatigue tests. A strict application of DEFSTAN 00-970 would therefore require the use of severe life reduction factors, which may lead to unacceptably short Safe Life Limits and an extensive Safety-By-Inspection program. Most of the critical structure in the outer wing requires substantial disassembly to allow inspection, including removal of the upper wing skin, which comes with significant costs and impact to aircraft availability. However, these tests have been useful in demonstrating the likely fail-safety of the outer wing structure as well as location of potential cracking. Both the test wings sustained loads above limit with damage including severed spars. It is thought that this excess load carrying capacity comes from the carbon fibre/epoxy upper and lower wing skins.

A new representative fatigue test would take at least several years to prepare and carry out to allow useful conclusions about the actual fatigue life of the outer wing. Considering that the RAAF F/A-18A/B fleet is currently projected to retire around the 2020 timeframe, the results would be available too late to be useful for the Aircraft Structural Integrity Program.

The F/A-18A/B Hornet Outer Wing StAtic Testing (HOWSAT) program is intended to substantiate a Through Life Management Strategy for the F/A-18A/B Hornet OW internal metallic structure by testing it with significant representative damage present [0]. The static test program will use damage scenarios derived from worldwide structural condition data, in addition to the fatigue damage demonstrated in the previous full-scale fatigue tests, to underpin a fatigue control plan for the OW in RAAF service.

Three representative damage load cases have been successfully applied to HOWSAT using the test rig shown in Figure 1. The testing of each representative damage load case involves the application 120% design limit loads for 12 static load cases. Ground vibration testing is also conducted to assess any changes in dynamic response due to the introduction of the representative damage. The deflections resulting from the maximum wing bending up and maximum wing bending down load cases are shown in the composite photograph of Figure 2.

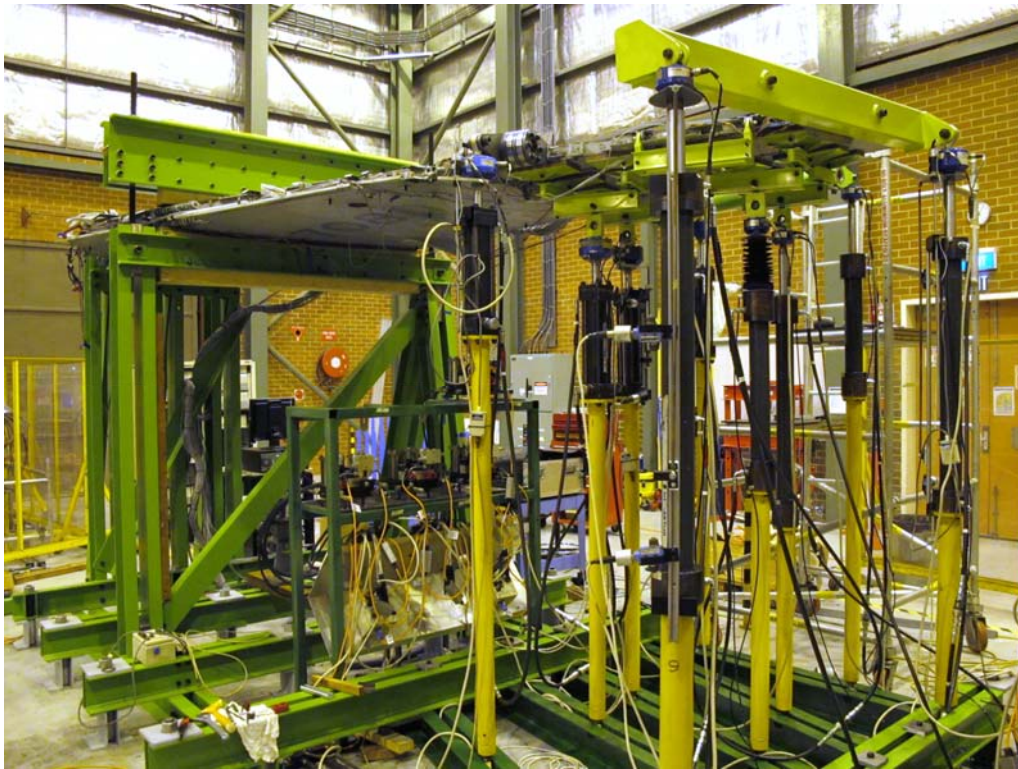


Figure 1 HOWSAT test rig configuration

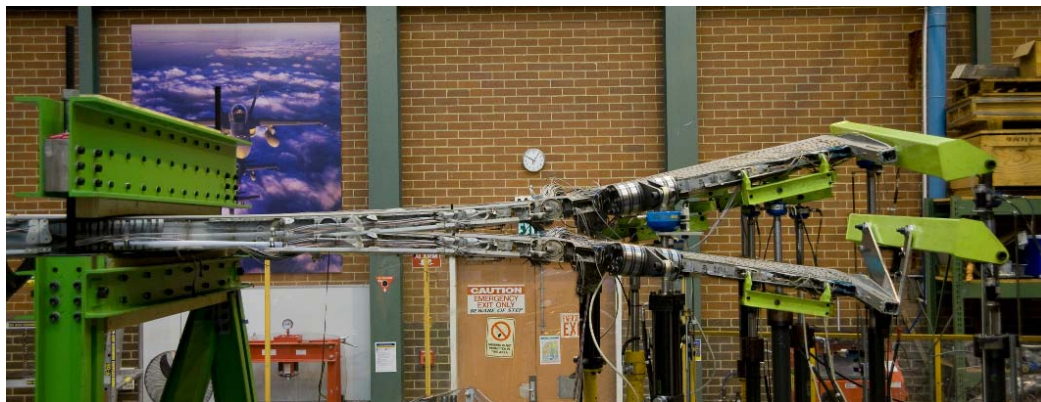


Figure 2 Composite photograph showing the deflections resulting from the maximum wing bending up and maximum wing bending down load cases. A different wing tip loading configuration is required for the wing down bending load cases due to load actuator displacement constraints.

Reference:

FLTLT G. Needham, SQNLDR R. Kloeden, The F/A-18A/B Hornet Outer Wing Static Test Program (HOWSAT), proc. Fourteenth Australian International Aerospace Congress, Melbourne, Aust., Mar 2011.

2.2.2 F/A-18A-D Flaw Identification through the Application of Loads (FINAL) Program - Geoff Swanton, (DSTO)

2013 marks the 10th year of structural testing of Classic Hornet aluminium alloy (AA) 7050-T7451 “centre barrels” (CBs) via DSTO’s “Flaw Identification through the Application of Loads” (FINAL) program. Since ICAF 2011 [1] a further two CB tests have been completed, bringing the total to 16. This is comprised of retired articles from the United States Navy, USN (7), Royal Canadian Air Force, RCAF (1), Royal Australian Air Force, RAAF (7) and the FT46 fatigue test article (1). The testing involves the application of representative flight spectrum wing root bending moment loads to the AA 7050-T7451 CBs via the wing attachment lugs. The main goal up until now has been to grow fatigue cracks to a point where they can be readily found, either by causing structural failure or through conventional non-destructive inspection (NDI) techniques. These cracks are subsequently analysed using quantitative fractography (QF) and the data are typically used in reassessing the safe life limit (SLL) of various discrete fatigue critical locations. In several cases the SLL has been extended such that the need for alternative costly and time consuming modifications has been eliminated. The number of QF reports stands at approximately 160 with over 1000 individual cracks examined to date.

Testing and teardown of the RAAF CBs with known service usage has also provided an unique opportunity to verify the RAAF Hornet individual aircraft fatigue monitoring system known as the Mission Severity Monitoring Program version 2 (MSMP2) [2]. It is believed that this work is the first example of using the crack growth in retired structure of known usage to verify a fatigue tracking system that incorporated significant ASI elements including tracking philosophy, structural fatigue lifing methodology, full-scale fatigue test results, design standard interpretation and retirement considerations. This work is ongoing.

The 17th CB test article is ex-USN and has been designated FINAL CB19, see Figure 1. This test started cycling in February 2013 and is being used to support several activities as summarised below:

- Validation/verification of a DSTO-designed bonded metallic doubler for the Y488 bulkhead “kick point” region. Although unmodified in fleet aircraft, previous FINAL testing has revealed cracking in this area. Therefore a proof-of-concept demonstrator on a full-scale test article is intended to support engineering investigations should this modification be considered for future structural integrity management options. (Reference 1, Section 2.2.2, mentioned testing this modification on an early configuration bulkhead).
- Reference 1 (section 2.1.4) presented an overview of supersonic particle deposition (SPD) being used primarily for protective coating applications as well as restoring the geometry of damaged or worn components. Preliminary coupon testing has also highlighted that the SPD layer is load bearing thus offering the potential to repair damaged structure. This CB is being used to test the durability of SPD applications on highly stressed regions of a full-scale aircraft structure subjected to representative

combat aircraft loads. Figure 2 shows the SPD application to FINAL CB19 at the Rosebank Engineering facility.

- In conjunction with the RCAF, a “hole salvaging” assessment activity will be conducted. This will involve oversizing certain fatigue critical holes (to simulate cracks that have been reamed out) at some midpoint in the test to assess the fatigue performance of these modifications for possible implementation into the fleet.
- Fibre optic sensors known as Fibre Bragg Gratings are being collocated or placed at mirror-image locations to the conventional foil strain gauges usually employed for monitoring strains. This test offers the opportunity to assess the accuracy and practicalities of using this technology for large component structural tests [3], see Figure 3.
- Previous CB tests have used DSTO’s portable thermoelastic stress analysis (TSA) technology to generate real-time stress contour imagery of highly loaded locations [4]. This has been used to provide visual comparisons of the effects of the pre- and post-modification of locations, as well as to validate finite element models. The TSA measurements typically rely on covering the area of interest in high emissivity black paint. This current CB test has been used to test the effectiveness of the TSA measurements using the aircraft’s default primer paint scheme, see Figure 4.



Figure 1: FINAL CB19 in the test rig at DSTO-Melbourne.



Figure 2: Robotic SPD application to the FINAL CB19 test article at Rosebank Engineering facility.



Figure 3: FBG sensor (labelled 20-04) collocated with conventional strain gauge foil on FINAL CB19 Y470.5 bulkhead.



Figure 4: DSTO's portable TSA capability showing IR camera mounted to test article and focussed on highly loaded bulkhead region coated in primer.

References:

1. Jackson, P. and Trasteli, C. "A Review of Australian and New Zealand Investigations on Aeronautical Fatigue During the period April 2009 to March 2011", DSTO-TN-0993. Defence Science and Technology Organisation, Australia, May 2011.
2. Molent, L., Barter, S. and Foster, W., "Verification of an Individual Aircraft Fatigue Monitoring System", Journal of Fatigue 2012; 43: 128-133.
3. Schembri, T., Tejedor, S., and Davis, C., "Strain Measurements using Fibre Bragg Gratings during Full-Scale Structural Testing of an F/A-18 Centre Barrel", Proceedings of the 4th Asia-Pacific Workshop on Structural Health Monitoring, Melbourne, Australia, 5-7 December 2012.
4. Rajic, N., Weinberg, S., and Rowlands, D., "Low-cost Thermoelastic Stress Analysis", Materials Australia Journal, March/April 2007.

2.3 IN-SERVICE STRUCTURAL INTEGRITY MANAGEMENT

2.3.1 Beta solutions for C-130J-30 wing damage tolerance locations based on handbook methods - Rebecca Evans, Manfred Heller (DSTO), Rebecca Gravina, A Clarke, and C Rock (QinetiQ Australia)

This work follows on from the ICAF 2011 input 'Computational approaches for the development of improved beta factor solutions for C-130J-30 DTA locations'. Background of this work is reiterated here. Beta factor determination work has been undertaken in the context of structural through-life support of the C-130J-30 Hercules fleet in service with the Royal Australian Air Force (RAAF). An indigenous Damage Tolerance Analysis (DTA) capability underpinning the adopted safety-by-inspection (SBI) management approach is being employed. Crack-front stress intensity factors; typically referred to as beta (or geometry) factors when given in non-dimensionalised form, represent a fundamental input to generating crack-growth curves on which to base the SBI thresholds and intervals.

Beta solutions have been determined using handbook methods and implemented using electronic spreadsheets (Microsoft® Excel) – refer to References [1] to [4]. One aspect of the work is that the C-130J-30 wing DTA locations have been categorised into five common structural configurations, whereby each configuration shares similar geometry, loading and crack phases, and thus the methods used to determine their beta solutions are similar. There is a separate spreadsheet for each of the thirty-three wing DTA locations analysed. For each location, cracking is typically split into multiple phases, and for each phase beta factors are determined for multiple crack sizes. These handbook results are obtained by compounding idealised handbook solutions and some new generic Finite Element Analysis (FEA) solutions (developed in support of this task) for specific phases. The pin and remote loads are applied separately and superposition is utilised to calculate the total beta from their corresponding individual beta contributions. Thus enabling the results (if loading is varied) to be transferable; eliminating the need to re-run analyses. The spreadsheets have been designed to allow variation of key parameters such as plate thickness, hole diameter, edge distance, and relative pin or remote loads. A comparison of handbook results with detailed 3D FEA for select cases has been undertaken for validation. For example, Figure 1 shows handbook solutions compared to the parametric FEA results for each crack phase for one of the integrally stiffened DTA geometries analysed (location OW-7D).

These beta solutions will provide the RAAF with an efficient indigenous capability to interpret results of the full-scale fatigue test and to support ongoing structural integrity management of their C-130J-30 fleet (including efficient DTA-based repair or re-design). The current results may be refined in the future based on the availability of more accurate local loading details from physical testing, large-scale FE loads models or through other stakeholders in the C-130 community via The Technical Cooperation Program.

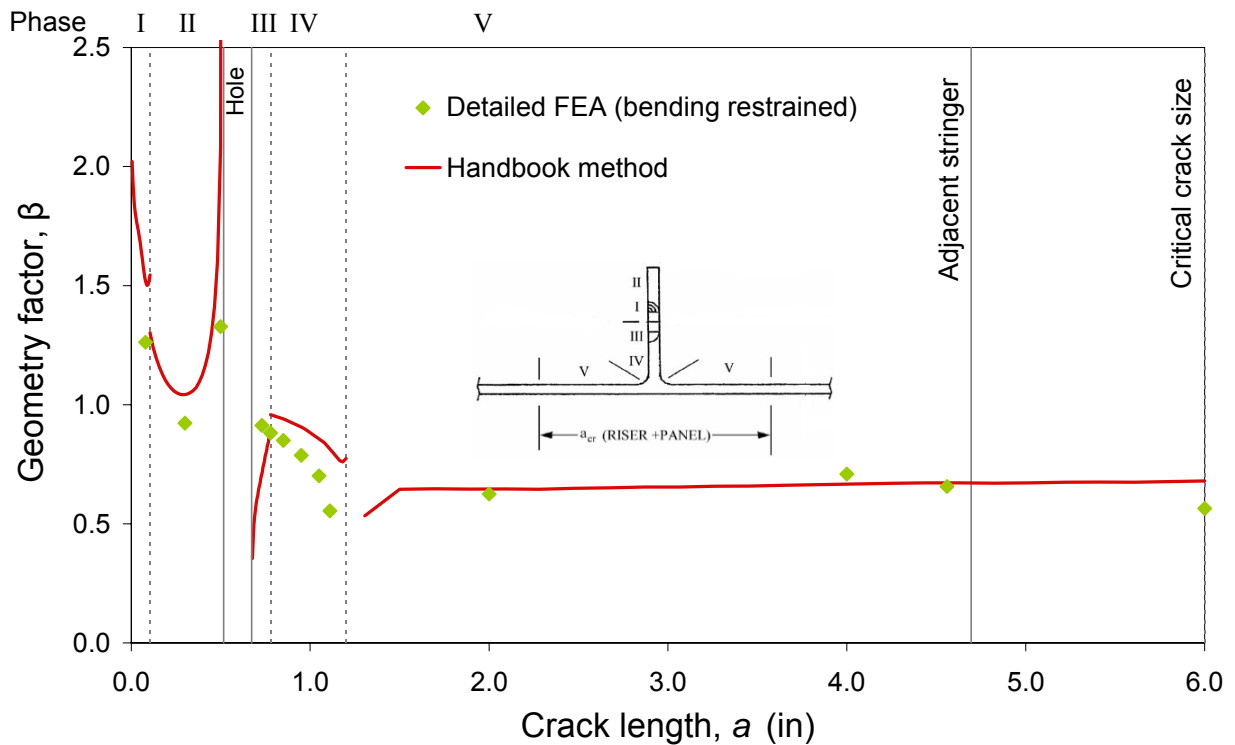


Figure 1: Typical handbook data and comparison with parametric 3D FEA (location OW-7D example, combined pin and remote loading).

References:

- [1] Clarke, A., Evans, R. and Heller, M., 'Beta Solutions for C-130J Wing DTA Locations Based on Handbook Methods, Configuration 3: Crack Growth in a Skin Panel with Integral Stringers', DSTO Minute, DSTO B2/129 Pt4, 23 February 2011.
- [2] Gravina, R., Evans, R. and Clarke, A., 'Beta Solutions for C-130J Wing DTA Locations Based on Handbook Methods, Configuration 1: Crack Growth in an 'L' Spar Cap Growing from a Horizontal or Vertical Section', DSTO Minute, DSTO B2/129 Pt4, 9 May 2011.
- [3] Evans, R., Clarke, A., Gravina, R., Heller, M. and Rock, C., 'Beta solutions for C-130J-30 wing damage tolerance locations based on handbook methods', DSTO report, DSTO-TR-2714, May 2012.
- [4] Evans, R., Clarke, A., Gravina, R., Heller, M. and Rock, C., 'Beta solutions for C-130J-30 wing damage tolerance locations based on handbook methods', presented at the 2012 Aircraft Airworthiness & Sustainment Conference, Brisbane QLD, 24-26 July 2012.

2.3.2 User Manual for the C-130J DSTO Global Finite Element Model Version C130J-DSTO-v1.0 - Michael Opie, (DSTO)

A global Finite Element Model (FEM) of the C-130J airframe is an important supplementary tool to aid in support of both current and future Royal Australian Air Force (RAAF) C-130J structural integrity management. The finite element model described in this document was originally developed by the Mercer Engineering Research Center (MERCER) in Georgia, USA and made available to the Defence Science and Technology Organisation (DSTO). It has recently formed a major element of the United States Navy (USN) Naval Air Systems Command (NAVAIR) ongoing C-130 structural integrity support program.

This document has been provided as a user manual for the DSTO version of the C-130J NASTRAN FEM. The purpose of this manual is to provide enough detail to allow a user of this FEM to understand how the model is organised and to easily incorporate changes to the model. A brief history of the FEM is presented which describes the current C-130J model's development from its origin as a Naval Air System Command (NAVAIR) sponsored C-130H model. The configuration of the current C-130J representation is described. The global model is organised into sub-models (see Figure 1) with defined numbering ranges in order to make it more efficient to work with. Most of the descriptions of the model entities are provided as annotated figures showing the finite element idealisations of the aircraft substructures. Model quality checks similar to those described in [1] and [2] were developed and applied to this FEM and the results summarised as shown in Figure 2. This user manual is an important document to aid in the use of the C-130J global FEM to support on-going and future wing fatigue test (WFT) test interpretation activities. It will also be useful for the future conversion of this model into the stretched C-130J-30 RAAF version of the aircraft.

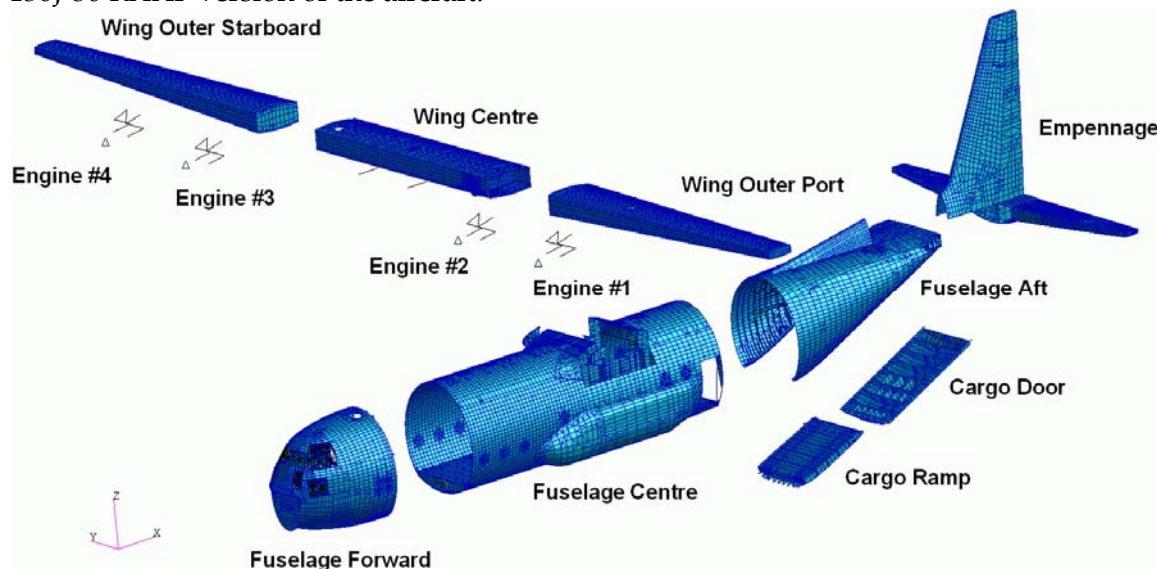


Figure 1 - C-130J global finite element model separated into sub-models

Mass					
	FEM	Expected	Difference		
Total	9.166076E+04	9.166076E+04	0.000000E+00	0.00%	FAIL
					1% WARNING
					0.01% PASS
CG					
	FEM	Expected	Difference		
X	5.169232E+02	5.169232E+02	0.000000E+00	0.00%	FAIL
Y	4.353496E-01	4.353496E-01	0.000000E+00	0.00%	1% WARNING
Z	2.363472E+02	2.363472E+02	0.000000E+00	0.00%	0.01% PASS
Maximum Displacements for 1G Load					
	FEM	Expected	Difference		
X	2.276141E+00	2.276141E+00	0.000000E+00	0.00%	FAIL
Y	3.846798E+00	3.846798E+00	0.000000E+00	0.00%	5% WARNING
Z	6.368333E+00	6.368333E+00	0.000000E+00	0.00%	1.00% PASS
Work Error (Epsilon) Check					
1Gx	7.61998E-12				FAIL
1Gy	-4.29224E-12				1.00E-06 WARNING
1Gz	-1.00100E-11				1.00E+09 PASS
Load Equilibrium Check					
1Gx	0.00%				FAIL
1Gy	0.00%				1% WARNING
1Gz	0.00%				0.10% PASS
Rigid Body Residual Strain Energy Check					
G Set	PASS				FAIL
N Set	PASS				PASS
F Set	PASS				
A Set	PASS				
Free-Free Normal Modes Check					
Mode	Frequency	F7/F Ratio			
1	1.192628E-05	1.673913E+05			FAIL
2	1.108211E-05	1.801421E+05			1.00E+04 WARNING
3	9.372503E-06	2.130013E+05			1.00E+05 PASS
4	8.011481E-06	2.491868E+05			
5	5.163072E-06	3.866603E+05			
6	1.001406E-05	1.993552E+05			
7	1.996355E+00				

Figure 2 – Nastran C-130J finite element model quality check summary

References:

1. Stockwell, A.E., *A Verification Procedure for MSC/NASTRAN Finite Element Models*, NASA Contractor Report 4675, June 2005.
2. Tillman, F., Galletly, R., Zins, J., *MSC/NASTRAN Model Checkout*, MSC NASTRAN User's Conference, Universal City, California, 20-21 March 1986.

2.3.3 C-130J Wing Fatigue Test Article Finite Element Model Validation and Determination of Test Representativeness - Michael Opie, (DSTO) and Jack Lubacz, (Qinetiq Australia)

The primary aim of the C-130J Finite Element Model (FEM) correlation activity was to develop the extant C-130 global FEM to the point whereupon correlation/validation against Wing Fatigue Test (WFT) structural response can be performed at key structural locations. The model is intended to be utilised to assess key areas on test where loading/constraint representativeness is potentially compromised. The objectives of the C-130 Finite Element Analysis (FEA) activities were the following:

1. Creation and validation of a FEM representing the Wing Fatigue Test article (WFTA).

2. Validation of WFT as representative of actual aircraft structure by correlating WFT FEA results to C-130J FEA results for equivalent loading.

A FEM representing the C-130J WFTA was created by using the wing sub-model from the DSTO C-130J global FEM (see Figure 1). This WFTA FEM was validated by correlation of the WFTA FEA predictions to the actual WFTA strain and displacement data. A small set of the WFT strain gauges were chosen for correlation. The criteria for selection of these gauges were: i) linear response, ii) response level above a minimum threshold, iii) location in an area of low strain gradient. The correlation shows that for the strain gauge locations chosen, the predictions match the test data to within about 10% in most cases (see Figure 2).

In order to validate the WFTA as representative of the behaviour of full aircraft structure, correlation of the WFTA FEM predictions to the global aircraft FEM predictions for equivalent load cases was performed. Some variability between the two models was found, although this was expected since the WFTA FEM lacks both the curved portions of the fuselage and an accurate representation of the engine nacelle structures. Overall, the FEA results presented show that the WFTA FEM correlates well with the general behaviour of the global C-130J FEM to within about 20% for strain and about 15% for displacements (except for some inboard wing stations with phase 3 loads which can be in error by more than 25%). Specifically, the areas validated were the wing to fuselage interface and the wing carry through lower surface subject to pressurisation. Both the WFTA FEM and C-130J global FEM can be used for future test interpretation activities provided that the areas of interest are well covered by the correlated strain gauges and that appropriate uncertainty factors are used.

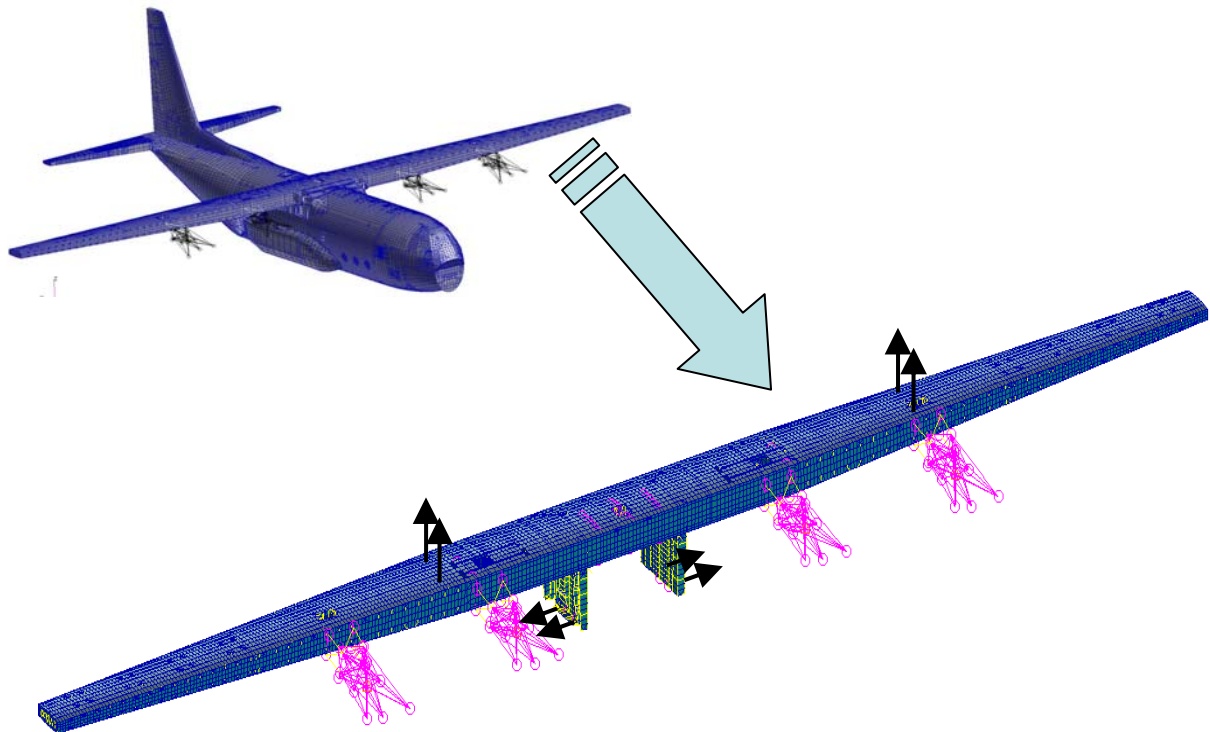


Figure 1 - A FEM representing the C-130J wing fatigue test article (WFTA) was created by using the wing sub-model from the DSTO C-130J global FEM.

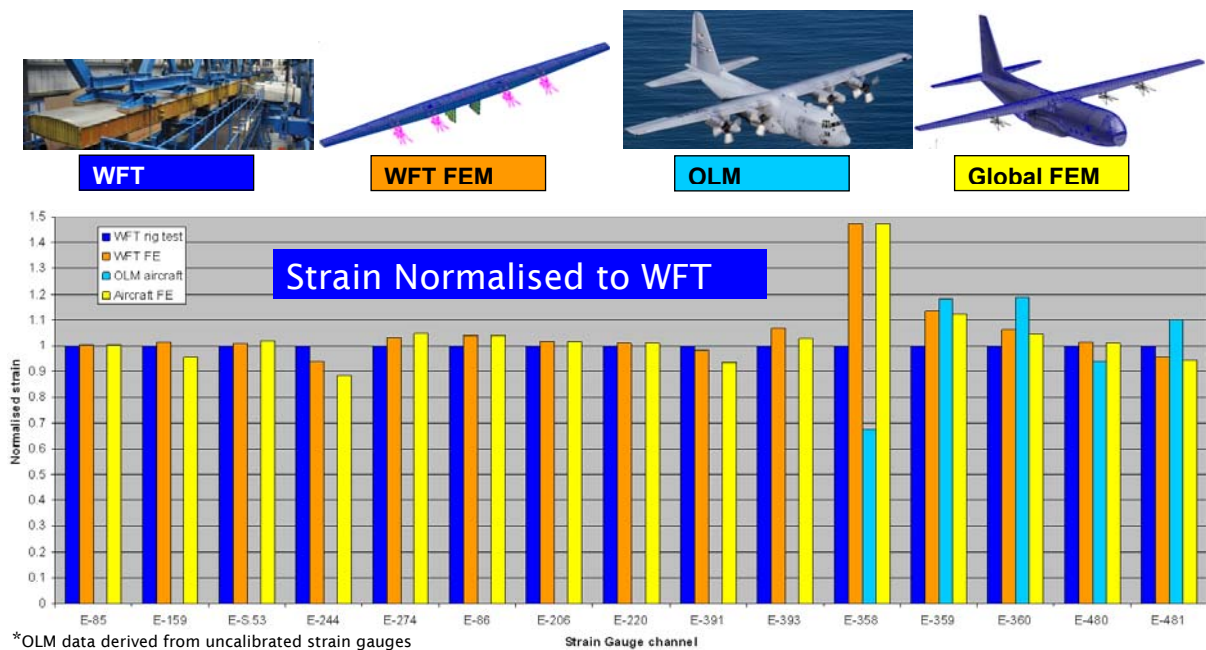


Figure 2 - Validation of the wing fatigue test by strain correlation for maximum bending. WFT validated as representative of actual aircraft structure

2.3.4 P-3C Structural Management Update - Andrew Walliker (DSTO), Kevin Watters (QinetiQ Australia) and FLTLT Greg Brick (ASI-DGTA)

This update describes efforts and achievements for management of the safety by inspection program for the P-3C aircraft.

Background

As reported in the previous National Review, structural integrity assurance and certification for the RAAF P-3C fleet was originally achieved through a safe life approach under CAR4b regulations. About 10 years ago the fleet were approaching their calculated safe life and other operators around the world were facing similar issues. Australia then entered into a program called the Service Life Assessment Program (SLAP). The SLAP was a comprehensive international collaborative program involving Australia, the United States, Canada and the Netherlands. Key aspects of the SLAP included full scale fatigue tests, coupon testing and analytical model development. In Australia the results from the SLAP were interpreted using a Test Interpretation (TI) methodology suitable to then construct a Structural Management Plan (SMP) which would achieve a transition of the

fleet to a safety by inspection certification basis under FAR 25.571. The SMP has now been implemented on the RAAF fleet and about three quarters of the fleet have so far been inducted into the first (SBI1) inspection regime. In late 2009 the RAAF formalised their objectives in terms of specific increases in thresholds and inspection intervals. Achievement of these goals will both enable the fleet to meet the Planned Withdrawal Date (PWD, currently 2019+), and to realise major cost savings and enhanced fleet availability. The ultimate aim of this change in management was to reduce the number of major SBI servicings from four to three, as shown in figure 1. Despite the aircraft nearing its end, there are several major tasks requiring completion in order to realize a PWD of 19,000 P-3C AFHRs. The following program elements are essential to enabling this:

- 2010 Structural Management Plan (SMP) Review Update
- Individual Aircraft Tracking System Software Input Updates
- Structural Data Recording Set (SDRS) Calibration
- Intergranular Corrosion - Fatigue Interactions.

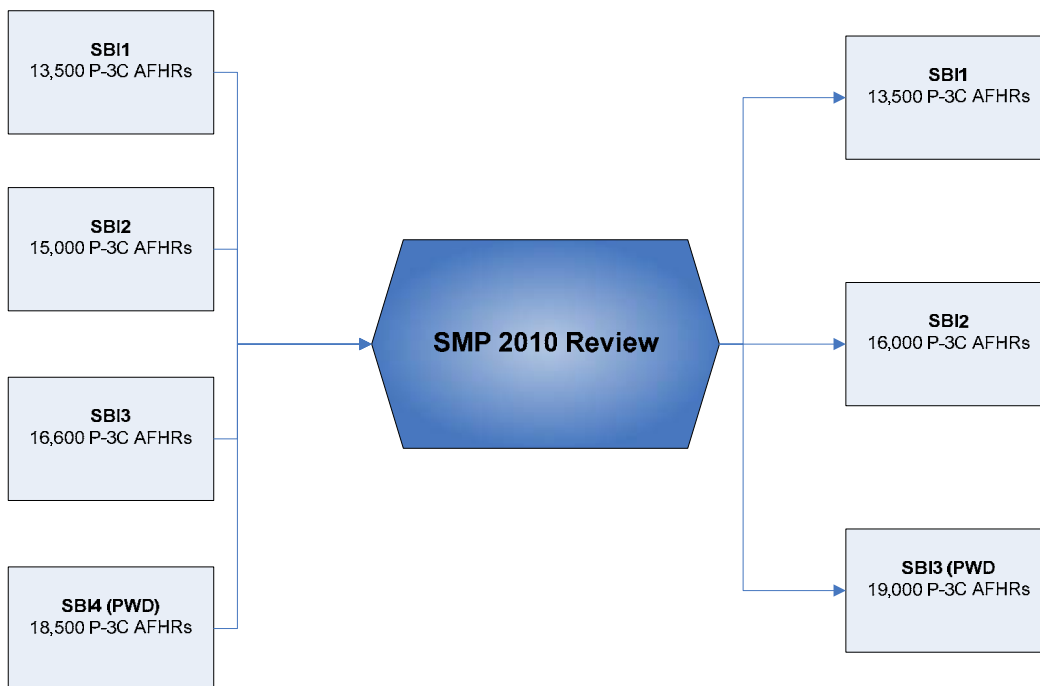


Figure 1: Reduction in SBI servicing requirements

2010 Structural Management Plan (SMP) Review Update

From 2009-2011, DSTO planned and conducted a large scale re-examination of the inspection requirements of the P-3C. This involved applying the results of improved lifing tools, such as FAMS and FASTRAN, as well as additional testing of Coupons and Components, with a variety of preconditions (such as Cold Working) introduced. This additional and extensive testing provided the conditions for the new and extended inspection thresholds and intervals to be achieved. In the last two years, the focus has been

on the reporting of the results of that testing, and the extensive and elaborate activities required to gain RAAF acceptance. The final reporting extends to some three thousand pages of results, spread over more than half a dozen different documents, all interrelated. With planning aspects requiring significant lead time to be effective, report results were released in draft form, prior to publication, so that questions could be answered and problems identified. Several issues have been identified that require further work to satisfy all the requirements outlined in the original 2010 SMP Review Functional Specification.

In rectifying the issues identified with the draft SMP, Independent Validation and Verification (IV&V) on the DSTO draft SMP and development of the RAAF issue of the SMP was conducted by QinetiQ, a defence contractor. This also included some engineering development to cover gaps identified by the IV&V. Areas of engineering development included:

- life improvement factors for various cold worked hole configurations,
- adjustment of inspection thresholds and intervals to account for SLAP residual strength testing deficiencies,
- engineering judgment assessment for the management of structural locations not adequately tested or analysed in the SLAP, and
- assessment of RAAF fleet condition data as a potential adjustment of the SMP.

In the lead up to the SMP update, QinetiQ performed two related engineering assessments. The first was a thorough audit of the transition of the fatigue management of the RAAF P-3 fleet to durability and damage tolerance management against the requirements of FAR 25.571. A number of issues from that audit were resolved during the development of the updated RAAF SMP. The second assessment was of the full operational loads monitoring database from 6 instrumented RAAF P-3Cs to re-characterise the RAAF P-3C operations into 36 missions and sub-missions with updated profiles for speed, altitude, landings, weights, etc.

One particular fatigue critical area which required additional consideration during the 2010 SMP review update was the aft pressure bulkhead frame at Fuselage Station (FS) 1117. Cracking in the frame was first reported during the RNZAF Kestrel program, but has since been identified by the CF in their entire fleet and the USN has noted cracking in several aircraft. The RAAF conducted initial inspections in 2008 and has since identified various forms of FS1117 cracking in several airframes, necessitating the creation of a refurbishment program. This program, to be conducted in conjunction with the SBI servicing, will seek to repair or replace the FS1117 frames in order to provide suitable structural life out to the PWD. Figure 2 below shows the FS1117 frame replacement prototyping at Australian Aerospace conducted in late 2012. Complete removal of the rear tail required additional development and new GSE developed by the maintenance organisation; AA. Beyond a repair developed by Lockheed Martin, AA has also conducted development of a repair option that is suitable for incorporation without removal of the tail; a significant saving in maintenance effort.



Figure 2: Empennage removal for FS1117 refurbishment

Individual Aircraft Tracking System Software Input Updates

Over this same period of time, extensive effort has been expended on determining the unit Damage inputs for software that supports Individual Aircraft Usage Tracking. This work utilises the tools already developed for the 2010 SMP Review. The product of this effort will be Unit Damage values for different Mission Types, along with the damage changes for changes in duration and Touch and Go landings.

This work has built upon the redefinition of typical usage profiles for current AP-3C flying, based on the accumulation of flight profile information from the SDRS system. Also, as the IAT system is moving from an 8 profile model to a 32 profile model, additional UDMs would be required. Update to this system will ensure accurate modeling of fatigue accrual for the aircraft out to PWD. It will ensure maximum use of available airframe hours whilst maintaining compliance within the P-3 certification basis.

SDRS Calibration

The RAAF AP-3C fleet has several aircraft fitted out with the Structural Data Recording Set (SDRS) system, but the strain gauge installation has never been calibrated, and thus is not used to its full potential. DSTO, ASI-DGTA, MPSPO and QinetiQ have embarked upon a programme to get the system calibrated. Due to significant operational pressures and a lack of available aircraft, it has proven extremely challenging to get the requisite hanger space, flight crew and platform available for the duration needed to achieve a ground calibration for all of the sub-fleet. So, to offset this, a substantial effort has been invested in trying to validate a Flight Calibration Approach. To date, lack of aircraft with a suitable

permissible flight envelope has prevented this from occurring, but further efforts over the next calendar year should see this situation change. Eventually, this calibrated data will be used to validate the IAT software and updates ensuring a robust and compliant system out to PWD.

Intergranular Corrosion – Fatigue Interactions.

With a solid understanding of AP-3C Fatigue, it was decided that next major hurdle for getting the fleet to PWD would be the presence of substantial corrosion in the fleet. While pitting and surface corrosion have been studied in some detail in the past, Intergranular Corrosion, particularly its influence on Fatigue life, was not so well understood. So, capitalising upon the recent extensive experience of fatigue through the SMP 2010 review, a new coupon test program was generated with the difference being that these coupons would have Intergranular Corrosion introduced and grown prior to testing. Several corrosion protocols were trialled and one was selected that would grow IGC to a depth of at least 2mm. This would ensure that the results would be reflective of corrosion within the granular layers and not purely the introduction of surface damage in the holes. Several coupons have already been tested through this process and the effort to examine the degree of corrosion and peg it back to the fatigue has begun.

Summary

The SBI and associated programs represents a huge level of effort from the RAAF, DSTO and QinetiQ organisations. They are essential to providing an enduring maritime and surveillance capability for the ADF. A reduction in SBI from four to three servicings represents an estimated 25% reduction in total maintenance costs.

Alternative activities that may have provided a similar life extension to the RAAF P-3 was structural refurbishment in the form of new wings, similar to that being undertaken by the Canadian Force, United States Navy and already completed by the Royal New Zealand Air Force. It is estimated that the SBI program for the entire RAAF fleet was achieved for the same cost as the structural refurbishment of four aircraft. This figure considers both the development/engineering costs of the SBI program as well as the actual maintenance and inspection costs of the servicing.

Despite its proximity to PWD, there are still major tasks yet to be completed that will ensure maximum exploitation of available airframe hours. This is essential given the P-3's continuing role in high profile tasks of maritime surveillance and patrol in Australia's Northern approaches.

2.3.5 P-3 Skin Panel Assessment - S. Bandara, T. Cooper, Kevin Watters (QinetiQ Australia)

The Royal Australian Air Force (RAAF) operates a fleet of 18 P-3 aircraft. A flight test program identified vibration issues with P-3 aft fuselage lower skin panels. QinetiQ were tasked with conducting an assessment to determine the fatigue implications of the aft fuselage lower skin panel vibration.

QinetiQ conducted vibration analysis using both classical and Finite Element Analysis (FEA) methods. FEA models of the skin panels were developed for a range of configurations covering both flat and curved skin panels. It was indicated that the boundary conditions for the skin panels are in between Simply Supported (SS) and Fully Fixed (FF) conditions and therefore both these conditions were also considered. Figure 1 shows FEA of the P-3 aft fuselage skin panel.

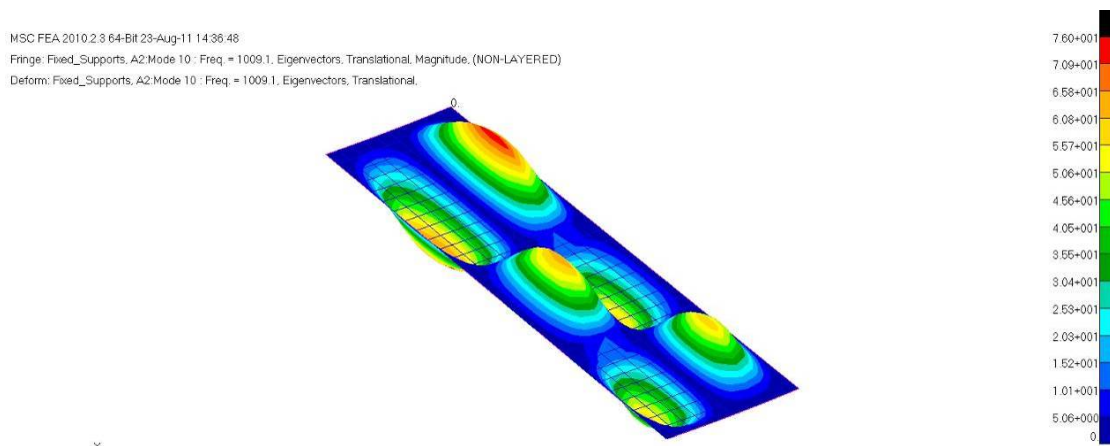


Figure 1: FEA model of P-3 Aft Fuselage Skin Panel

Ground Vibration Test (GVT) data and flight test acceleration and strain response data was available for the skin panels. Defence Science and Technology Organisation (DSTO) reviewed this data and generated Power Spectral Density (PSD) data files which were then provided to QinetiQ. These PSDs spanned a frequency range of 1 Hz to 2000 Hz and contained all relevant test events. QinetiQ used this data to develop PSDs representing average flight levels ('Avg PSD', likely scenario) and maximum flight levels ('Max PSD', conservative scenario) for use in vibration analysis. Typical 'Max PSD' data used for vibration analysis is shown in Figure 2.

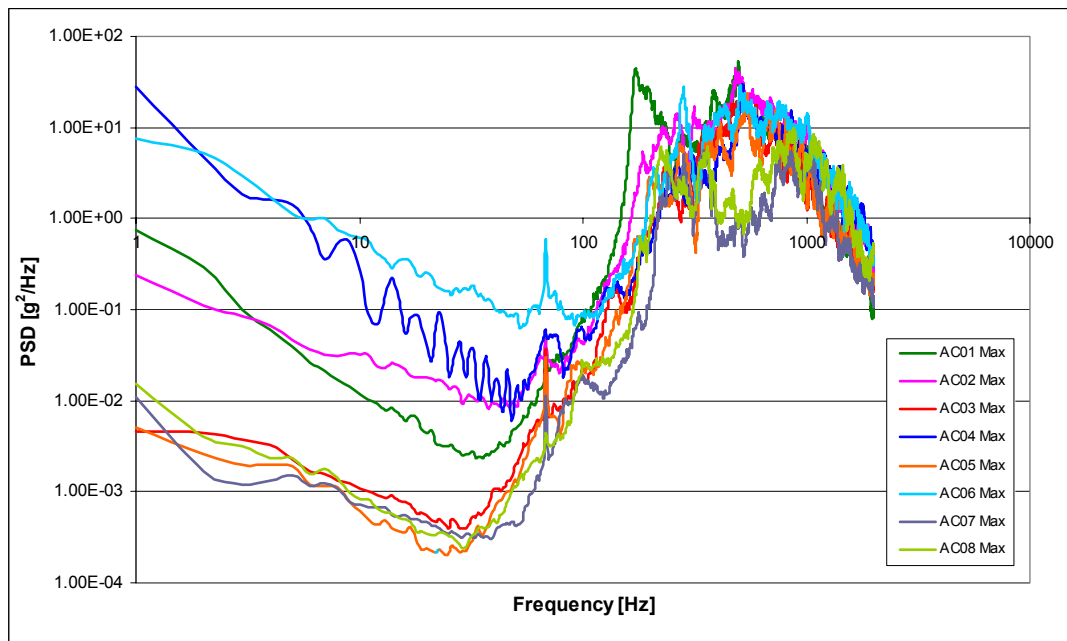


Figure 2: Max PSD Levels for Accelerometers

Using transfer functions allowing for the damping measured in the GVT, input functions were derived to reproduce the flight measured response using the FEA. Using the response PSD curves, it was possible to calculate Root Mean Square (RMS) G levels which could then be used with a 1 G static stress distribution to develop peak stresses at various panel locations. These peak stresses were then used with 2024-T3 fatigue data to derive fatigue lives. For the 'Avg PSD' case, the 'Three Band Technique' which employs a Gaussian distribution was used. For the 'Max PSD' case, the RMS stress arising from the RMS G level was assumed to act unfactored for 100 per cent of the time, since this was an envelope case encompassing the peak load condition.

The S-N data in the MMPDS is limited to $1.00E+08$ cycles. Because of the high frequency range of the response (fundamental frequencies up to 500 Hz), the data limit of $1.00E+08$ cycles would provide an artificial unrepresentative limit to the analysis. Therefore, extrapolations of the MMPDS data were developed. Three fatigue analysis scenarios were considered including the use of a linearly extended S-N data range as well as cut-off scenarios of $1.00E+10$ cycles and $1.00E+12$ cycles. The use of large fatigue lives based on the complete extended S-N curves which were significantly beyond the material test range was considered to present a significantly increased risk. Therefore, the cut-off scenarios were considered a more practical approach, with the $1.00E+10$ cycle cut-off incurring the least risk.

The fatigue lives calculated may be used with suitable factors to develop safe lives and Safety By Inspection (SBI) intervals for the aft fuselage skin panels.

2.3.6 C-130J Counter Measure Dispenser System Structural Substantiation - S. Bandara, Kevin Watters, R. Stewart (QinetiQ Australia)

The Royal Australian Air Force (RAAF) C-130J contains an AN/ALE-47 Counter Measure Dispenser System (CMDS) which provides the airplane with a means of defence against threats from surface-to-air missiles and air-to-air infrared and radar guided missiles. QinetiQ was tasked to carry out structural substantiation of the CMDS and support structure for RAAF operations.

The CMDS consists of dispensers which are mounted on a number of locations on the C-130J including the nose, mid-fuselage and tail. The panel used to mount the mid-fuselage dispensers is shown in Figure 1.



Figure 1: C-130J Mid-Fuselage Dispenser Panels

The assessment involved identifying the key structure that supports the dispensers at the nose, mid-fuselage and tail locations. A simple dynamic model was developed to characterise the motion of the structure when stores were dispensed. The firing frequency of dispenser stores overlaps the natural frequency of the support structure and induces significant structural vibration. At each dispenser location, the system was characterised by estimating the key parameters of the support structure including mass, inertia, stiffness, damping, and natural frequency using GVT data available from Defence Science and Technology Organisation (DSTO) testing. Typical response of the CMDS for a generic firing sequence is shown in Figure 2.

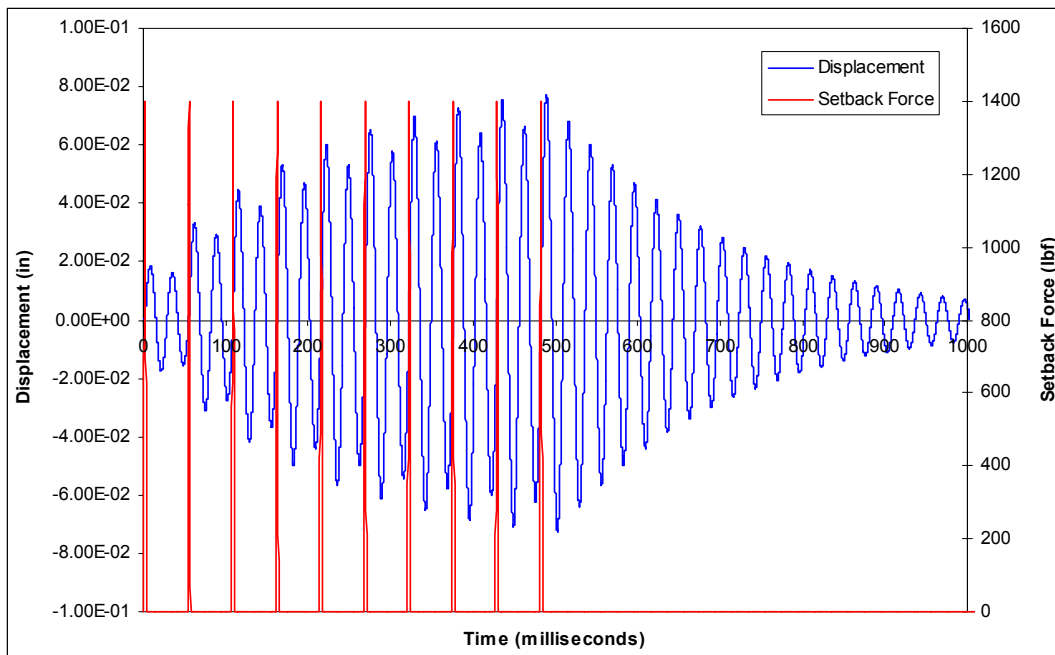


Figure 2: C-130J CMDS Response

The dynamic loads that were obtained from the dynamic model were assessed relative to known baselines where possible. These baselines were previously Original Equipment Manufacturer (OEM) cleared dispensing intervals for specific store types. Observations from the load assessment where the dispense intervals were integer multiples of the system period produced the most severe response. These were recommended to be avoided in programming the flare/chaff sequences.

For the mid-fuselage dispenser, it was found that the structural natural frequency was very sensitive to the mass which changes as the dispenser empties. The response builds and decays as the mass of the dispenser changes as stores are ejected which affects the natural frequency of the supporting structure. The CMDS response which shows the interaction between the structural natural frequency and the store firing frequency is shown in Figure 3. This required that some frequency bands needed to be avoided to ensure resonance did not occur.

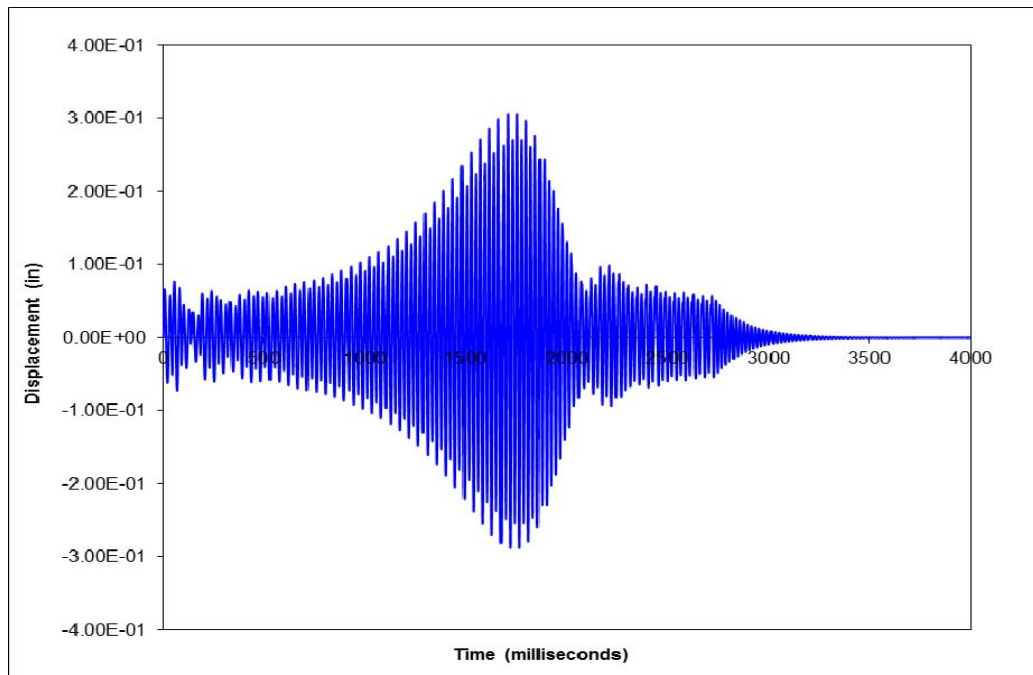


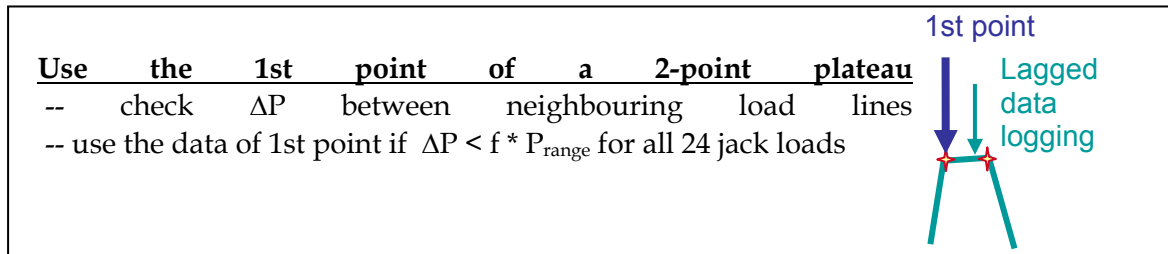
Figure 3: C-130J CMDS Response with Mass Reduction

The use of OEM baselines ensured that static and damage tolerance considerations were already covered for some locations. Additional limited static analyses were conducted to demonstrate high margins of safety. Durability and damage tolerance analyses were also conducted to demonstrate that the structure was both durable and damage tolerant with reasonably large lives. It was recommended that the RAAF manage the dispenser support structure via inspection of the structure.

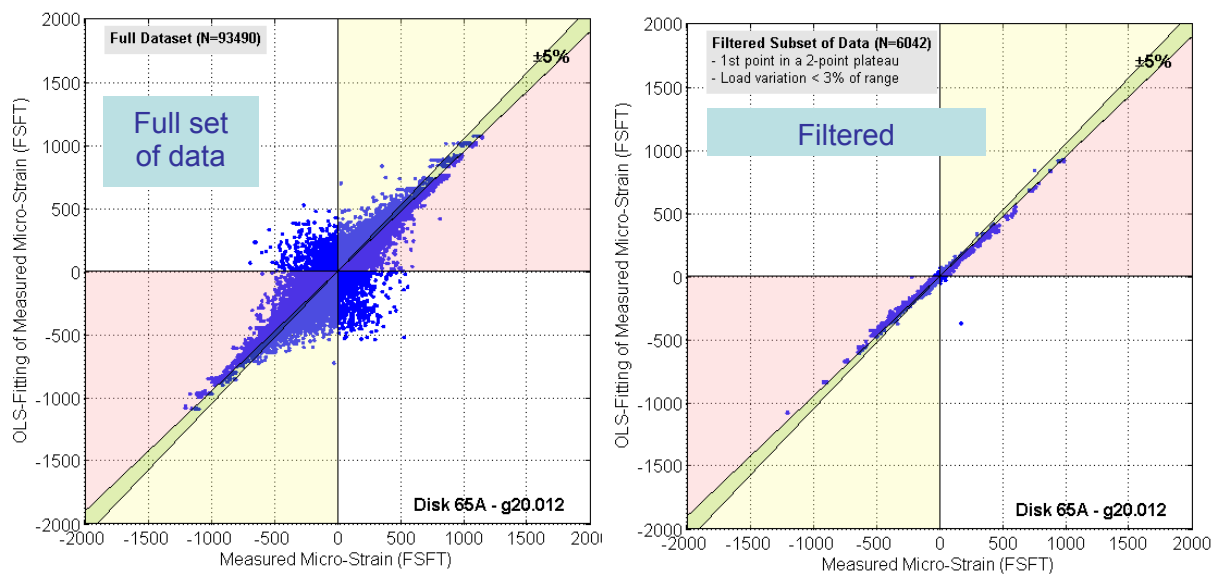
2.3.7 Assessment of Training Aircraft Full Scale Fatigue Test Data for Reliable Validation of Global Finite Element Models - Xiaobo Yu, Robert Kaye and Michael Opie, (DSTO)

A current training aircraft structural recertification program plans to use computational structural mechanics to reveal hot spots and support fatigue and residual strength analysis. The correctness and applicability of finite element models therefore need to be assessed, by processes including verification and validation. This paper [see reference] spins off an investigation that used archived DSTO full scale fatigue test (FSFT) data to validate global finite element models. It reports a set of approaches that can be used to achieve a more reliable validation. These include: (i) spectrum asymmetry analysis and reverse-engineering of existing test data to retrospectively reveal jack load sign conventions of the as-recorded data; and (ii) linearity check and load line filtering to tackle out-of-phase data logging in test. The effectiveness of these approaches is demonstrated by comparing finite element model predications with full scale fatigue test data.

Figure 1 illustrates the scheme of load-line filtering and its effectiveness in reducing non-linearity within the FSFT data.



(a) Scheme of load-line filtering



(b) Correlation plot of the full set of data

(c) Correlation plot of the filtered data

Figure 1. (a) Scheme of load-line filtering; (b) and (c) Correlation between as-recorded and OLS-fitting of FSFT data, showing that the non-linearity within the FSFT data was significantly reduced by applying a load-line filter. (OLS refers to Ordinary Least Square, which is an approach to linearly fit the FSFT data)

Reference:

Xiaobo Yu, Robert Kaye and Michael Opie, Assessment of training aircraft full scale fatigue test data for reliable validation of global finite element models, In: 15th Australian International Aerospace Congress, AIAC15, 25-28 February, Melbourne, Australia.

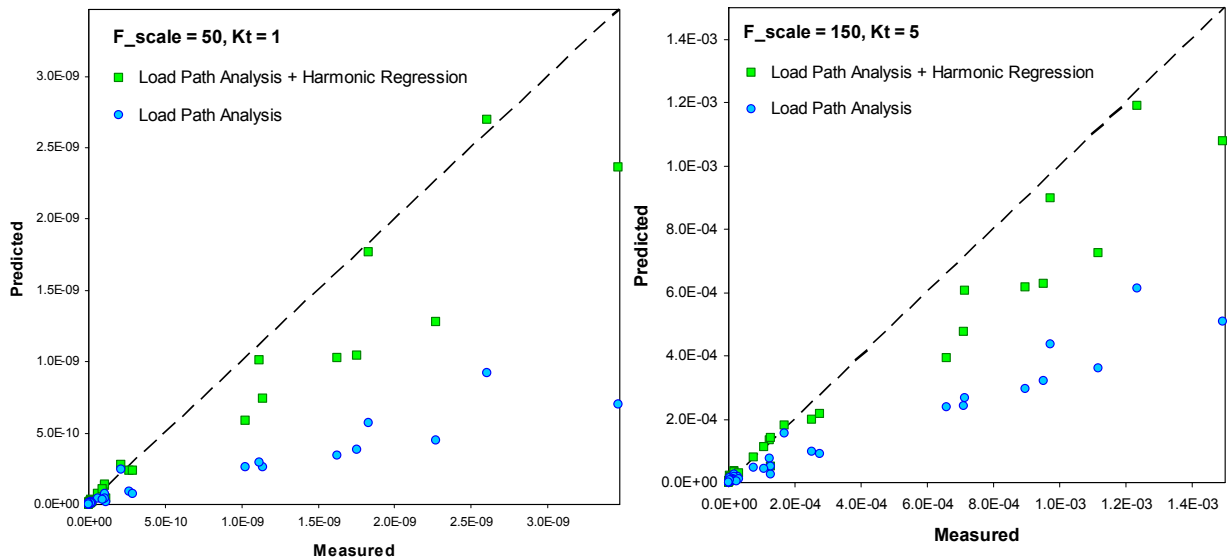
2.3.8 Integration of Load Path Analysis and Harmonic Regression for Usage Monitoring of Helicopter Dynamic Components - Xiaobo Yu and John Vine, (DSTO)

Usage monitoring of individual fatigue-critical dynamic components on helicopters can lead to reductions in maintenance costs and improvements in fleet management. Around the world, many approaches have been proposed and investigated, which can be catalogued into: flight region recognition, flight load remote synthesis, and flight load direct measurements, ordered in a sequence of increasing level of accuracy. Nevertheless, an increasing level of accuracy in usage monitoring is usually associated with increasing level of instrumental complexity and costs, and/or, lower level of technical readiness. In the Defence Science and Technology Organisation (DSTO) in Australia, the balance between the accuracy, costs and potential technical readiness has been assessed and it was decided to pursue the remote load syntheses approach.

Based on the Joint USAF-ADF S-70A-9 Blackhawk flight strain survey data, DSTO has investigated a number of remote load synthesis approaches. From this, the load path analysis and harmonic regression were recognized as two of the most promising approaches. The load path analysis is a deterministic approach based on the force and moment equilibrium across the swashplate assembly. As demonstrated in a number of level flight cases, it allows accurate synthesis of the collective and cyclic components of the main rotor pitch link (MRPR) load from the measurements on three stationary servo links. This is a forward-engineering approach, allowing no parameter tuning, therefore the transfer function for load synthesis is not affected by measurement errors. However, the structural layout of the swashplate assembly has prohibited the reactionless component of the MRPR load to be synthesized by this approach. On the other hand, the harmonic (amplitude-phase) regression is a reverse-engineering approach, which is able to reveal either deterministic or non-deterministic relationships. Apart from the difficulties in phase prediction, the harmonic regression has demonstrated to be a promising approach.

A follow-up study [see reference] was thus performed, integrating the load path analysis with the harmonic regression. The role of the load path analysis was to predict the collective and cyclic components of the MRPR load, and the role of the harmonic regression was to predict the $2f_{MR}$ term of the reactionless component of the MRPR load. For all 42 level flight runs under investigation, only five strain gauge channels are selected as prediction parameters.

Figure 1 compares the relative damage calculated from the measured and predicted MRPR load histories. For each of the 42 level flight runs, the relative damage was calculated using the Miner's rule after a rain-flow cycle counting according to the ASTM standard. The MRPR load was treated as an indication load. Therefore sign-reversal was applied and a range of scaling factor (F_{scale}) and K_t values were assumed. The plots indicate that the integrated approach is able to predict relative damage within an approximated -30% and +5% error range for the runs that accumulate the most damages per second. This result is encouraging given that only five prediction parameters were used.



(a) $F_{scale} = 50, Kt = 1$ (max rDps = $3.46e-9$) (b) $F_{scale} = 150, Kt = 5$ (max rDps = $1.49e-3$)

Figure 1. Comparison of relative damage calculated from the measured and predicted MRPR load histories of 42 level flight runs. (rDps refers to relative damage per second)

Reference:

Xiaobo Yu and John Vine, Integration of load path analysis and harmonic regression for usage monitoring of helicopter dynamic components, In: 15th Australian International Aerospace Congress, AIAC15, 25-28 February, Melbourne, Australia.

2.3.9 Helicopter Airframe Fatigue Spectrum Generation and Truncation – Luther Krake (DSTO)

Helicopter airframe fatigue cracking is a cause of significant and growing cost of ownership and operational readiness concerns for the operators of (primarily) metallic airframe helicopters. Airframe fatigue has often been overlooked for helicopters with research and design concentrated on understanding the fatigue of the rotating structural components such as rotor blades and pitch links due to their safety implications. The Australian Defence Science and Technology Organisation (DSTO) and Naval Air Systems Command (NAVAIR) are collaborating to develop improved methods and technologies that can be used to assess the fatigue damage endured by helicopter airframes thereby opening the way for more modern and cost-effective analysis or test-based fatigue management programs for their service customers.

A key preparatory step in any analysis or test of a helicopter airframe is to develop a detailed understanding of the flight load sequences – or fatigue spectra – it experiences. In the past, ‘standard’ loading sequences such as Helix and Felix have been developed for rotating components but these are not directly applicable to the airframe. Airframe fatigue spectra have been developed for several previous helicopter airframe certification tests; however, these spectra were generally heavily simplified for reasons such as computational efficiency, test practicality and cost. Real airframe fatigue spectra are likely to be influenced by the modes of vibration that might be present on the airframe, the attenuation of the vibratory loading that is introduced at the main and tail rotors and the relative magnitudes and influences of both quasi-static (manoeuvre induced) and vibratory loading. To better capture such complexity, more realistic, higher fidelity fatigue spectra are required.

To this end, DSTO has developed novel computer-automated fatigue spectrum generation and truncation algorithms. Fatigue spectrum generation is the process of pseudo-randomly creating realistic flight-by-flight sequences of flight conditions and assigning flight loads data to those sequences. The sequencing part of this operation involves randomly selecting flight conditions and arranging them according to a set of so-called ‘regime sequencing rules’ (i.e. piloting heuristics). The rates of occurrence and time allocations for each flight condition in the sequence have been, initially, based on those defined in the Design Usage Spectrum (DUS) for the subject helicopter. Loads data can consist of measured airframe stress responses, applied rotor loads (i.e. forces and moments) or flight state parameters as required. For the current work, fatigue spectra have principally been generated using data from a Flight Strain Survey (FSS) conducted on the H-60 Black Hawk.

Once generated, a raw fatigue spectrum will typically consist of substantially more load cycles than it is practical to apply in a laboratory-based FSFT. Because the rotors of a helicopter are turning constantly and in all flight conditions, the airframe will be subjected to hundreds of millions – if not billions – of potentially fatigue damaging load cycles over its lifetime and recreating this many load cycles in the laboratory could take decades. Therefore, truncation is a technique that is commonly applied to fatigue spectra to eliminate non- or lesser- damaging load cycles, producing a spectrum that is equivalent in terms of the theoretical fatigue damage it produces but with substantially fewer load Turning Points (TPs). DSTO has adapted known truncation techniques to develop a truncation method called the Indexed Rainflow Filter (IRF) method, which allows fatigue spectra to be truncated to an infinitely variable degree while preserving the original sequence and magnitudes of the remaining TPs. The process is shown diagrammatically in Figure 1 and an example of an assembled stress sequence for an airframe location for a single flight is shown in Figure 2.

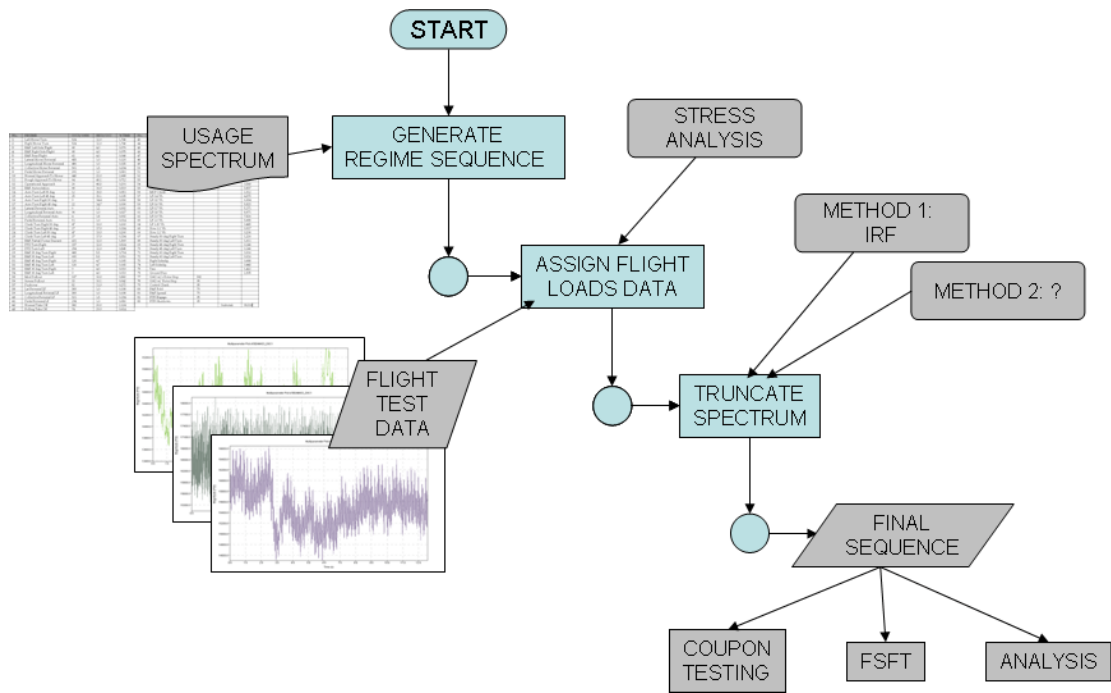


Figure 1: Spectrum generation and truncation process description

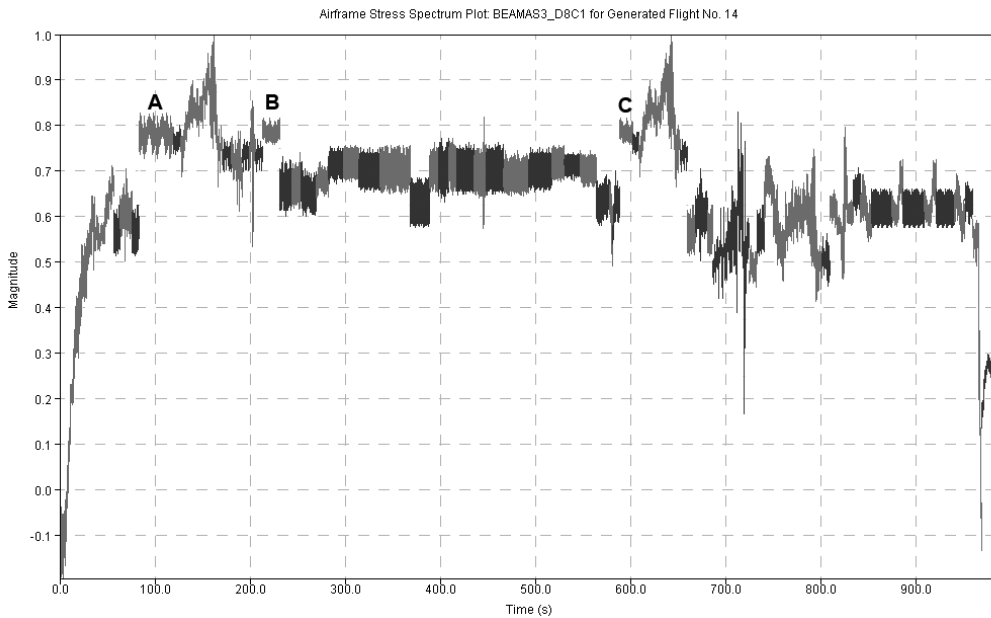


Figure 2: Stress sequence for an airframe location for one flight

2.3.10 E-7A Wedgetail Usage Monitoring System Certification, Testing and Implementation - Tom Matley, (DSTO) and Ian Coker, (Directorate General Technical Airworthiness)



Background

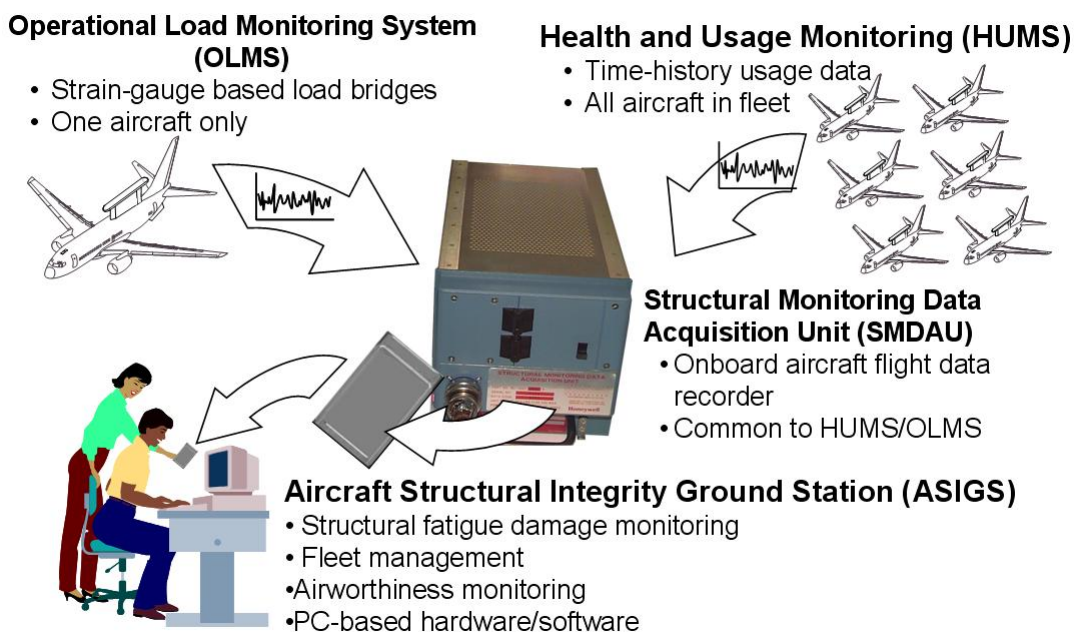
An effective Aircraft Structural Integrity Program (ASIP) requires an accurate Usage Monitoring (UM) system. The Health Usage Monitoring System (HUMS), Operational Loads Monitoring System (OLMS) and Aircraft Structural Integrity Ground Station (ASIGS) are the key elements of the E-7A Wedgetail UM system. The system provides the data and analyses necessary to assess if each individual aircraft is being operated within the defined usage spectrum of the fleet and therefore assess if the certification basis remains valid, enable structural life assessments to be based on actual individual aircraft usage and provide historical data on which to base predicted usage spectra for future acquisitions.

The onboard HUMS and OLMS provide the data necessary to monitor and assess the usage of individual aircraft and the fleet and provide guidance on operational and maintenance strategies. The OLMS data is useful for investigating loading responses to flight environments and comparing the recorded responses against HUMS flight performance and acceleration data. The OLMS data is also used to investigate and characterise repeated load exceedence spectra encountered during service and compare the collected data against design predictions.

Onboard Hardware

The HUMS is a permanently installed system included on all six RAAF E-7A Wedgetail aircraft. The primary component of the HUMS is the Structural Monitoring Data Acquisition Unit (SMDAU) data recorder. The SMDAU is a durable and capable data recorder, developed for the E-7A fleet by Honeywell. The primary SMDAU design feature was to add the capability to record 100 samples per second high rate analogue data.

The analogue recording capability uses an inertial sensing unit to measure aircraft acceleration and angular rate data in each axis, a flight data recorder and structural bending moment measurements provided by the Operational Loads Monitoring System (OLMS). The SMDAU is also connected to the baseline aircraft standard ARINC-429 data bus to gather flight performance data. This includes high sample rate motion data and comprehensive flight performance data including altitude, speed, attitude, control surface positions, and engine revolutions per minute. The same SMDAU is used for both the HUMS and the OLMS recording functions. The HUMS functions are always available, and connecting a discrete measurement input to ground also enables the OLMS recording functionality for aircraft so equipped.



Aircraft Structural Integrity Ground Station

ASIGS consists of a custom software build hosted on a high-end Commercial off the Shelf (COTS) Windows Server platform. ASIGS is capable of assessing accumulated fatigue damage for the aircraft based on the actual aircraft usage. Flight parameter plotting functions allow investigation of entire flights or portions of flights. ASIGS provides comprehensive individual aircraft and fleet usage statistics, fatigue damage data, service life plots, exceedance data and excess load and usage information.

ASIGS post-processes HUMS data recorded in flight on a flight-by-flight basis, before calculating usage statistics and fatigue damage. ASIGS uses a parametric approach to the calculation of fatigue damage at each fatigue critical location. The fatigue damage is calculated as a function of the critical flight parameters (airspeed, altitude and gross weight). ASIGS fatigue damage algorithm parses each flight into a set of mission segments that have an assigned damage rate (damage per hour, distance or event). The fatigue damage is then calculated by multiplying the time distance or number of events in a certain flight segment by the associated damage rate stored in the database. The parametric approach and fidelity of the flight segmentation routine results in representative fatigue calculation of flights that are both more and less severe than the assumed usage profiles.

ASIGS reporting functionality includes individual and fleet wide usage and service life data analysis and generation of Routine Usage Status Reports, Usage Analysis Reports and annual Fatigue Assessment Reports.

ASIGS Certification

The Commonwealth of Australia (CoA) conducted certification testing to assess if the system was fit for purpose and complies with both contractual and Australian Defence Force airworthiness requirements.

The key document in the certification of ASIGS was the Health and Usage Monitoring Validation Plan (HUMSVP). The HUMSVP was developed using a requirements based testing methodology and took a holistic approach and included not just the ASIGS software but all the systems, data and processes supporting it.

ASIGS certification testing required a multi faceted approach including:

- Compliance auditing that the system implementation met specifications
- Software testing using both clear and black box testing methodologies
- System functional testing to evaluate that that ASIGS was fit for purpose

After a number of iterations of the certification testing process, ASIGS was certified by ASI-DGTA in August 2012.

2.3.11 Regulation of UAS for use by the ADF - Callum Wright, (DSTO)

Over the past 4 years there has been increased effort to develop and apply a robust, yet sympathetic, set of regulations that govern the use of UAS within Australia by Defence. Up to this point the Australian Defence Force (ADF) used rapid acquisition to procure or lease platforms for specific operations outside Australia. This application in an environment of heightened threat allowed for the waiver of regulations. However, increased integration into the force structure and draw down of overseas operations made it apparent that the operation of UAS within Australia was becoming a necessity.

The existing regulatory bodies have been tackling this problem in iterative cycles with the goal of reaching a mature system as quickly as possible; in parallel with ongoing operations, acquisition programs and support activities. In essence three broad categories are being considered:

- a. Full certification with stringent operational controls: this would be for UAS that were, large, fast, dangerous, expensive, weaponised, flying in unrestricted airspace or over the general population.
- b. Partial risk based certification and operation: Only to be flown in military restricted airspace, not over the general populous and posing a contained and manageable risk.
- c. No certification or oversight: Small non-lethal UAS that can be operated with no certification or operational oversight. These are extremely low risk operations.

Whilst this general construct is widely believe to be correct, the specific generation and agreement of category boundaries is more problematic and is taking significant time to work through and remains an unsolved problem. Kinetic energy is the most likely measure that will establish the boundary for the third category (extremely low risk operations) and most discussion centres on what is a tolerable consequence. The boundary between the first and second categories is also uncertain with only a few factors consistently embraced: carriage of munitions and flight in uncontrolled airspace or over populous areas forcing the use of the most stringent category.

The ADF is also engaged with the civil regulator (CASA), who is tackling similar issues, to ensure regulations can be as harmonised as possible. CASA was the first regulator in the world to issue UAS regulations (CASR Pt101 issued in 1998) as is also looking to update, but is experiencing similar issues to those within Defence.

With this backdrop DSTO has been assisting both Technical and Operational regulators with regulation formation and to understand the differences and limitations in the traditional code of requirements based approaches to certification versus a risk target approach. DSTO has also conducted small investigations into structural regulations to assess if there are any specific issues with the proposed approaches and has run risk analysis to understand the issues with such calculations. As part of this an assessment of a flight planning model that calculates the third party risk due to UAV platform failures was performed. Despite these challenges Defence has conducted a risk based approval for two UAS types to operate within military controlled airspace.

Concurrently, DGTA and DACPA have progressed with the assessment of both Shadow and Heron for operation on Australian military ranges within the “partial risk based certification and operation” category.

DSTO has been contemplating future investigations into the likelihood of injury during loss of control of a UAS.

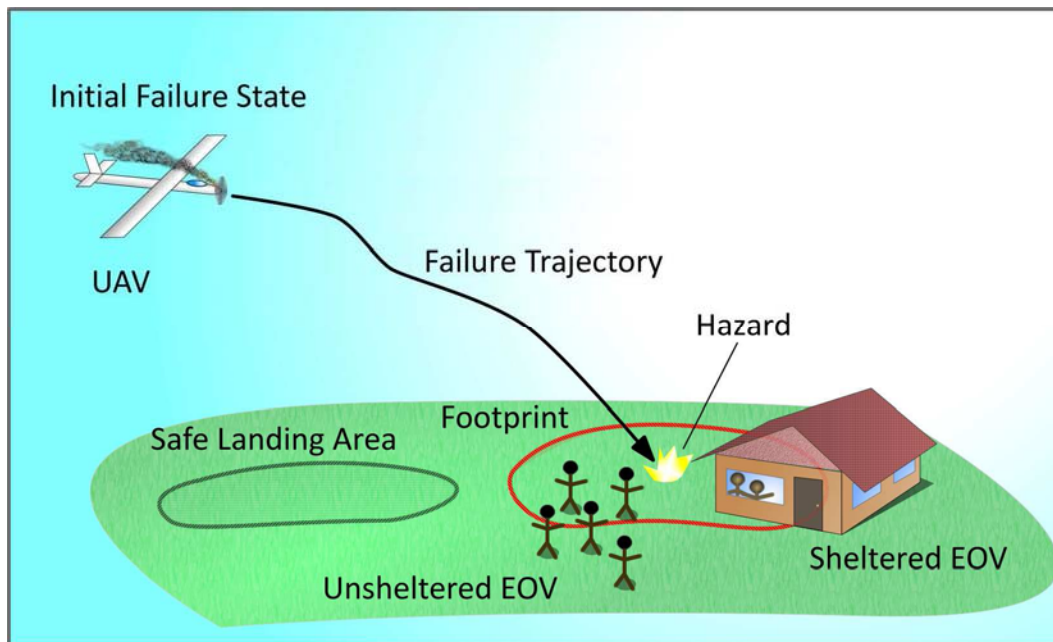


Figure 1. A graphical representation of the general risk model.[1]

Reference:

Clothier, R. *URAT Risk Model Definition*, ARCAA-URAT-RM-MD-001, Version: 1.1, 13-Jan-10

2.3.12 DEF STAN 00 970 Equivalent Safety Finding Methodology for RAAF PC-9/A FAR23 Certified Repairs - Z. Louli, S. Trezise, Kevin Watters (QinetiQ Australia)

The Royal Australian Air Force (RAAF) operates a fleet of 63 Pilatus PC-9/A turboprop trainer aircraft. The aircraft was designed and originally certified to Federal Aviation Regulation (FAR) Part 23 Amendment 28 requirements. However, with the clearance of the RAAF PC-9/A to 10000 Airframe Hours (AFHRS) based on the in-country Full Scale Fatigue Test (FSFT) demonstration, the certification standard for fatigue management was transitioned to Defence Standard (DEF STAN) 00 970.

As part of the through life management of the RAAF PC-9/A, the Original Equipment Manufacturer (OEM) continues to design repairs for the PC-9/A aircraft in accordance with FAR 23. Hence, a method was required to allow assessment of repair compliance with the current fatigue certification basis (ie DEF STAN 00 970). To this end, QinetiQ developed a checklist which could be applied to OEM repairs to rapidly assess DEF STAN compliance.

The checklist was developed with consideration for the following factors:

- The differing requirements of FAR23 and DEF STAN 00 970 with regard to fatigue assessment
- The methods of fatigue assessment typically employed in OEM repair assessment
- A comparison of crack growth analysis methods commonly used by the RAAF PC-9/A ASIP stakeholder community
- Known limitations of the FSFT

The final checklist was applied to a selection of historical repairs to demonstrate the use of the approach, and also to provide a compliance finding for these repairs. It was generally found that repair fatigue analyses met the criteria outlined in DEFSTAN 00 970. However, some aspects of the DEFSTAN 00 970 requirements safety by inspection programs were not met, particularly the application of analytical and/or unmonitored factors in determining the inspection intervals.

2.3.13 Development of Flight Manoeuvre Recognition Software for Rotary Wing Platforms - A. Castelow, A. McArlein, C. McGregor (QinetiQ Australia)

The current Usage Monitoring (UM) system used to characterise usage of the majority of Australian Defence Force (ADF) Rotary Wing (RW) aircraft is based on the manual completion of usage forms by aircrew at the end of each flight. Annual Fatigue Assessments (AFAs) performed for ADF RW platforms compare the recorded usage data to an approved baseline Design Usage Spectrum (DUS), and provide an assessment of the fatigue accrual and the ongoing validity of the component fatigue lives.

Critical review of UM systems undertaken for a number of RW platforms, however, identified that a number of significant fatigue damaging flight regimes are currently unable to be accurately monitored via the extant UM systems (i.e. turns, descents, climbs, pull-ups, high speed flight, etc.), with aircrew required to be able to detect and recall manoeuvres post-flight. This restricts the level of comparison able to be made between in-service usage and the baseline DUS, in turn, limiting the ability of AFAs to make judgements regarding the validity of component lifing. Review of UM systems undertaken for a number of RW platforms highlighted the potential use of Flight Data Recorder (FDR) data to capture in-service occurrences of those flight regimes not currently monitored.

A series of algorithms for identifying fatigue damaging flight regimes in the S-70B-2 Seahawk DUS in data downloaded from the FDR have been developed [1]. These algorithms are currently being used as the basis for development of Flight Manoeuvre Recognition (FMR) software. Initial development focussing on recognition of S-70B-2 Seahawk fatigue damaging flight regimes in FDR data, has been completed, with the software currently undergoing a two phased Verification and Validation (V&V) program.

The first phase involved the analysis of data extracted from DSTO flight simulator models for the Seahawk, where missions comprised of known manoeuvres were flown by a qualified member of ADF aircrew (with a working knowledge of the platform) in the Air Operations Simulations Centre (AOSC) simulator. Software outputs were compared against expected results, with further investigation undertaken where any discrepancies

were found to exist. Modifications to original logic and algorithms to improve the quality of software manoeuvre recognition have been proposed where required, however, current indications are that the software will be capable of monitoring a significant number of additional flight regimes unable to be captured by the extant UM system.

The second phase will involve analysis of actual S-70B-2 FDR data from monitored ADF flights. It is intended that an on-board observer will record the sequence and approximate duration of manoeuvres performed, providing a means of confirming the functionality of the software and potential improvements identified. Work is also underway to assess the feasibility of expanding the FMR software to incorporate other RW platforms, with the S-70A-9 Black Hawk considered a primary candidate for inclusion.

References:

1. Raytheon Australia, Seahawk Usage Monitoring Software Development – Flowchart Development, SHUMS-RPT-001, Revision 1.0, 25 July 2006.

2.3.14 Black Hawk CRT Calculations/Individual Asset Calculations - A. Jackson, T. Frisch, C. Cowx, B. Hindmarsh, D. Moorhead, J. Turner, J. Lamshed, K. Watters, R. Lockett, K. Jackson, J. Moews (QinetiQ Australia)

In 2010 QinetiQ, with support from DSTO, developed a revised usage spectrum (AUUS2) to represent Australian Defence Force (ADF) Black Hawk usage. The revised spectrum was based on a spectrum previously developed by the Black Hawk OEM, Sikorsky, which was modified using usage data manually recorded on EE360 sheets.

Fatigue damage calculations were performed using Miners rule to produce Component Retirement Times (CRTs) for 28 critical components. This process followed standard industry practice using a working S-N curve and suitable component flight loads. The S-N curves and flight loads used in the revised CRT calculations were sourced from OEM damage calculations. The revised usage spectrum allowed the authorised throw-away lives for all components to be increased.

Following the calculation of revised CRTs, the effects of variations in fleet usage between individual aircraft on CRTs were assessed. This study showed that, for some components, variations in recorded gross weight and altitude data between aircraft could result in fatigue damage accrual rates for some aircraft to be greater than predicted by the AUUS2 CRT calculations. These findings resulted in the identification of a number of individual components whose estimated fatigue accrual placed them at risk of exceeding their fatigue damage limits prior to reaching their CRT. Since individual components can be moved between different aircraft within the fleet, the location history of each asset was used to determine the usage history for each individual asset. The recorded usage for each asset was used to develop a usage spectrum for each asset, and fatigue damage calculations were performed to predict the actual fatigue life consumed. The calculations showed that the fatigue accrual rates for 20 out of the 22 assets assessed were less than that predicted by the AUUS2.

2.4 FATIGUE INVESTIGATIONS OF MILITARY AIRCRAFT

2.4.1 Failure Analysis Examples in Military Aircraft - Nick Athiniotis, (DSTO)

Fatigue cracking at Wing Leading Edge Ribs of C130 aircraft.

Cracking initiated at the edges of fastener heads and/or at the edges of the pressed bead panel stiffeners due to out-of-plane bending of the rib material.

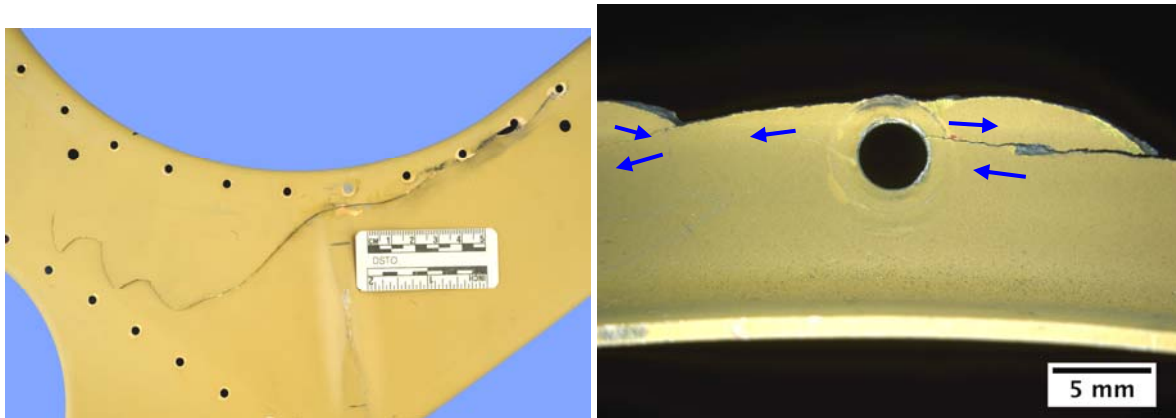


Figure 1: Fatigue cracking originating at the edge of at least two fastener heads. Typical region of crack initiation located at the edge of a fastener head; direction of growth shown by arrows.

Aircraft Transmission Support Beam Cracking in the Black Hawk helicopter.

Cracking initiated due to fretting at the upper corners of the first row of fastener holes. This location likely experienced considerable tensile stress due to bending of the beam during ground-air-ground cycles, with contributions to crack growth from manoeuvre (flight) loads and vibration.



Figure 2: Upper flange showing the crack intersecting two fastener holes. Macroscopic features indicated that crack initiation occurred at the upper corners of the fastener holes

Cracking due to Residual Stress in a trainer aircraft.

Fatigue cracking occurred from a number of fastener holes. A lack of damage observed on the fracture surface, the large number of fatigue crack origins on the outboard surface, and the crack not reaching the inboard surface all suggested that a significant level of residual stress was contained in the component. This tensile residual stress is likely to have been produced from the cold bending of the radius of the component.

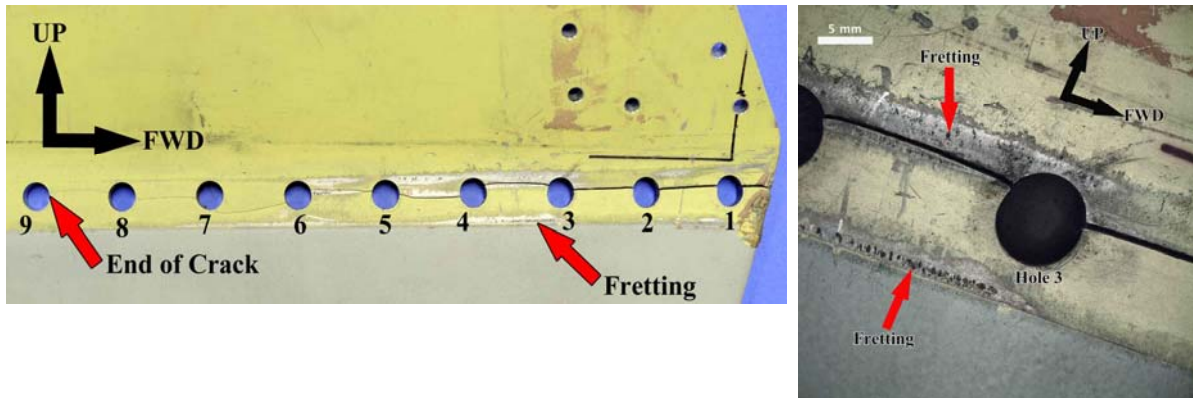


Figure 3: Fatigue crack extending from the leading edge to the start of the 9th hole, and associated fretting (right image).

Air Turbine Starter in F/A-18 aircraft.

Examination of two Air Turbine Starters (ATS) revealed fatigue cracking which originated from machining marks on the forward face of the turbines. New Non Destructive Inspection techniques introduced after a previous Forensic investigation were capable of detecting the cracking. Fatigue progression marks were believed to have formed by loading similar to that which occurred during functional testing at overhaul.



Figure 4: Upper flange showing the crack intersecting two fastener holes. Macroscopic features indicated that crack initiation occurred at the upper corners of the fastener holes

2.4.2 Life Extension of F/A-18 LAU-7 Missile Launchers Using Rework Shape Optimisation and Cold Rolling - Manfred Heller, Jaime Calero, Simon Barter, Ron Wescott, Jireh Choi, (DSTO)

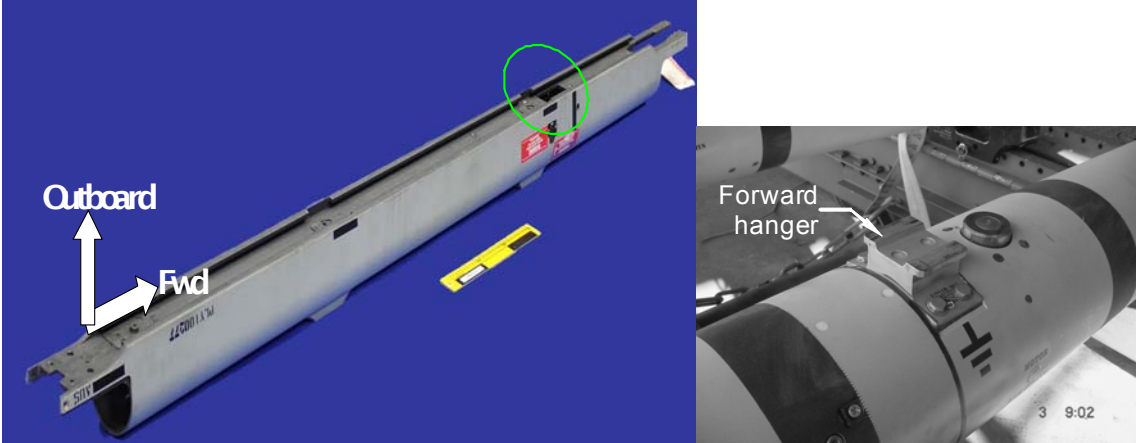
For more than twenty years, the Royal Australian Air Force (RAAF) has reported cracking of the housing guide rails of the LAU-7 missile launchers, in their F/A-18 aircraft. Positioned at the wing tip, the LAU-7 missile launcher (Figure 1 (a)) carries the Advanced Short Range Air-to-Air Missile (ASRAAM). One point of attachment of the missile to the launcher is via the forward hanger (Figure 1 (b)). Multiple fatigue cracks have been found to propagate in the guide rail at the corner adjacent to the missile forward hanger (Figure 1 (c)). The RAAF has been managing the issue by replacing housings when the cracks reach a surface length of 19 mm (3/4 inch). This length typically corresponds to a crack depth of 0.5 mm or less.

DSTO has developed a relatively unique life extension technology that uses an FEA-based stress optimisation approach to create optimised rework shapes that significantly reduce peak operating stresses. An overview of this DSTO technology was presented at ICAF 2009. In previously reported work DSTO designed a repair approach for the launcher rails based on optimum rework shaping at the critical fatigue location. Two design options were developed: (i) an optimised blend shape that removes cracks to a depth of 1.1 mm, and (ii) a very shallow optimised blend shape that will inhibit initial crack growth. The stress reductions resulting from both designs can provide substantial economic benefits by avoiding the need for component replacement and increasing the interval between costly periodic in-service inspections.

Successfully completed stages in launcher repair development were: (i) FEA to design the optimised shapes, (ii) making prototype in-situ tooling to manufacture the new shapes, (iii) fatigue testing of coupons, and (iv) Quantitative Fractography (QF) to assess crack growth. The shape and typical stress distribution for the shallow rework design are shown in Figure 2. Figure 3 shows the manufacturing jig on the launcher in position to carry out the repair. A typical fracture surface for coupons with the 1.1 mm deep optimised profile is shown in Figure 4.

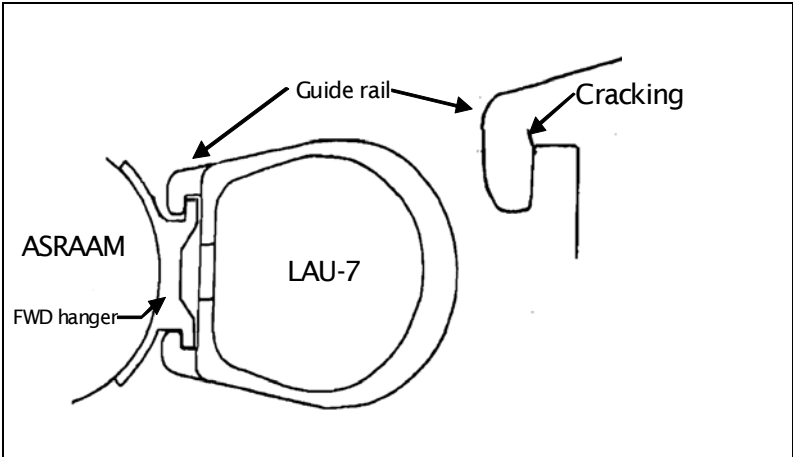
Cold rolling can lead to component life extension by introducing beneficial residual stresses and improving the surface finish. In the current work the procedure to cold roll coupons has been enhanced. At first a cold rolling tool with the same shape as the cutting tool was adopted. FEA was then used to re-design the cold rolling tool. Coupons with the 1.1 mm deep rework have been cold rolled with the new tool and then undergone fatigue testing. Figure 5 is a summary of crack depth versus component life (in terms of numbers of loading blocks) for coupons with the nominal and 1.1 mm deep optimised shape, with and without cold rolling. Results show that on average cold rolling increases the component life by 40% for the 1.1 mm deep rework up to a crack depth of 0.5 mm (Figure 5).

Development of an NDI procedure using a specialised eddy current probe has also been completed in collaboration with the RAAF and Australian industry. The RAAF is currently conducting trials of the life extension technology to repair launcher housings.



(a)

(b)



(c)

Figure 1: (a) LAU-7 missile launcher (b) close up of ASRAAM missile with forward hanger, and (c) cross-section of launcher at forward hanger showing location of cracking

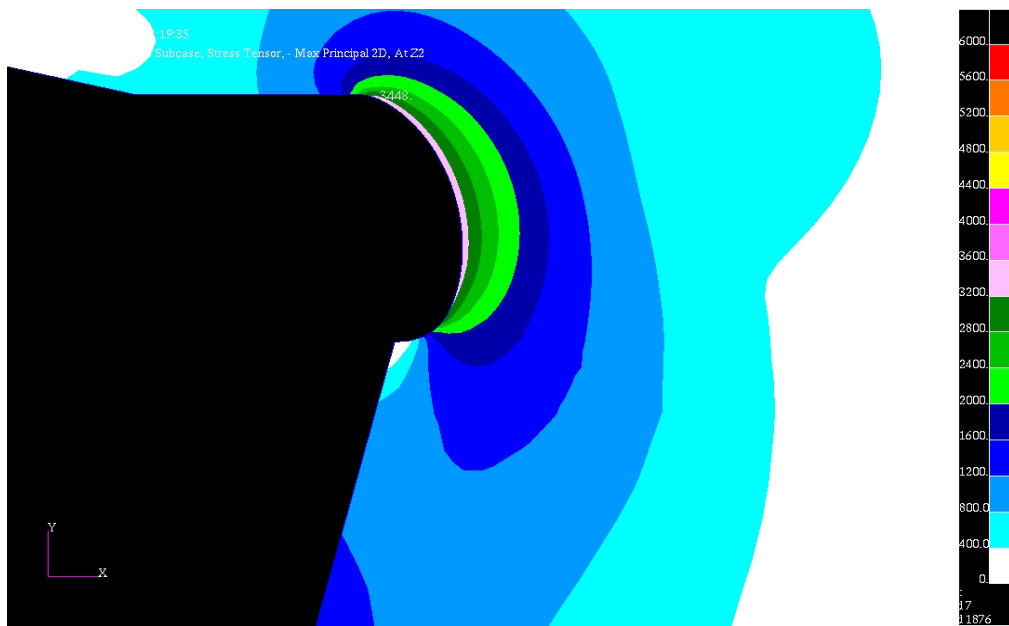


Figure 2: Shape and stress distribution for the shallow rework (peak stress concentration reduced by 45%)

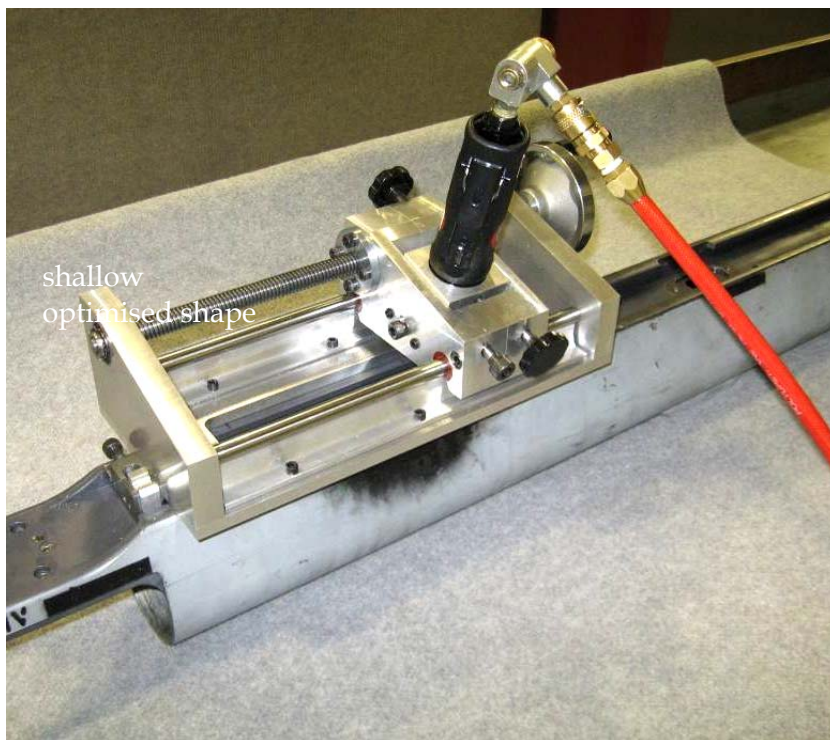


Figure 3: Manufacturing jig

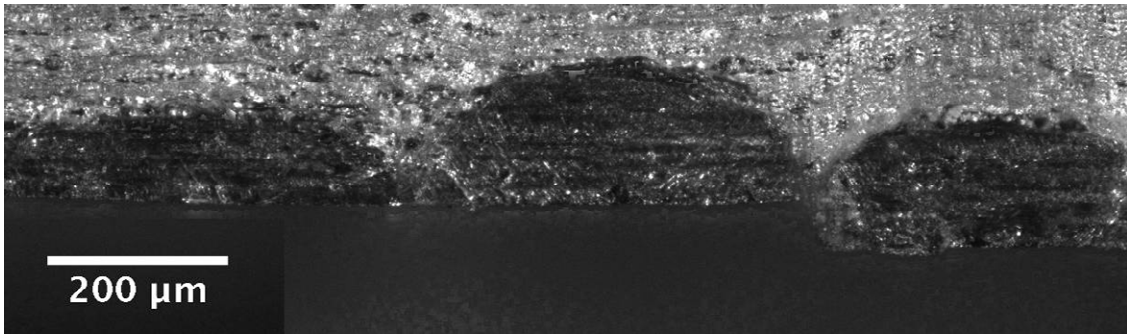


Figure 4: Typical shapes and spacing of small cracks in coupons with 1.1 mm deep optimised profiles

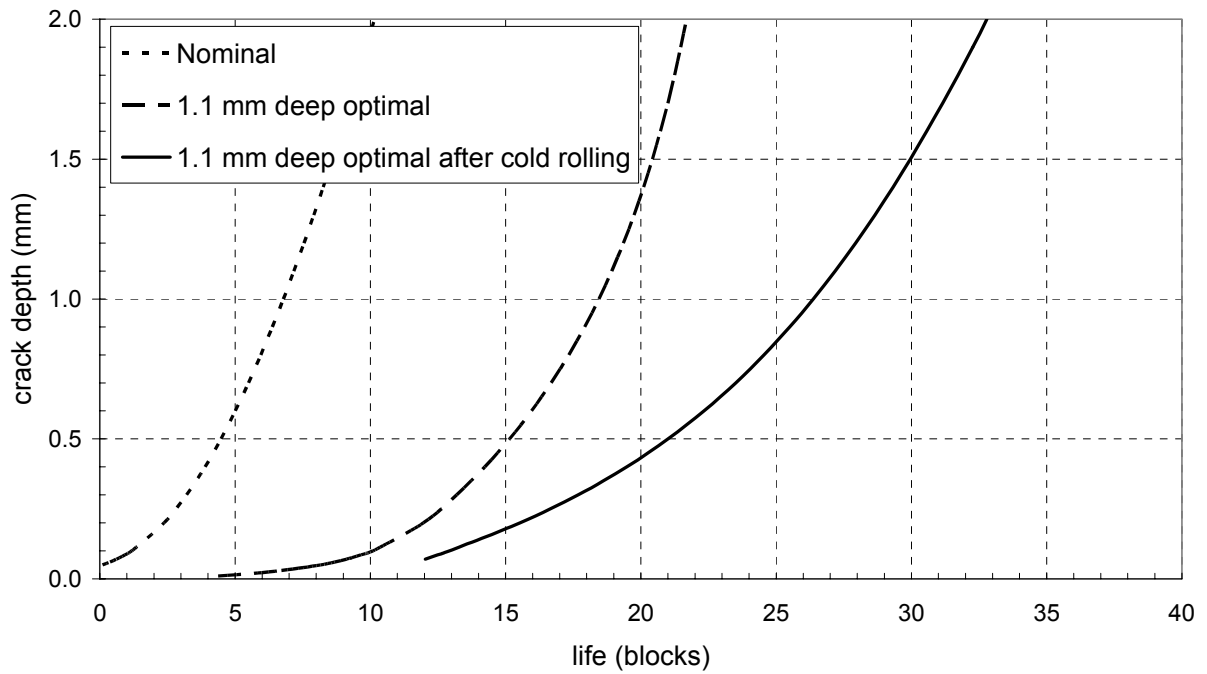


Figure 5: Average fatigue crack depth as a function of loading block number for coupons with (i) nominal profile, (ii) 1.1 mm deep optimised profile, and (iii) 1.1 mm deep optimised profile with cold rolling.

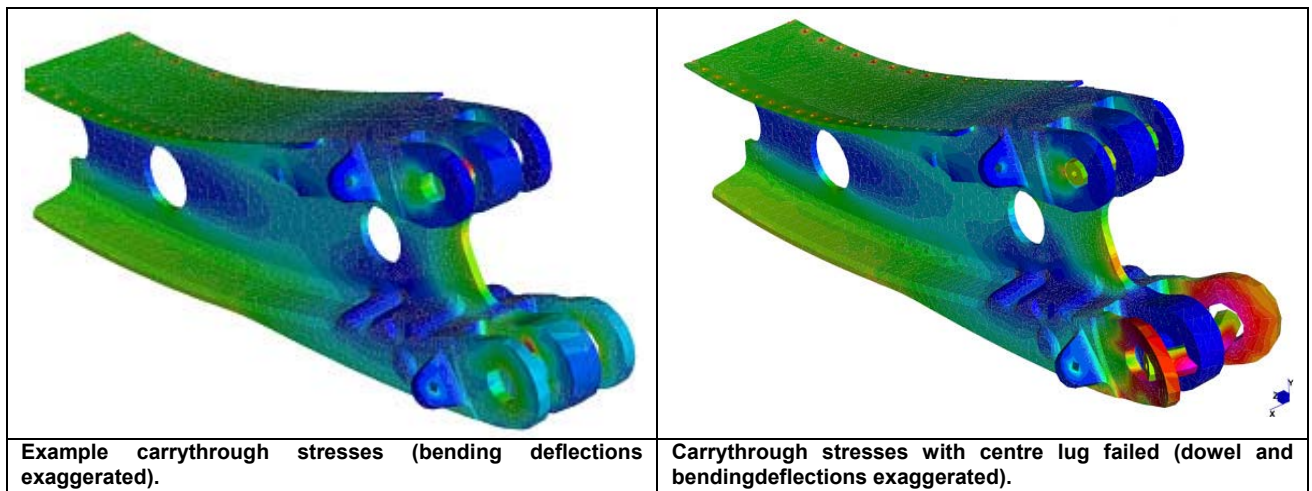
2.5 FATIGUE INVESTIGATIONS OF CIVIL AIRCRAFT

2.5.1 Fatigue and Structural Integrity of Light Aircraft - AEA Aerospace Group Pty Ltd and Dave Morris, (Civil Aviation Safety Authority)

2.5.1.1 Cessna 210 Carry through rework

A recent investigation and repair design was conducted on the wing main spar attachment and carry-through of the Cessna 210 aircraft. This six seat high performance aircraft is a typical example of light aircraft used in the 'little airliner' role, carrying passengers and cargo throughout regional Australia. These 'little airliners' have generally accrued far more flight hours than was originally intended when they were first designed. The original design standard of this and many similar aircraft was CAR 3, which had no requirement to establish a fatigue life or ensure failsafe behaviour in any part of the airframe. A consequence of this is that as they age, become damaged and corroded, their ongoing residual strength and remaining fatigue life are unknown.

The carry-through structure in question has both single and multiple load-path features, which means each critical point must be treated on a unique case-by-case basis. Also, carry-through components were forged from 2014 alloy which while being high strength is sensitive to stress corrosion cracking, load direction and high crack growth rate. Classical static and Finite Element Analysis (elastic-plastic) was conducted to determine the residual strength of the various critical points in both their baseline and reworked configurations. Finally, the remaining fatigue life and inspection intervals were determined using all three options available in the modern FAR 23 requirements; safe-life, failsafe and damage tolerance evaluation. Crack growth modelling was applied to all components to determine ongoing inspection intervals.



As modern damage tolerance requirements were originally developed from military and large commercial aviation experience, there were surprises and unusual outcomes of applying these requirements to this type of 'little airliner' structure. These outcomes also apply more generally to any compact, highly loaded and single load path structure of older design. The implication for light aircraft, when covered by maintenance programmes derived from the damage tolerant requirements, is that they are predicted to be more prone to fast crack growth with correspondingly short inspection intervals. However options exist to mitigate against these effects, particularly at the design stage:

- Due to the small number of critical parts, the probability of a flaw at a critical location may be much lower. Closer or more detailed inspection of parts is possible at the production stage.
- Although corrosion acts as stress raiser, because attachment details are relatively heavy sections, the 'effective crack' size may give stress intensities below the threshold value for crack growth. For lower stress levels, this improves the crack growth period.

For Further information : eric.whitney@aeroengaus.com.au

2.5.1.2 Cessna 441 life extension STC.

The Cessna 441 performs an important role in the commuter passenger sector of the Australian Civil Aviation industry. The Cessna Structural inspection Document manages the fatigue of the aircraft structure up to its published validity limit of 22,500 flight hours. This limit was mandated by the Australian Civil Aviation Safety Authority in 2007. Many C441 aircraft in Australia are close to or have reached the SID Limit of Validity (LOV). A project was undertaken to extend the fatigue life limit of the C441 to 40,000 hours or cycles whichever is reached first. The project involved the replacement of parts, reinforcement of parts and the addition of supplementary structure to ensure that the stresses were reduced to a level that yielded appropriate inspection intervals. The structure was made damage tolerant where possible. Strain gauging was carried out to the wing and fuselage sections to verify the FEA model developed. The C441 systems were assessed and many components were similar to Cessna 404 models that have SID LOV of 40,000 hours. The FEA model allowed modelling of failed structural members and observation of load re-distribution and demonstration of fail-safe characteristics. Damage tolerant inspections were developed for structure with predictable/stable crack growth rates.



For Further information : kim.white@aeroengaus.com.au

2.5.1.3 CASA 212 fatigue assessment of landing gear following Antarctic operations

Australian STC SVA519 was issued in September 2009 for the installation of retractable plate skis to the landing gear of increased gross weight CASA 212 aircraft for operations in the Antarctic. Due to inadequate data for the fatigue substantiation of the landing gear and associated components at the time of certification a conservative life limit was applied with the requirement to re-evaluate the fatigue on the landing gear within 3 years. This timeframe allowed for the gathering of data by way of sensors attached to the landing gear for the trial period. With the relevant data logger records, the stress spectra for the aircraft modification was evaluated. The data loggers recorded strut positions and accelerations. The data also allowed Airbus Military to provide advice on the implications for the unmodified airframe. For each PSE that was found to have a more restrictive life limit than an unmodified aircraft, a usage factor was determined to apply to each landing or cycle count. The manufacturer's maintenance schedule was altered to ensure that the inspections were adequate for the operations.

For Further information : don.love@aeroengaus.com.au

**Aeronautical
Engineers
Australia**

Working Together



3. NEW ZEALAND

3.1.1 CT4-E Fatigue Life – Stephen Campbell, (Defence Technology Agency)

The RNZAF operate a fleet of Pacific Aerospace CT 4-E Airtrainers. The CT-4E is utilised for Ab initio flight training as well as having a role in the RNZAF formation aerobatic display team.

The CT 4-E is an evolution model of the CT 4-B, which has seen service in both the RNZAF and RAAF. The -E derivative incorporates a new engine and propeller combination and operates at an increased all up weight when compared to the -B variant.



The original fatigue life of the CT 4-B was determined by a full scale fatigue test conducted on behalf of the RAAF in the early 80's. On introduction to service, the fatigue life of the CT 4-E was based on the original -B data with analytical corrections to account for the additional mass.

Recently, the RNZAF initiated a usage evaluation of their CT 4-E fleet. This survey indicated that the RNZAF usage severity has increased over the -B usage. This is a likely result of the extra performance of the -E. In addition to the usage severity increase and the structural weight change between variants, it was found that the original design calculations included unconservative estimates of pilot and equipment weights.

After review of the design data, OEM fatigue test on the -B variant and combined with the new RNZAF severity and operational weights, it was decided that the RNZAF had consumed or nearly consumed the fatigue life of the CT 4-E at one structurally significant location, and that a second location was likely to exceed its revised fatigue life before the planned withdrawal for the fleet. A fleet wide inspection programme of both locations was initiated.

The CT 4 has empennage is a single spar structure. The RNZAF fleet had consumed the majority of the revised fatigue life for this location. A fleet wide inspection and replacement programme was initiated. The inspections revealed fatigue cracking in the spar caps and some of the support structure on the majority of the RNZAF fleet. The spar cap replacement programme has been implemented.

The CT 4-B wing includes a built up "laminated" spar cap, that is spliced at a wing carry through joint. It was estimated that the RNZAF fleet would approach or exceed the remaining fatigue life at approximately the planned withdrawal date for the CT 4-E. A fleet wide inspection programme was initiated, with the intention of conducting active fleet management of the fleet. The inspection programme revealed fatigue damage in a portion of the fleet, and it was decided that a fleet wide wing splice replacement programme would be initiated. The splice replacement programme included changing the spar cap in the area to single machined pieces (as opposed to the original laminated stack). To date, the replacement programme has been incorporated in the majority of the RNZAF fleet.

3.1.2 C-130 Gust Spectrum- Stephen Campbell, (Defence Technology Agency)

The RNZAF have recently upgraded their C-130 fleet. The upgrade encompassed mission systems, incorporation of a glass cockpit, an avionics system re-wire and a structural enhancement package. The structural enhancement package included number of fatigue life enhancements, structural replacements and re-establishing RNZAF usage baselines.

As part of the programme to re-establish RNZAF usage baselines, the aircraft OEM was contracted to conduct an Operational Usage Evaluation (OUE) for the RNZAF fleet. During the course of the OUE, the RNZAF raised a number of questions regarding how to estimate the gust spectrum for their C-130 fleet.

Anecdotally, the gust environment in which the RNZAF fleet operates is considered more severe than often assumed by OEM's in designing their aircraft. To date, there has been only one significant published set of data that contains gust information from the

environment that the RNZAF fleet typically operates. This report was conducted by the Royal Aircraft Establishment in 1958, and utilised data from a fleet of Bristol Freighter aircraft.

In late 2005, the RNZAF installed a prototype usage monitoring system in one of their C-130 aircraft. This system remained on the aircraft until 2011, when the aircraft on which it was installed was inducted into the RNZAF C-130 upgrade programme. The usage monitoring system is somewhat unique in that it continuously recorded normal acceleration (N_z) data from a dedicated high sensitivity accelerometer at a sampling rate of 100 Hz. Upon error checking, the OEM was able identify and utilise this N_z data for 455 full flights (1552 flight hours) in the RNZAF operational environment.

Due to the combination of a high sensitivity accelerometer and high data recording rates, it was possible to filter the RNZAF N_z data using a local peak detection algorithm with a 0.03g rise fall threshold. It was further possible to filter the data using a two second dead band criteria around the individual peaks. N_z events that maintained the peak value for more than two seconds were classed as manoeuvre events, and those of shorter duration were classified as gust.

Further analysis of the events classified as gust indicated that the RNZAF operational environment contained significantly more gust events with incremental peaks in the range 0.1-0.5 g than the standard gust models employed by the OEM. It was concluded that the RNZAF gust environment was more severe than the spectrum typically used by the OEM. The RNZAF OUE was modified to incorporate a new (more severe) gust model.